To the Graduate Council:

I am submitting herewith a dissertation written by Frederick John Snow entitled "Geometric Morphometry Analysis of the Scapula: Implications for the Determination of Sex and Ancestry." I have examined the final paper copy of this dissertation for form and content and recommend that it be accepted in partial fulfillment of the requirements for the degree of Doctor of Philosophy, with a major in Anthropology.

William M. Bass, Major Professor

We have read this dissertation
and recommend its acceptance:

Accepted for the Council:

Vice Provost and Dean of
Graduate Studies

# Geometric Morphometry Analysis of the Scapula: Implications for the Determination of Sex and Ancestry

A Dissertation
Presented for the
Doctor of Philosophy
Degree
The University of Tennessee, Knoxville

Frederick John Snow
May 2004

Thesis
2004b
.S66

## Dedication

This dissertation is dedicated to my wife, Cindy,
and parents, Fred and Helen Schneeberger.

# Acknowledgments

There are many people to whom I am indebted for making this project possible. First, I would like to thank my chair, Dr. William M. Bass, and my other committee members, Dr. Richard L. Jantz, Dr. Walter Klippel, and Dr. David Icove for providing direction for this dissertation.

Thanks also to Dr. Ann Reed, Dr. Dennis Slice, Dr. Robert Muenchen, and Scott Snyder for providing statistical assistance.

I am also indebted to Dr. Mark Koponen, Dr. Kris Sperry, and Scott Roberts of the Georgia Bureau of Investigation for giving me time away from work to complete this dissertation.

I also owe a huge debt of gratitude to my parents, Fred and Helen Schneeberger, for encouraging a nascent interest in archaeology and the human skeleton while I was a child and for their unwavering support. Little did we know that this budding interest as a child would develop into a career as an adult, nor did we envision the circuitous route I would take to get there.

Finally, I would like to thank my wife, Cindy, who endured long periods of time alone while I was in the Balkans gaining international experience and whose organizational skills kept me on track. Without her help, support, and unflagging encouragement this dissertation would not have been possible.

## Abstract

The nascent but growing field of geometric morphometrics has proved to be a useful tool in the investigation of shape differences of skeletal elements of various populations. Until recently, most anthropological studies using geometric morphometrics have focused on shape differences of the skull, largely to the neglect of the postcrania. This research uses coordinate data derived from three-dimensional digitizing to quantify morphological variation in left and right scapulae of Blacks and Whites of both sexes. The sample analyzed was from a collection of present day Americans, making it particularly germane for forensic applications.

Left and right scapulae of Black males, Black females, White males, and White females were digitized, producing three-dimensional coordinates that were subsequently subjected to Procrustes analysis, and residuals were analyzed by traditional statistical analyses. Consensus configurations were superimposed using thin-plate splines to investigate shape variability among groups.

Canonical discriminant function analysis suggested that shape differences exist between scapulae of Blacks and Whites and between the sexes. Principal component analysis showed that principal components loaded differently on the canonical discriminant functions of left and right scapulae. Centroid sizes effectively discriminated between males and females but did not discriminate between Blacks and Whites.

The success of this study in differentiating shape variability between scapulae of males and females and between Blacks and Whites demonstrates the benefit of using geometric morphometry to examine biological variability of human subpopulations. In addition, the use of non-traditional landmarks allowed for a more complete analysis of scapular shape. The use of non-traditional landmarks showed that much of the variability in scapular shape between the sexes and between Blacks and Whites lies in previously neglected areas of the scapula.

# Table of Contents


**Chapter 1. Introduction** ..... 1

**Chapter 2. Geometric Morphometry** ..... 4
Methods of Geometric Morphometry Analysis ..... 6
Finite Element Scaling Analysis ..... 7
Euclidean Distance Matrix Analysis ..... 7
Procrustes Analysis ..... 8
Thin-plate Spline Analysis ..... 10
Anthropological Applications ..... 11

**Chapter 3. The Scapula** ..... 14
Previous Research ..... 14
Scapular Morphology ..... 18
Ossification of the Scapula ..... 34

**Chapter 4. Materials and Methods** ..... 46
Scapulae ..... 46
Landmarks ..... 46
Missing Landmarks ..... 54
Data Collection Protocol ..... 55

**Chapter 5. Analytical Methods** ..... 56
Procrustes Analysis ..... 57
Principal Component Analysis ..... 60
Canonical Discriminant Function Analysis ..... 62
Thin-plate Spline Analysis ..... 62

**Chapter 6. Results** ..... 64
Procrustes Analysis ..... 64
Centroid Size ..... 64
Principal Component Analysis ..... 68
Left scapulae ..... 72
Right scapulae ..... 73
Canonical Discriminant Function Analysis ..... 74
Left scapulae ..... 75
Right scapulae ..... 78
Thin-plate Spline Analysis ..... 81

**Chapter 7. Discussion and Conclusions** ..... 87
Future Research ..... 95

**List of References** ..... 97

**Vita** ..... 114

# List of Tables


Table 4.1. Scapular Landmarks and Descriptions.....48

Table 6.1. Descriptive Statistics of Centroid Sizes of Left Scapulae of Black Females (BF), Black Males (BM), White Females (WF), and White Males (WM).....65

Table 6.2. Descriptive Statistics of Centroid Sizes of Right Scapulae of Black Females (BF), Black Males (BM), White Females (WF), and White Males (WM).....65

Table 6.3. Analysis of Variance of Centroid Sizes of Left Scapulae.....69

Table 6.4. Analysis of Variance of Centroid Sizes of Right Scapulae.....69

Table 6.5. Eigenvalues of the Covariance Matrix of Left Scapulae.....70

Table 6.6. Eigenvalues of the Covariance Matrix of Right Scapulae.....71

Table 6.7. Generalized Squared Distance of Left Scapulae of Black Females (BF), Black Males (BM), White Females (WF), and White Males (WM).....79

Table 6.8. F Statistics for Generalized Squared Distance of Left Scapulae of Black Females (BF), Black Males (BM), White Females (WF), and White Males (WM).....79

Table 6.9. P-Values for F Statistics of Generalized Squared Distance of Left Scapulae of Black Females (BF), Black Males (BM), White Females (WF), and White Males (WM).....79

Table 6.10. Generalized Squared Distance of Right Scapulae of Black Females (BF), Black Males (BM), White Females (WF), and White Males (WM).....80

Table 6.11. F Statistics for Generalized Squared Distance of Right Scapulae of Black Females (BF), Black Males (BM), White Females (WF), and White Males (WM).....80

Table 6.12. P-Values for F Statistics of Generalized Squared Distance of Right Scapulae of Black Females (BF), Black Males (BM), White Females (WF), and White Males (WM).....80

# List of Figures


Figure 3.1. Adult scapular morphology (right scapula, dorsal view)..... 20

Figure 3.2. Muscle attachments of the scapula (right scapula, dorsal view)..... 22

Figure 3.3. Muscle attachments of the scapula (right scapula, ventral view)..... 24

Figure 3.4. Muscle attachments of the scapula (right scapula, lateral view)..... 26

Figure 3.5. Scapula of neonate showing nutrient foramen (right scapula, superior view) ..... 28

Figure 3.6. Epiphyseal fusion of the acromion (ca. 16 years, right scapula, dorsal view)..... 31

Figure 3.7. Growth and morphological change of the scapula. ..... 35

Figure 3.8. Neonate scapular morphology (right scapula, dorsal view)..... 36

Figure 3.9. Neonate scapular morphology (right scapula, ventral view)..... 37

Figure 3.10. Neonate scapular morphology (right scapula, lateral view)..... 39

Figure 3.11. Juvenile scapular morphology (ca. 6 years, right scapula, lateral view)..... 40

Figure 3.12. Age of epiphyseal fusion of the scapula (right scapula, lateral view)..... 41

Figure 3.13. Age of epiphyseal fusion of the scapula (right scapula, dorsal view)..... 45

Figure 4.1. Scapular landmarks (dorsal view) ..... 49

Figure 4.2. Scapular landmarks (lateral view) ..... 50

Figure 4.3. Scapular landmarks (scapular notch) ..... 51

Figure 6.1. Means and standard deviations of centroid sizes of left scapulae ..... 66

Figure 6.2. Means and standard deviations of centroid sizes of right scapulae ..... 67

Figure 6.3. Class means on canonical variables of left scapulae ..... 76

Figure 6.4. Class means on canonical variables of right scapulae ..... 77

Figure 6.5. Thin-plate spline plot of mean White male and Black male configurations of left scapulae ..... 82

Figure 6.6. Thin-plate spline plot of mean White male and White female configurations of left scapulae ..... 83

Figure 6.7. Thin-plate spline plot of mean White male and Black male configurations of right scapulae ..... 84

Figure 6.8. Thin-plate spline plot of mean White male and White female configurations of right scapulae ..... 86

# CHAPTER 1

## Introduction

The determination of sex and ancestry are two of the major challenges for the forensic anthropologist and are essential steps in personal identification of human skeletal remains. Sex and ancestry may be determined by examination of morphological characteristics of the skeletal material or by performing morphometric analyses using selected skeletal measurements. Morphological analysis is generally applied to unfragmented skeletal remains and relies heavily on the experience of the examiner.

Morphometric analysis, on the other hand, is more objective, repeatable, often requires less technical experience, and approximates or exceeds the success rate of morphological examination. In addition, quantitative analysis often can be performed on fragmented remains making it particularly useful in mass disasters.

For decades, morphometric assessment of sex and ancestry was dominated by studies of the skull and, rarely, the postcrania, using discriminant function analyses of linear measurements. The one-dimensionality of these measurements, however, failed to adequately capture the shape variability that exists in skeletal elements, which are three-dimensional. Recent advances in microcomputers coupled with a powerful new tool, often referred as the "new" or geometric morphometry,

now allow biological size and shape variation to be assessed in two and three dimensions, which previously was not possible.

Although increasingly common in the literature, studies employing geometric morphometry to address questions of group affiliation continue to focus on cranial morphology variability within and among groups. This is not surprising, given the abundance of cranial landmarks and the relative ease in locating them. Postcranial elements have received far less attention, and their usefulness in determining sex and ancestry remains largely unexplored.

This dissertation tests the hypothesis that sex and ancestry differences in shape are present in the scapula and that this variation can be quantified using non-traditional measurements and the "new morphometry." The scapula is particularly amenable to analysis by geometric morphometrics, given its large size, high relief, and irregular, three-dimensional shape. Although relatively fragile and easily broken, in an archaeological or forensic context the scapula typically survives at least as well as many other postcranial elements, few of which have the characteristics best suited for geometric morphometry analysis. Scapular landmarks are recorded in three-dimensional form and analyzed using traditional statistical methods as well as geometric morphometric methods. As with traditional methods of statistical analysis, geometric morphometrics allow absolute size to be compared within and among groups; only geometric morphometry, however, permits absolute size to be removed,

such that only information on shape variation remains. Thin-plate spline and Procrustes analyses, in particular, provide insight into not only the magnitude of variation, but also where it occurs. If geometric morphometry is successful in differentiating between scapulae of different sexes and ancestries, forensic anthropology will have gained a useful tool in developing a biological profile, particularly in instances where skeletal elements that are more traditionally used for determining sex and ancestry are absent.

The following chapters describe the rise of geometric morphometry, its application to this dissertation, the methods employed, the demographics of the sample, and the results of this study. Chapter 2 focuses on a brief history of geometric morphometry, methods associated with it, and its advantages over more traditional methods. Chapter 3 provides a detailed account of early studies of the scapula, osteological landmarks, associated musculature, development, and centers of ossification. A description of the skeletal sample, landmark selection, and data collection protocols are presented in Chapter 4. In Chapter 5, analytical methods employed to assess morphological variability are discussed, and Chapter 6 presents the results of the analyses. Chapter 7 provides a summary of the results and presents conclusions regarding the usefulness of geometric morphometry in assessing sex and ancestry from the scapula.

# CHAPTER 2

## Geometric Morphometry

Morphometry is often described as the investigation of biological change using geometric form or, as Bookstein (1982) describes it, "the fusion of biology and geometry, and statistics." Unlike traditional morphometry, which uses linear measurements to investigate biological change and relationships, geometric morphometry uses multi-dimensional landmark data to express size and shape variation of structures.

Modern geometric morphometry has its roots in two widely divergent methodologies. The multivariate biometric method, which emphasizes the geometry of the covariance matrix over geometric form, originated with Francis Galton, developed by Karl Pearson, and brought into its modern form by Sewall Wright (Bookstein, 1992). The other methodology relies primarily on visualization of changes in biological form. Often attributed to D'Arcy Thompson (1917), this method actually dates to the Renaissance. As with the multivariate biometric method, which lacked visual representation of changes in biological form, this method lacked a testable statistical method.

Attempts to fuse the two seemingly incompatible methods continued through the years, and the two forms finally became united in the late 1970's and 1980's. The key to the combining of the two techniques was the restriction of landmarks to discrete points that were believed to be

homologous from form to form. Statistical analysis of landmark locations was expressible in geometric diagrams that were directly interpretable in the original picture plane. Likewise, results of shape change could be graphically represented through deformation analysis.

The new or geometric morphometry became increasingly popular in the 1990s, when advances in computer technology enabled the management of large data sets, and sophisticated software programs enabled the calculation of two- and three-dimensional landmark data. There are many advantages of using geometric morphometry over traditional morphometrics, including the ability to archive data on size, shape and landmark relationships in a two- or three-dimensional form. Data analyses of such relationships are not possible using traditional methods, which record only linear distances, nor can traditional methods reconstruct interlandmark distances, as geometric morphometry can. Because geometric morphometry can represent shape variation in three dimensions, it can also be used with three-dimensional plotting software that enables landmark coordinates to be scaled and rotated, enabling a visual representation of the structures of interest (Marcus and Corti, 1996). This pictorial representation of the results is one of the primary benefits of geometric morphometry, as it allows change to be evaluated and results to be interpreted more easily than with tables of numerical coefficients. Further, use of homologous landmarks allows for a more complete biological representation of the results. Movement of landmarks relative to one

another can be assessed, rather than simply reporting that shape has changed.

In addition, because geometric morphometry scales the structures in question by removing size, orientation, and location differences leaving only shape differences to be investigated, the coordinate data are more amenable to more traditional multivariate analyses, such as canonical correlation, factor analysis, cluster and principal component analysis, and analysis of variance and covariance (Marcus and Corti, 1996). Existing in two or three dimensions, geometric landmarks enable shape variability to be investigated in all directions, unlike the single dimensionality of linear landmarks. As a result, more powerful statistical methods for detecting shape variation can be employed (Bookstein, 1982).

**Methods of Geometric Morphometry Analysis**

Of the many methods of geometric morphometry analysis, four are most commonly employed. Finite element scaling analysis is one of the earlier methods and uses small closed regions of triangles or tetrahedra to connect landmarks. Each region is then compared to its counterpart in a second organism and displayed as strain crosses that indicate directions and magnitudes of strain within each element. Euclidean distance matrix analysis uses the ratios of landmark distances between two specimens to assess shape change (Lele, 1993). Procrustes analysis is based on the idea that two or more specimens can be overlain, such that this

superimposition allows differences in landmark position to be evaluated graphically. Thin-plate spline analysis, which was originally developed for computer graphics and computational surface theory, maps reference configurations on a Cartesian grid. A more in-depth assessment of these methods follows.

**Finite Element Scaling Analysis**

Finite element scaling analysis (FESA) is an early method of geometric morphometry analysis and uses a series of small closed regions of triangles in two dimensions or tetrahedra in three dimensions to connect homologous landmarks of the form in question. By computing affine (uniform) transformations between corresponding regions, strain crosses are generated within each element or at each landmark that show the direction and magnitude of the principal strains (Cheverud, et al., 1983), and these graphical representations show changes in shape. A major problem with FESA is that the principal strain or the variance of its angle depends on how the organism is divided into elements. As a result, it becomes difficult to recognize uniform shape change. For this reason, FESA is seldom used.

**Euclidean Distance Matrix Analysis**

Euclidean distance matrix analysis (EDMA) compares shapes before they have been scaled by examining the ratios of distances between all pairs of landmarks of two specimens (Lele, 1993; Lele and Richtsmeier, 1991). Two specimens having the same ratios must have the same shape

and vary only in size. Interlandmark distances that are unusually large or unusually small between specimens are shown in lists that are not easy to interpret in terms of shape change. In some applications the method has low statistical power, and although coordinate-free and invariate to rotation and translation, other more widely accepted methods, such as Procrustes analysis and shape coordinates also are coordinate-free. In addition, there is concern that the results could be biased due to the use of a particular coordinate system, even though it may be used only for displaying the results of a statistical analysis (Rohlf and Marcus, 1993). Consequently, EDMA is seldom used in geometric morphometric analyses.

**Procrustes Analysis**

Although seldom cited, Boas (1905) and Phelps (1932) laid the groundwork for later work involving superposition of two-dimensional forms. Most geometric morphometric studies use registration systems, which place organisms into a common frame of reference in order that differences in orientation are not mistaken for biologically meaningful differences in form. Many investigators, however, argue that arbitrarily chosen points of reference, such as porion and orbitale in the Frankfurt Horizontal that permit comparisons of human skull form, may lead to differences in interpretation regarding differences and variations in form. Boas further recognized that other points may be as biologically significant as porion and orbitale, and

that there was no justification in selecting only two points and disregarding all others.

Despite publication in major journals, Boas' work lapsed into obscurity. It has been speculated that firm adherence to the typological approach of cranial variation by anthropologists rather than embracing statistical craniometrics caused it to fall from favor (Cole, 1996). An early proponent of what would later become known as Procrustes analysis, Phelps (1932) revived the Boas data and used distance measures to quantify differences in form (Cole, 1996).

Sneath (1967) investigated the problem of optimal translation, which involves the fitting of a model that describes the differences between two organisms while taking into account differences in rotation, translation, and scale. Essentially, this involves the superimposition of one organism on top of the other so that corresponding landmarks align as closely as possible. Differences in alignment are then shown as differences in shape, as represented by the residuals (Cole, 1996).

Further work by Gower (1975) produced an algebraic method of superimposition using least squares, which, although appealing, resulted in a general lack of fit at most points even when the forms being compared were identical except for a few landmarks. Siegel and Benson's (1982) resistant-fit method largely resolved this problem by adopting a nonparametric analog of least squares regression. This method allows differences in two organisms to be revealed more accurately, particularly

when the major differences are limited to the relative positions of a few landmarks. Later work by Gower (1975) extended Procrustes methods to include any number of objects. More recently, Goodall (1991) extended Procrustes analysis by developing the F ratio and Hotelling's $T^2$ tests. Bookstein (1996) states that Procrustes analysis combines all the tools of geometric morphometrics and insists that it should be the "sole statistically meaningful shape distance for landmark data...". Today, virtually all landmark-based geometric morphometry studies use Procrustes analysis to analyze shape.

**Thin-plate Spline Analysis**

Thin-plate spline analysis has its origins in Renaissance art but is generally associated with Thompson's (1917) concept of Cartesian transformation, which depicts the shape of an organism as a distortion in the shape of a reference organism. With this method, a Cartesian coordinate grid is placed over the organism and both organism and grid are distorted until the form of the second organism is achieved. Shape differences between the two organisms are shown by distortions of the grid. Although visually simple, the method was never fully described in a way that it could be repeated, and it failed to provide a statistical method.

In 1981, Bookstein incorporated methods of continuum mechanics with Thompson's Cartesian transformation grids as a way to bring statistical methods to bear on visualization. Thin-plate spline analysis maps all points

in the reference specimen (usually the mean of the sample) onto corresponding points on the target specimen (Bookstein, 1991). Initially, the two specimens are superimposed, removing differences in size and orientation by using shape coordinates. Using two baseline coordinates, the superimposed landmarks are recalculated relative to the baseline, resulting in a set of shape coordinates that contain morphometric information regarding size and shape, and are independent of the baseline (Bookstein, 1991). To obtain information on shape change, bending of the objects to the thin-plate spline transformation is measured, with small changes requiring less bending energy than large changes.

**Anthropological Applications**

Early applications of geometric morphometry to anthropological research focused on craniometric variation. The skull is particularly amenable to analysis, given its preponderance of easily located and traditional Type 1 landmarks. As defined by Bookstein (1986, 1990, 1991), Type 1 landmarks are generally located at the intersections of sutures or other distinct boundaries and represent recognizable points located between areas of distinct histology. True homologues, Type 1 landmarks are readily distinguishable and thus permit a more accurate baseline for subsequent analysis.

One of the earliest software programs examining three-dimensional coordinates was Benfer's (1975) SKULL, which used coordinate data to

examine variation in the height and breadth of the skull. Triangulation of Cartesian coordinates combined with principal component analysis allowed Benfer to observe morphological variation among crania. Additional studies using geometric morphometrics to compare crania have focused on answering questions of skull deformation (Cheverud et al., 1992), sexual dimorphism (O'Higgins and Dryden, 1993; Lynch et al., 1996; Wood and Lynch, 1996), racial affinity variation (Ross et al., 1999), and allometric growth (O'Higgins and Vidarsdottir, 1999).

To date, few studies have focused on the use of geometric morphometric analysis of the postcrania. Unlike the skull, which has an abundance of Type 1 landmarks, most postcranial landmarks are Type 2, which are local geometric features of extended tissue boundaries (Bookstein, 1990), or Type 3, described as extreme points along a linear dimension of the form (Bookstein, 1990). Although not as useful as Type 1 landmarks, Type 2 and 3 landmarks still can be used to assess variation in shape among objects.

More recently, geometric morphometry has been used to investigate differences in postcranial elements. Using Procrustes analysis of 14 two-dimensional landmarks on the distal humerus of Pliocene and recent hominids, Bacon (2000) found no clear affinity between KNM-KP 271 and modern *Homo*, nor with *Australopithecus afarensis*, as had been previously demonstrated.

Similarly, a phalanx from the Lower Pleistocene site of Cueva Victoria in Murcia, Spain was analyzed using principal and relative warp analyses as well as Fourier analysis to compare it with human, gorilla, and cercopithecid phalanges (Palmqvist et al., 1996). Results of the analyses indicated that the fossil phalanx was of human origin and suggested the presence of *Homo* in the southern Iberian Peninsula during the Lower Pleistocene.

Although geometric morphometry has shown its usefulness in answering questions involving cranial morphology, its use in the postcrania has languished. Nevertheless, shape variation in the postcrania is known to exist and may be best quantified by using geometric morphometry rather than more traditional methods of measurement.

# CHAPTER 3

# The Scapula

## Previous Research

The scapula, which comprises a major part of the pectoral girdle, has received considerable attention regarding the determination of age, racial affinity, sex, and stature. Early works by Broca (1878) focused on measurement of the scapula, particularly scapular height, scapular breadth, and infraspinous height. These measurements were used to measure primates, lower mammals, and children, adolescents, and adults of several nationalities. Later works by Livon (1879), Flower (1879), Turner (1886), Dwight (1887), Mendes-Corrêa (1919), Graves (1921, 1922, 1939), and Frey (1923) expanded Broca's sample to include other groups. These early works were often largely descriptive and primarily gave scapular measurements for certain groups. Others reported "racial" differences in scapular dimensions, which were suggested by variation in absolute and relative dimensions and variability in scapular indices.

Vallois (1924, 1926a, 1926b, 1927, 1928) made the first extensive study of the scapula. Following the tradition of the time, he compared measurements of humans to scapulae of other primates and proposed "racial" classifications based on scapular measurements and indices. In addition, he measured the scapulae of 20 fetuses and 32 children from birth

to ten years of age. Certain morphological traits, such as Vallois' classification of the spine of the scapula, were used to assign scapulae to various groups.

Similarly, Hrdlička (1942a, 1942b, 1942c) reported on traits such as the shape of the vertebral border and superior borders, the shape of the scapular notch, and their frequencies among various groups. Hrdlička (1942a) recognized that the scapulae "...phylogenetically is almost entirely a muscular product, aside of its articular parts is completely dependent on the development and activity of its muscles, and in response to these, at all times of its existence, is adaptable in shape, size, strength, and most other conditions." Hrdlička (1942a) and Wolffson (1950) realized that the genetic form of the scapula was modified by biomechanical stresses and that classifications of the shape of the vertebral border, inferior angle, and scapular notch actually existed as a continuum, thus precluding distinct categories.

Scapular measurements have been used in predicting sex. Both Broca (1878) and Hrdlička (1942a) reported that in most groups female scapular indices were greater than males, suggesting that female scapulae were not only absolutely shorter but also relatively shorter than males and more closely approximated those of juveniles. Hrdlička (1942a) reported that although differences in frequencies of morphological traits, such as the shape of the vertebral border, the shape of the superior border, and the shape of the scapular notch exist, they were not great enough to accurately

assign sex. Dwight (1905) stated that in addition to maximum length of the scapula, the length of the glenoid cavity between the supraglenoid tubercle and the most inferior point on the articular margin could be used to discriminate between males and females.

More recently, discriminant function analysis of the length of the spine of the scapula and the length of the glenoid cavity yielded correct sexing of over 97% in Chinese adults (Ren, 1987). Similarly, discriminant function analysis of the length of the glenoid cavity, maximum distance from the acromion to the coracoid process, and maximum length of the coracoid process correctly sexed 95% of a sample of southern Italians (Di Vella et al., 1994). Murphy (1995) used discriminant function analysis of the maximum height of the glenoid cavity and the maximum breadth of the glenoid cavity to obtain an expected accuracy of nearly 94% in a series of prehistoric New Zealand Polynesian scapulae. Stewart (1979) found that 79% of a sample of American blacks and whites could be correctly sexed using the maximum length of the scapula. Bainbridge and Tarazaga (1956), finding morphological traits of the scapula of limited use in determining sex, used a series of measurements to sex scapulae. Other researchers have also observed sexual dimorphism of the scapula (Olivier and Pineau, 1957; Hanihara, 1959; Iordanidis, 1961; Hojo, 1970; Guangjin, 1982; Sun, 1986; Sun, 1986; Penning and Müller, 1988).

As with other skeletal elements, scapulae have been studied for aging techniques. The acromion, coracoid process, glenoid cavity, part of

the neck, the vertebral border, and the inferior angle begin ossification during the third intrauterine month and become recognizable by the fourth month (Fazekas and Kosa, 1978; but see Last, 1973; Birkner, 1978; Basmajian and Slonecker, 1989). Generally, the epiphyses begin to unite in childhood and are completely fused by the 23rd year (Stevenson, 1924; McKern and Stewart, 1957; Krogman, 1962). Following epiphyseal fusion, age changes are manifested in marginal lipping of the acromial facet and glenoid cavity, but the onset of lipping is too variable to be used for anything but supporting evidence of age (McKern and Stewart, 1957). In older adults, reduced vascularity resulting from bone resorption may produce atrophic spots or even holes in the body of the scapula (Graves, 1922). In addition, bone thinning may accentuate lateral lines or even produce pleating or buckling of the scapula but, as with marginal lipping, these changes should only be used as supporting evidence of age. Similarly, it has been suggested that acromial morphology may change from Type I (flat) to Type III (hooked) with age (Wang and Shapiro, 1979; Barnett et al., 1995; MacGillivray et al., 1998; but see Getz et al., 1993; Nicholson et al., 1996).

Measurements of the scapula have been used in stature estimations, albeit with mixed results (Peng, 1983; Shulin and Fangwu, 1983; Campobasso et al., 1998).

## Scapular Morphology

The pectoral girdle is composed of the clavicle, which articulates medially with the manubrium and laterally with the scapula, and the scapula, which articulates with the humerus. Thus, the pectoral girdle articulates with the axial skeleton laterally, and without a corresponding articulation with the vertebral column. The clavicle is relatively immobile and serves primarily to brace the arm to the thorax; the scapula, however, is more mobile than any other joint (Peat, 1986), owing to its attachment to the thorax by ligaments and muscles. This arrangement permits power to be generated in the upper limb, yet allows sufficient mobility for grasping and manipulative activities.

Although the basic morphology of the pectoral girdle is similar among mammals, human bipedality has caused modifications in the function and morphology of the scapula and clavicle. Only humans and apes have a robust attachment of the clavicle to the sternum. This arrangement provides stability to the sternoclavicular joint, and increases pectoral mobility through lateral displacement of the shoulder joint (Steele and Bramblett, 1988).

The spade-like appearance of the scapula is believed to responsible for its name, since 'skapto' means 'I dig' in Greek (Field and Harrison, 1957). Classified as a flat bone, the scapula articulates with the clavicle at the acromioclavicular joint and the humerus at the glenohumeral joint. The scapula is isolated from the vertebral column and ribs by extensive musculature, which cushions it from shock and reduces the frequency of fractures (Rowe, 1968; Wilber and Evans, 1977; Hollinshead, 1982).

The function of the scapula is to articulate with the upper arm and secondarily to provide a platform for muscle attachment to increase mobility and power of the joint (Anetzberger and Putz, 1996). Despite its size, the scapula is often so thin that it is translucent (Steele and Bramblett, 1988) and often does not survive in an archaeological or forensic context. Surprisingly, it is rarely injured, (Rowe, 1968; Heyse-Moore and Stoker, 1982; Hollinshead, 1982), and when fractures do occur they are typically associated with trauma to other parts of the body (Imatani, 1975; McGahan et al., 1980; Thompson et al., 1985; Ada and Miller, 1991; Gupta et al., 1998).

The scapula is essentially triangular in shape and is characterized by a number of borders, angles, surfaces, and projections for muscle attachment (Figure 3.1). The shortest of the three borders, the superior border runs between the superior angle and the base of the coracoid process (Kuhns, 1945). The suprascapular notch lies adjacent to the coracoid process on the superior border and varies in shape from a shallow depression to a foramen (Hrdlička, 1942a). The suprascapular nerve traverses the notch, and conversion of the notch to a foramen has been shown to cause impingement of the nerve and corresponding weakness in abduction and rotation (Van Dongen, 1963; McClure and Raney, 1975; Rengachary et al., 1979; Ganzhorn et al., 1981; Garcia and McQueen, 1981; Pate et al., 1985; Edelson, 1995a ).

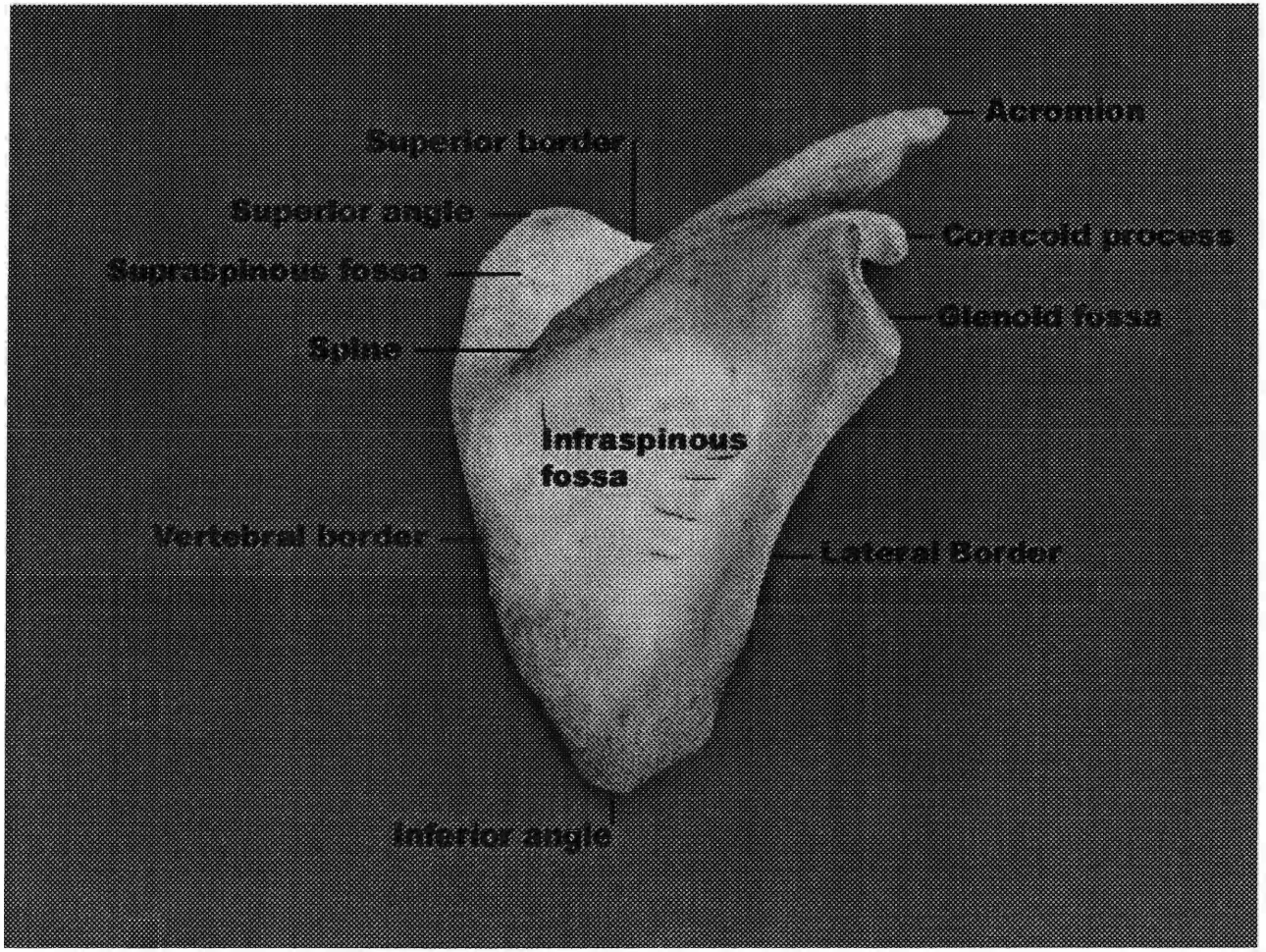



Figure 3.1. Adult scapular morphology (right scapula, dorsal view).

The vertebral border (Figure 3.1), which lies between the superior and inferior angles, is typically slightly convex and lies adjacent to thoracic vertebrae 2-7 (McMinn and Hutchings, 1977). The border superior of the scapular spine serves as the attachment point for the levator scapulae muscle (Figure 3.2). Slightly inferior to the scapular spine is the site of attachment for the rhomboid minor muscle, and the bottom two-thirds of the border serves as the attachment for the rhomboid major muscle (Stone and Stone, 1997). Acting in concert, the rhomboids and levator scapulae muscles suspend the scapula from the vertebral column as well as elevate and retract it during manipulative activities (Stone and Stone, 1997).

The lateral border (Figure 3.4) is composed of a thickened bar of bone and runs between the inferior angle and the inferior glenoid cavity. Slightly concave, the lateral border is the site of attachment for the long head of the triceps brachii muscle inferior to the glenoid, the teres minor and teres major, and the latissimus dorsi near the inferior angle (Figure 3.2). These muscles are primarily responsible for rotation and adduction, and extension of the arm (Stone and Stone, 1997). In Neanderthals, the presence of a dorsal sulcus on the lateral border has been viewed as evidence for a larger attachment area for the teres minor than that found in modern humans (Aiello and Dean, 1990). Alternatively, some believe that the dorsal sulcus arose in response to resisting dorsoventral bending movements (Churchill and Trinkaus, 1990), or biomechanical stress (Moran and Chamberlain, 1997).

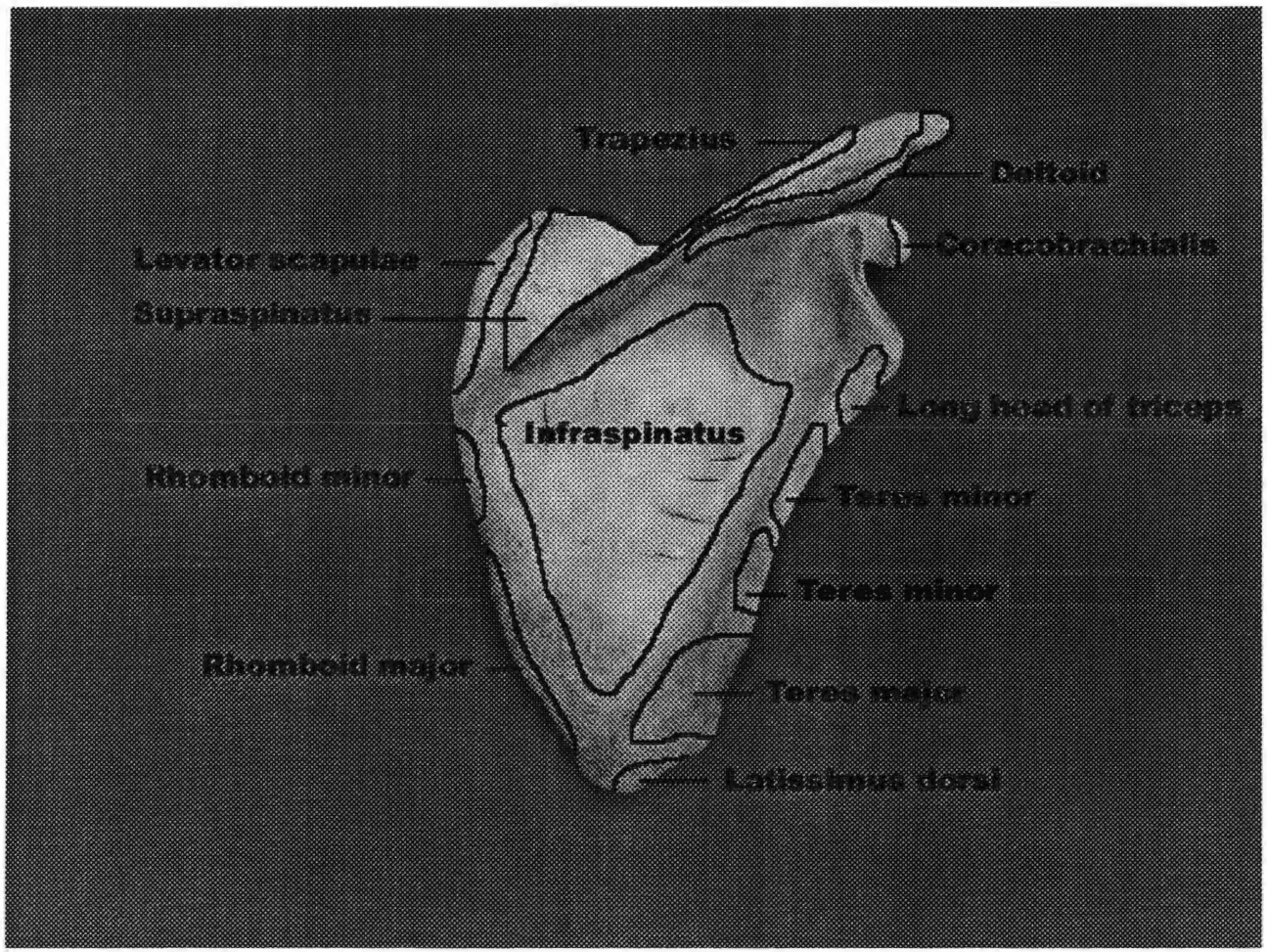



Figure 3.2. Muscle attachments of the scapula (right scapula, dorsal view).

The superior angle (Figure 3.1), which is formed by the intersection of the superior and vertebral borders, serves as the site of muscle attachment for the serratus anterior on the ventral side (Figure 3.3) and the levator scapulae on the dorsal side (Figure 3.2). The serratus anterior is responsible for rotation of the scapula for abduction and flexion of the arm and protraction of the scapula (McMinn and Hutchings, 1977). The levator scapulae muscle elevates the medial border of the scapulae and acts in concert with the trapezius and rhomboids to pull the scapula medially and upward.

The inferior angle (Figure 3.1) is formed by the intersection of the medial and lateral borders and lies adjacent to the seventh rib. The inferior angle is the site of attachment of the serratus anterior (Figure 3.3) and latissimus dorsi (Figure 3.2) muscles. Rarely, a costal facet appears on the ventral surface (Gray, 1942; Bainbridge and Tarazaga, 1956), and a separate infrascapular bone has been reported (McClure and Raney, 1974), although it typically fuses with the body of the scapula by age 20 (Keats, 1992).

The lateral angle is formed by the glenoid cavity and the neck of the scapula (McMinn and Hutchings, 1977). The glenoid cavity (Figure 3.1) is usually pear-shaped, lined with hyaline cartilage, and is concave (but see Brailsford, 1953) within the synovial capsule to accept the convex head of the humerus. The glenoid cavity is further deepened by the presence of the glenoidal labrum, which is thinnest at the center and thicker near the

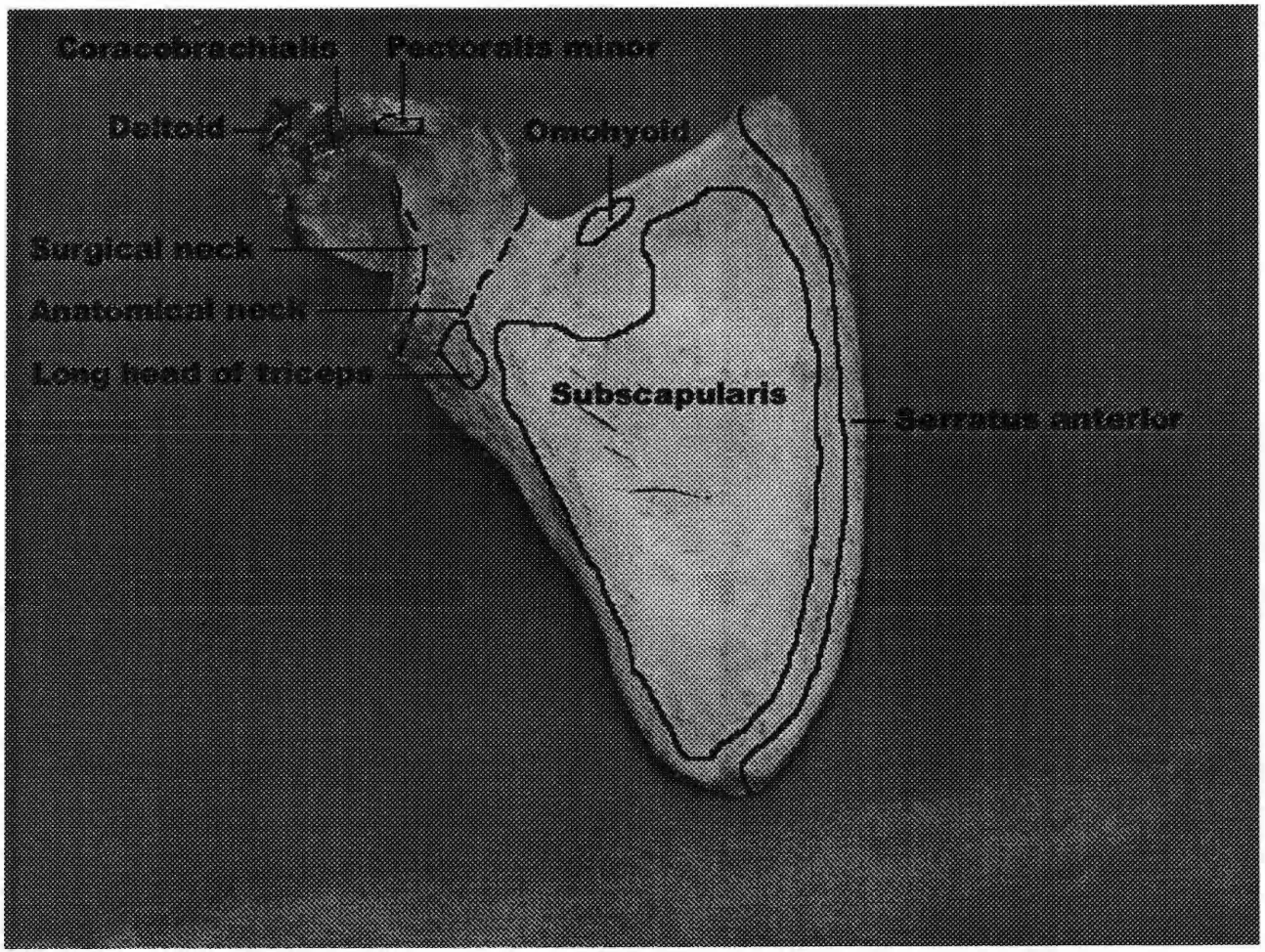



Figure 3.3. Muscle attachments of the scapula (right scapula, ventral view).

periphery of the joint. It tapers in diameter toward the supraglenoid tubercle (Gray, 1942), which is the site of attachment of the long head of the triceps brachii (Figure 3.4) (Vangsness et al., 1994), and a small notch is often present on the rim. The glenoid notch is believed to arise in response to pressure exerted by the tendon of the subscapularis muscle (Martin, 1933; Miles, 1997; Prescher and Klümpen, 1997). The joint is typically weak, owing to the fact that the humerus is held in place only by the tendons of muscles forming the rotator cuff, the supraspinatus, infraspinatus, subscapularis, and teres minor muscles (Figure 3.2, 3.3). Although this arrangement allows for maximum mobility of the joint, the tradeoff is a relatively unstable joint that is subject to injury and dislocation, which frequently occurs at the inferior aspect where musculature is weakest (Kanagasuntheram et al., 1987; Carola et al., 1992). The weakness of the joint also accounts for markers of occupational stress on the glenoid cavity, such as a supraglenoid facet, often associated with migrant citrus labor (Wienker and Wood, 1988).

The ventral surface of the scapula (Figure 3.3) is concave both laterally and superior-inferiorly due to a bending of the upper third at approximately the level of the scapular spine and a buttressing of bone along the lateral border. This buildup of bone is believed to be reinforcement against the strong musculature of the deltoid and serratus anterior (Anetzberger and Putz, 1996). The subscapularis muscle, which medially rotates the arm and stabilizes the glenohumeral joint, covers the

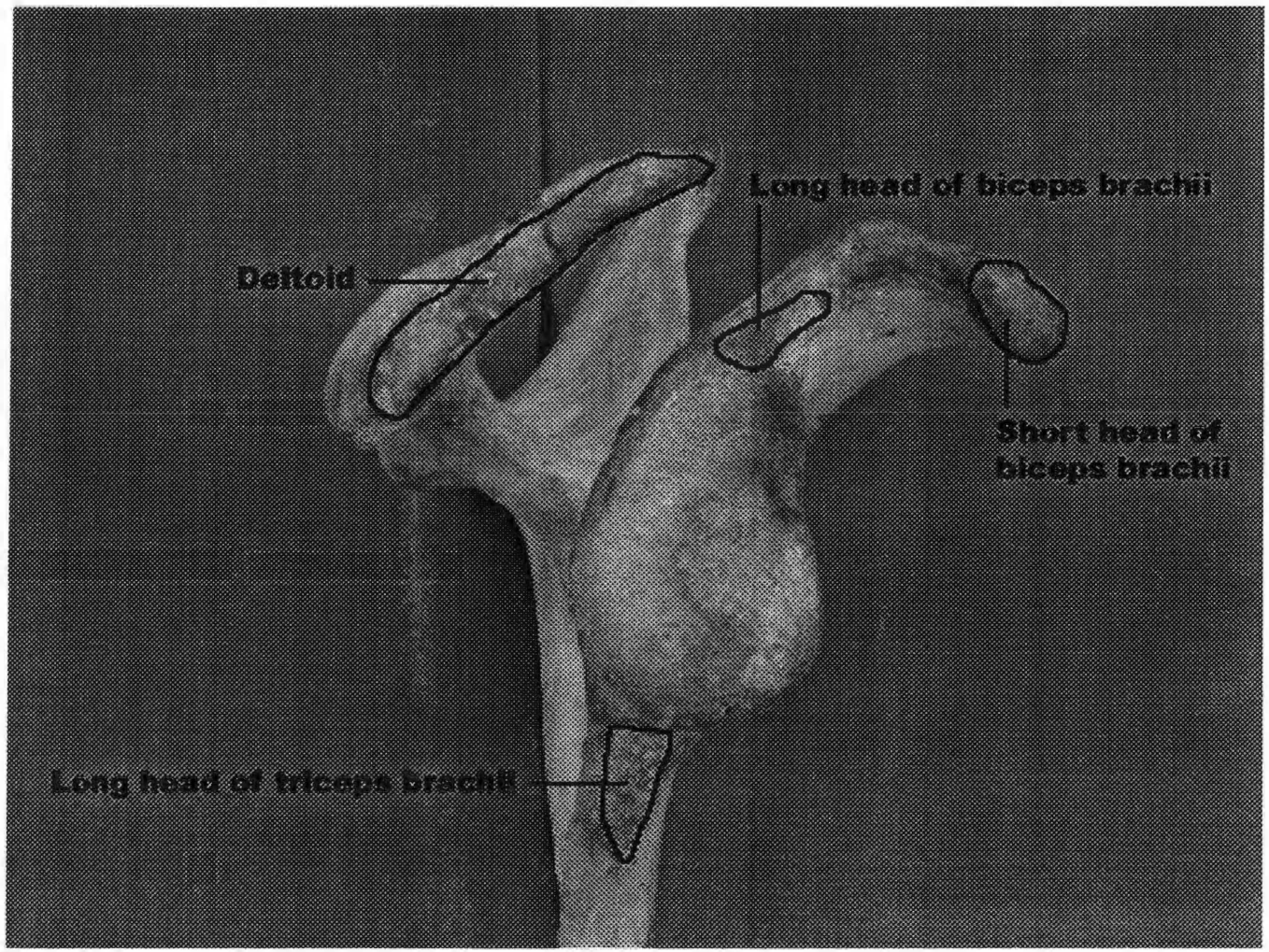



Figure 3.4. Muscle attachments of the scapula (right scapula, lateral view).

majority of the ventral surface of the scapula, attaching along the lateral border and the body by way of intramuscular tendons (Stone and Stone, 1997).

The scapular spine divides the dorsal surface of the scapula into a large infraspinous fossa and a smaller supraspinous fossa (Figure 3.1). The supraspinatus muscle is confined to the supraspinous fossa and spine except for the tendon, which is routed under the acromion and inserts on the greater tubercle of the humerus. Easily injured, the tendon of the supraspinatus can contribute to calcification of the subacromial bursa causing painful abduction of the arm at the shoulder (Kanagasuntheram et al., 1987). Medial to the glenoid cavity in the supraspinous fossa, a large nutrient foramen (Figure 3.5) serves as a conduit for the suprascapular artery, which provides blood to the spine of the scapula (Gray, 1942; Brookes and Revell, 1998). Additional vessels feed both the supraspinous and infraspinous fossas by going underneath the spinoglenoid ligament. Impingement of this ligament is known to cause nerve entrapment and subsequent reduction in mobility (Cummins et al. 1998).

The infraspinous fossa (Figure 3.1) is curved, concave inferior to the spine and convex laterally. The infraspinatus muscle (Figure 3.2) occupies the majority of the fossa and inserts at the middle facet of the greater tuberosity of the humerus (McMinn and Hutchings, 1977). The infraspinatus is particularly important in that it draws the humerus toward the glenoid fossa and thus resists posterior dislocation of the arm (Stone and

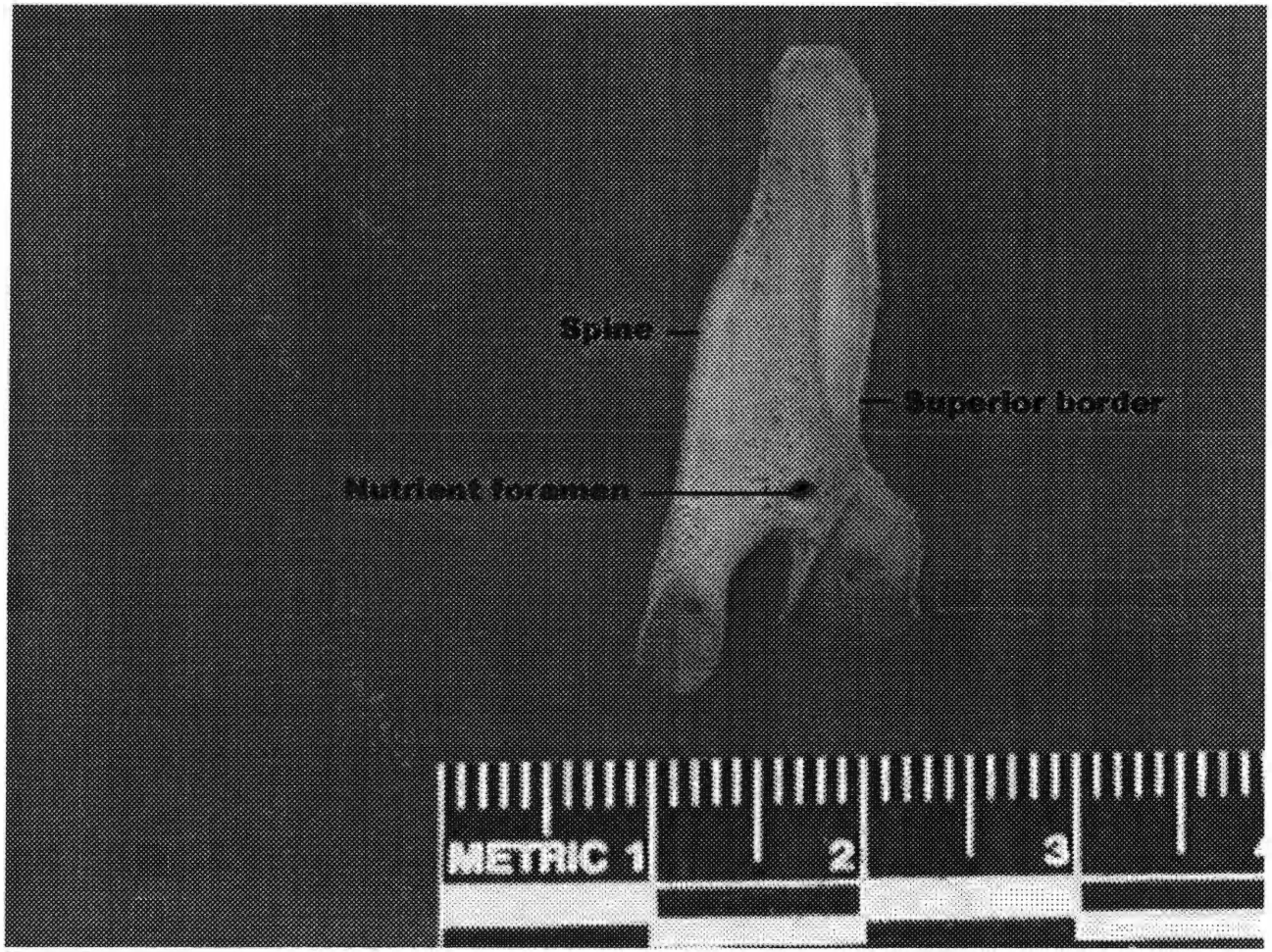



Figure 3.5. Scapula of neonate showing nutrient foramen (right scapula, superior view).

Stone, 1997). Both the teres minor and teres major have their origins on the lateral border of the infraspinous fossa (Figure 3.2).

Located on the dorsal surface of the scapula at the level of the third thoracic vertebra, the spine extends from the upper third of the vertebral border, angles superio-laterally across the width of the scapula, and terminates at the spinoglenoid notch (McMinn and Hutchings, 1977). At its lateral extremity, the margin of the spine turns superiorly and parallels the medial border of the supraspinous fossa. The superior border curves to become the medial border of the acromion (Figure 3.1), while the inferior border flares at the deltoid tubercle before extending laterally to become the lateral border of the acromion. The superior and inferior borders of the spine diverge at the medial border, forming a triangular area that is the site of attachment of the rhomboid minor muscle (Cartmill et al., 1987).

The acromion, which derives its name from the Greek *'acros'*, meaning top, is a flared lateral extension of the spine of the scapula that is located above the glenohumeral joint. Often classified as triangular, falciform, or quadrate (Macalister, 1893; Gray, 1942; Hrdlička, 1942a; Bainbridge and Tarazaga, 1956; Jacobson et al., 1995; Vanarthos and Monu, 1995; Yazici et al., 1995; Bright et al., 1997; Chambler and Emery, 1997; Zuckerman et al., 1997), acromial shape exists as a continuum and shapes grade into each other. Along with the coracoid process, the acromion forms a partial cup to prevent dislocation of the shoulder. The acromion has received much attention in recent years, particularly in regard

to its shape when relieved of stress. Howell (1917) observed morphological abnormalities of the acromion, coracoid, spine, and borders of dog scapulae when relieved of muscular forces. These abnormalities were induced by muscular hypofunction during the developmental phase of the scapula. Similarly, Riesenfeld (1966) reported a decrease in scapular breadth and an increase in scapular length when muscular hypofunction was experimentally induced in rats, as did Doyle (1976). This osteological response to reduction in associated musculature is termed the 'law of antagonistic expression.' Similar responses of the scapulae are believed to exist in humans.

The superior surface of the acromion is roughened and exhibits at least four laterally-extending ridges called the 'acromial rete' (Frazer, 1948) that serve as attachment points for the deltoid muscle. The inferior acromion, in contrast, is relatively smooth, owing to its proximity to the subacromial bursa, although it is roughened at the tip and along the medial margin for attachment of the coraco-acromial ligament (Wood Jones, 1953; Miles, 1998). It is believed that the tip of the acromion can adopt a "hooked" appearance with age as a result of calcification of the coraco-acromial ligament (Edelson 1995b, 1996; MacGillivray et al., 1998; but see Getz et al., 1996; Nicholson eteal., 1996).

The acromioclavicular joint (Figure 3.6) is the articulation between the scapula and the clavicle and is located on the medial aspect of the acromion. Due to its primary function of buttressing the pectoral girdle, movement is limited (de Palma, 1957; Kapandji, 1974). Upward

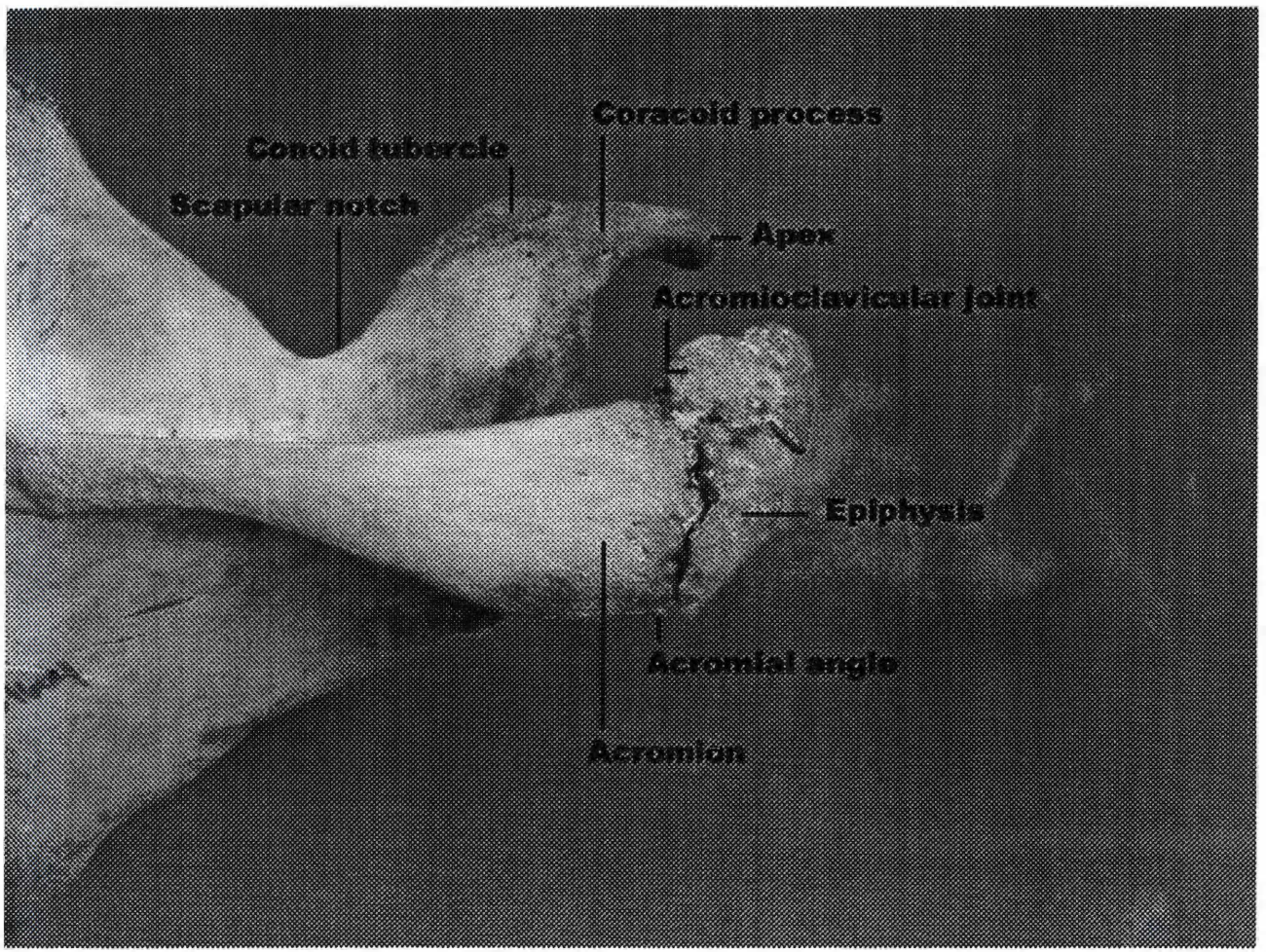



Figure 3.6. Epiphyseal fusion of the acromion (ca. 16 years, right scapula, dorsal view).

displacement of the humeral head that ruptures the supraspinatus tendon may cause a small accessory facet on the inferior acromion (Wilson and Duff, 1943; Weiner and McNab, 1970; Finnegan, 1978; Ozaki et al., 1988; Ulthoff et al., 1988; Ogata and Ulthoff, 1990; Patte, 1990; Williams et al., 1995; Miles, 1996, 1999).

The deltoid muscle (Figure 3.2) originates at the lateral end of the clavicle, crosses the anterior, lateral, and posterior borders of the acromion, continues along the inferior border of the scapular spine, and terminates at the deltoid tuberosity of the humerus (McMinn and Hutchings, 1977). The anterior portions of the deltoid are responsible for the flexion and medial rotation of the arm (Kumar et al., 1997). The medial portion abducts the arm, and the posterior portion extends and laterally rotates the arm (Cartmill et al., 1987). The middle fibers of the trapezius also have their insertion on the acromion and the crest of the spine of the scapula, and the lower fibers insert at the deltoid tubercle of the spine of the scapula (Stone and Stone, 1997; Gumina et al., 1999).

The coracoid process (Figure 3.1) lies ventral to the acromion and extends laterally from the superior border of the scapula. The base of the coracoid process extends from the supraglenoid tubercle to the lateral border of the suprascapular notch. Rising vertically from its base, the coronoid process bends laterally at the coracoid tubercle and terminates at the tip, which is slightly inferior to the process (McMinn and Hutchings, 1977). As with the acromion, the inferior surface of the coracoid process is

smooth, due to the underlying subcoracoid bursa, while the superior surface is roughened (Scheurer and Black, 2000). Muscle and ligament attachment to the superior surface aids in stability of the joint. The coracoclavicular ligament, comprised of the conoid ligament and trapezoid ligament, brace the inferior side of the clavicle and strengthen the joint. The ligament is stronger than the clavicle itself, such that a fall on the shoulder is more likely to break the clavicle than tear the ligaments (Cartmill et al., 1987). Replacement of the ligament by bone or an articulation has been observed (Anderson, 1891; Gowland, 1915; Gradoyevitch, 1939). The coracoacromial ligament, which has its origin along the lateral border of the coracoid process, serves to prevent upward dislocation of the humerus, and the coracohumeral ligament supports the superior aspect of the head of the humerus. The insertion of the pectoralis minor, which raises the ribs in forced respiration, is on the anterior surface of the coracoid process, as is the origin of the coracobrachialis, which weakly adducts the arm (Stone and Stone, 1997).

Due to protection by the overlying clavicle and acromion, fractures of the coracoid process are uncommon (Hollinshead, 1982). Repeated trauma to the pectoralis minor, coracobrachialis, and biceps brachii muscles, however, can induce fracturing (Boyer, 1975). Deformities of the scapula are similarly rare, the most common being Sprengel's deformity, which is the failure of one or both scapulae to descend to normal height, and often retaining its fetal form (Livingstone, 1937; McClure and Raney, 1975). The

etiology is uncertain but is believed to have a genetic component (Tachdjian, 1972).

**Ossification of the Scapula**

Ossification of the scapula is believed to originate from perichondrium located in the surgical neck during the second fetal month (Last, 1973; Birkner, 1978; Basmajian and Slonecker, 1989). The presence of a large nutrient foramen located in the supraspinous fossa medial to the glenoid fossa (Figure 3.5) corresponds closely to the site of ossification (Scheurer and Black, 2000). It is believed that the suprascapular artery, which traverses this foramen, serves as the principal source of blood flow to the primary center of ossification.

Ossification at the site spreads laterally and medially, reaching the spine of the scapula by the ninth week and the glenoid by week 12 (Ogden and Phillips, 1983). Ossification proceeds in a fan- or cone-shaped fashion with vertebral ossification proceeding faster than glenoid ossification, resulting in greater expansion of the vertebral border compared to the glenoid (Ogden and Phillips, 1983). Intramembranous ossification fills the spaces between the two cones, and by 12-14 fetal weeks its characteristic shape is achieved (Fazekas and Kosa, 1978; Ogden and Phillips, 1983). At birth, the scapula differs markedly from its adult form (Figure 3.7) (Elmiger, 1966). The superior border is often scalloped and the vertebral border broadly convex (Figure 3.8, 3.9). The supraspinous and infraspinous

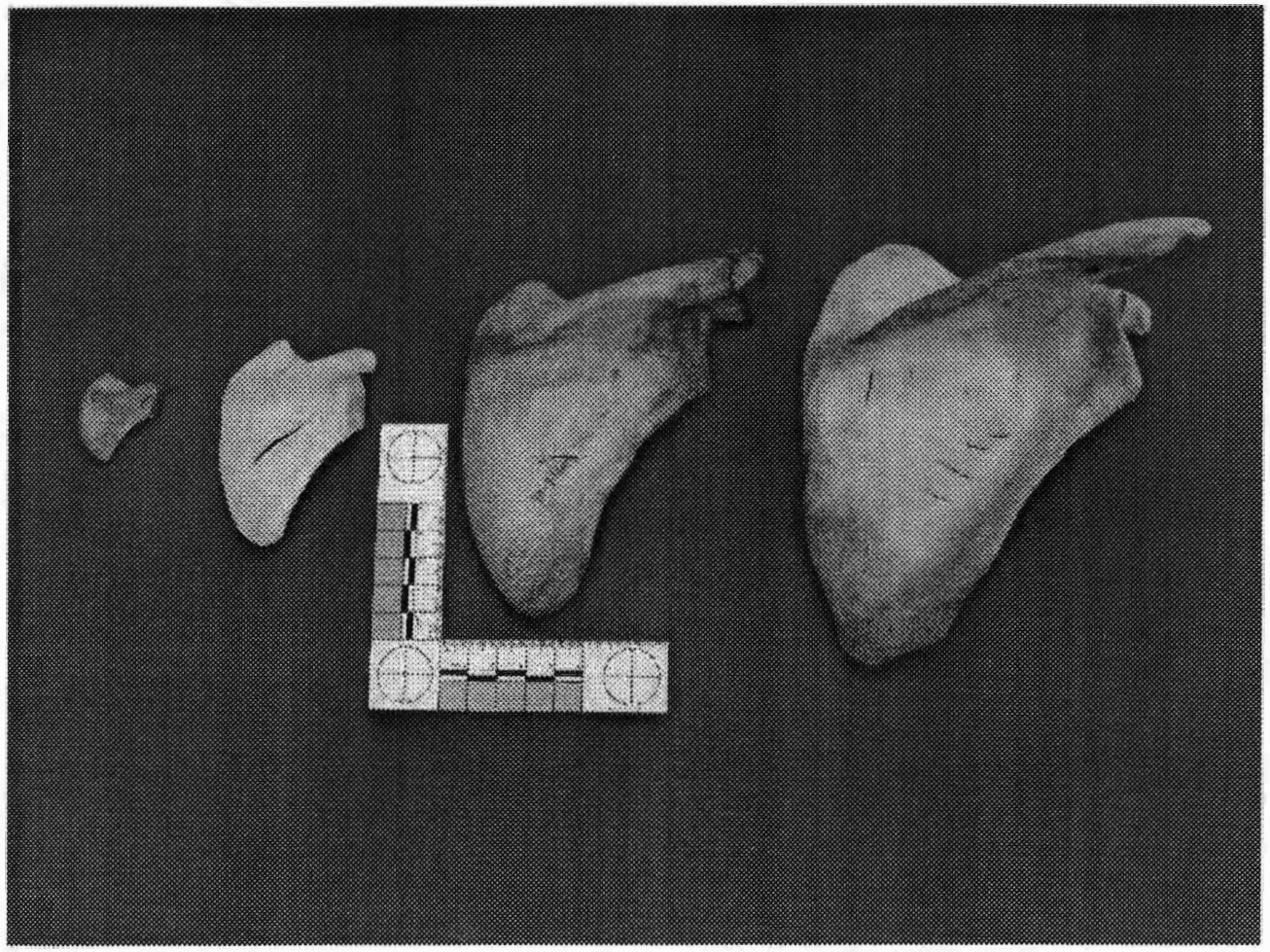


Figure 3.7. Growth and morphological change of the scapula.
From left: neonate, ca. 6 years, ca. 16 years, adult (right scapulae, dorsal view).

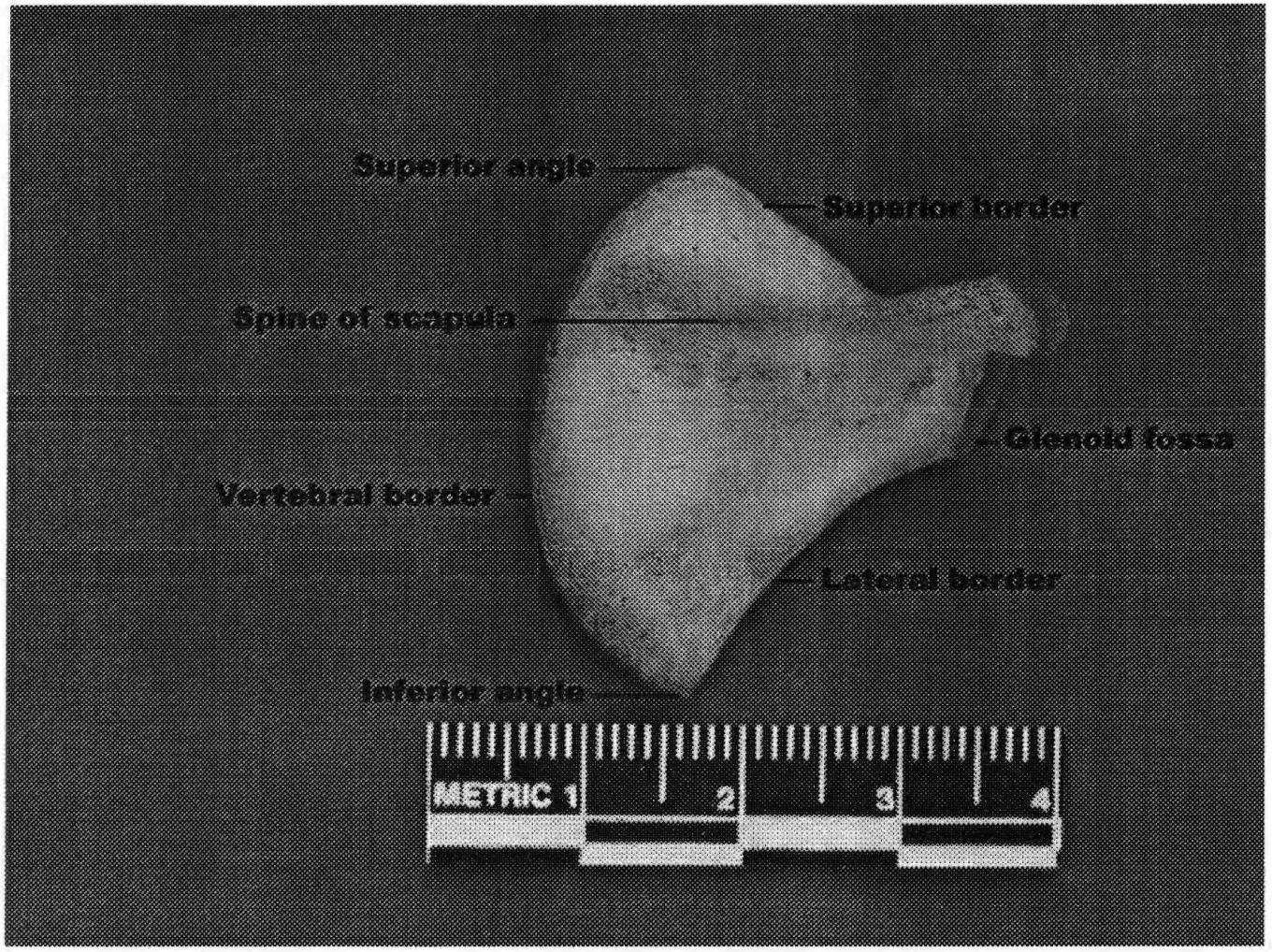



Figure 3.8. Neonate scapular morphology (right scapula, dorsal view).

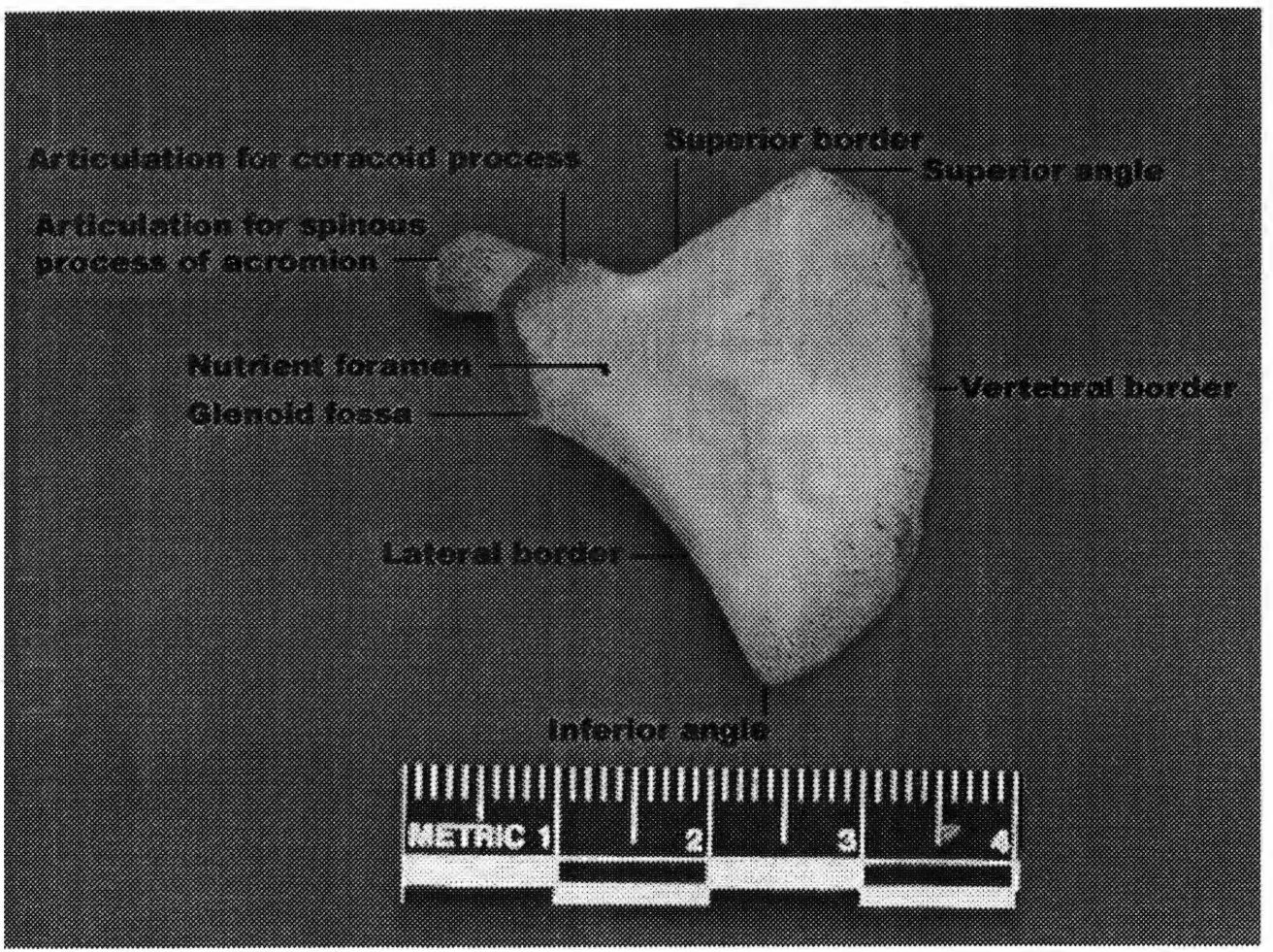



Figure 3.9. Neonate scapular morphology (right scapula, ventral view).

fossas are relatively flat, not having achieved their curved adult forms. The most lateral extension of the spine flares for articulation of the acromion and a flattened area superior and medial to the glenoid fossa marks the attachment of the coracoid process (Figure 3.10), both of which are still cartilaginous. Unlike the adult form, the neonate glenoid fossa is oval and flat or convex (Figure 3.10), and the scapular foramina are more conspicuous. The medial border, inferior angle, and glenoid fossa are cartilaginous (Frazer, 1948; Last, 1973).

The primary center for ossification of the coracoid process (Figure 3.11) is believed to be located near the middle of the process, and growth proceeds toward the scapula. It is believed to form during the first year of life (Girdnay and Golden, 1952; Birkner, 1978; Ogden and Phillips, 1983), and is always present by the second year (Cohn, 1921). A growth plate develops during the second year at the scapular and coracoid surfaces and fusion occurs at approximately 14-15 years of age (Stevenson, 1924).

Isolated ossification centers for the glenoid circumscribe the lower periphery of the rim of the glenoid fossa (Figure 3.12), forming at approximately age 14 to 15 years of age (Birkner, 1978). These centers of ossification begin to spread and eventually unite and attach to the lower portion of the glenoid cavity. Continuing growth permits attachment to the overlying subcoracoid center of ossification. From the periphery of the glenoid, the forming epiphysis then spreads toward the center of the glenoid,

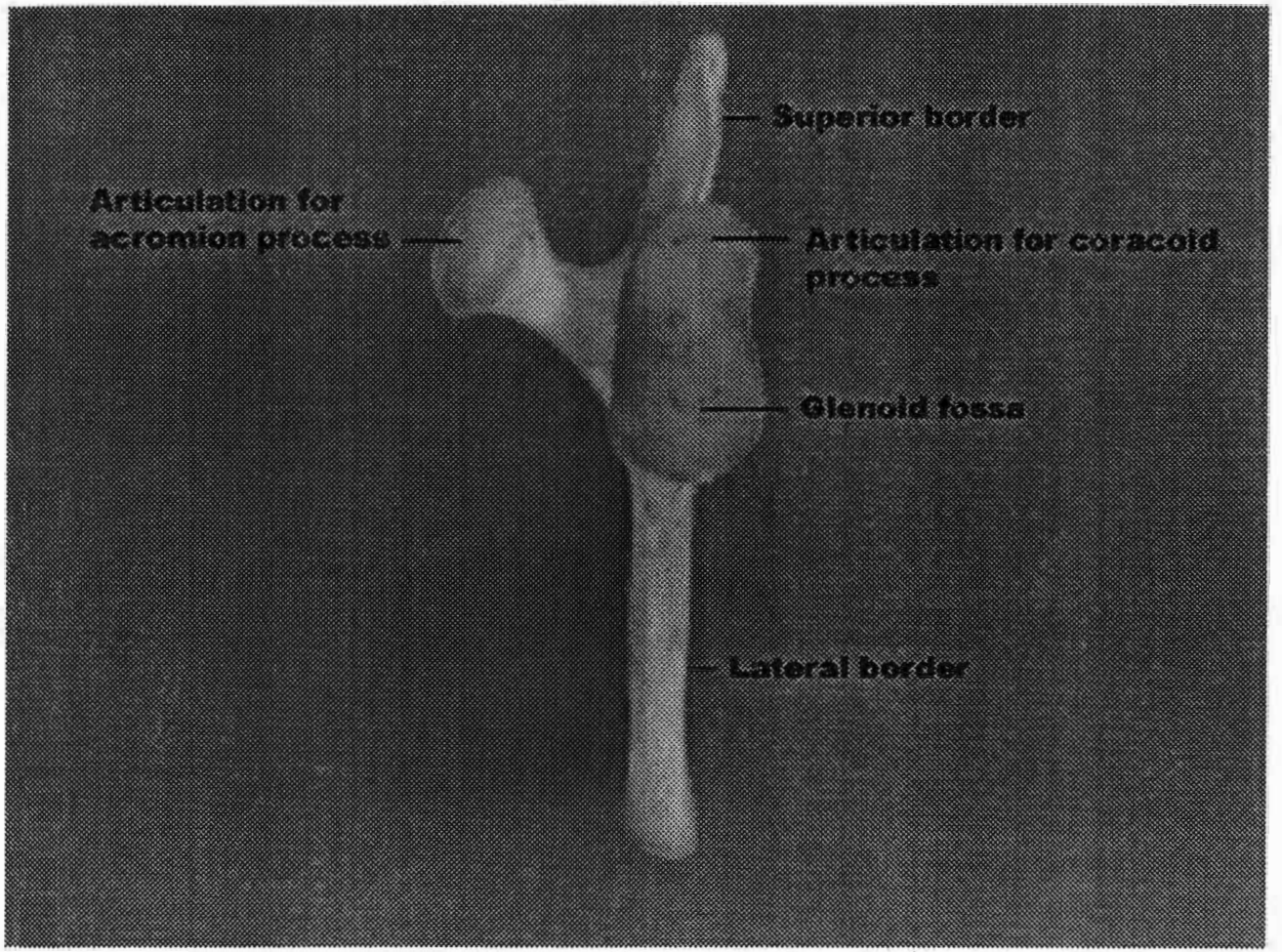



Figure 3.10. Neonate scapular morphology (right scapula, lateral view).

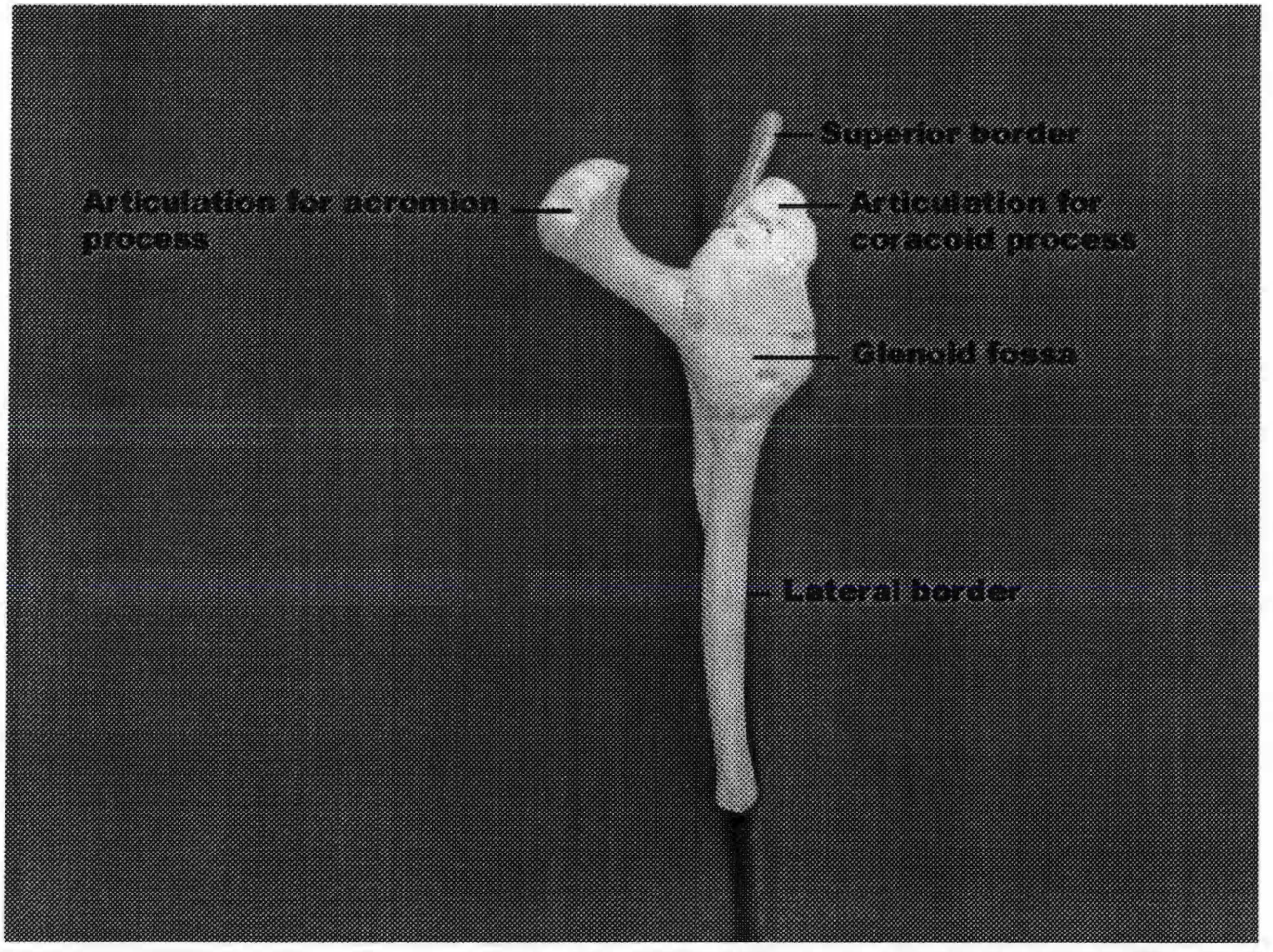



Figure 3.11. Juvenile scapular morphology (ca. 6 years, right scapula, lateral view).

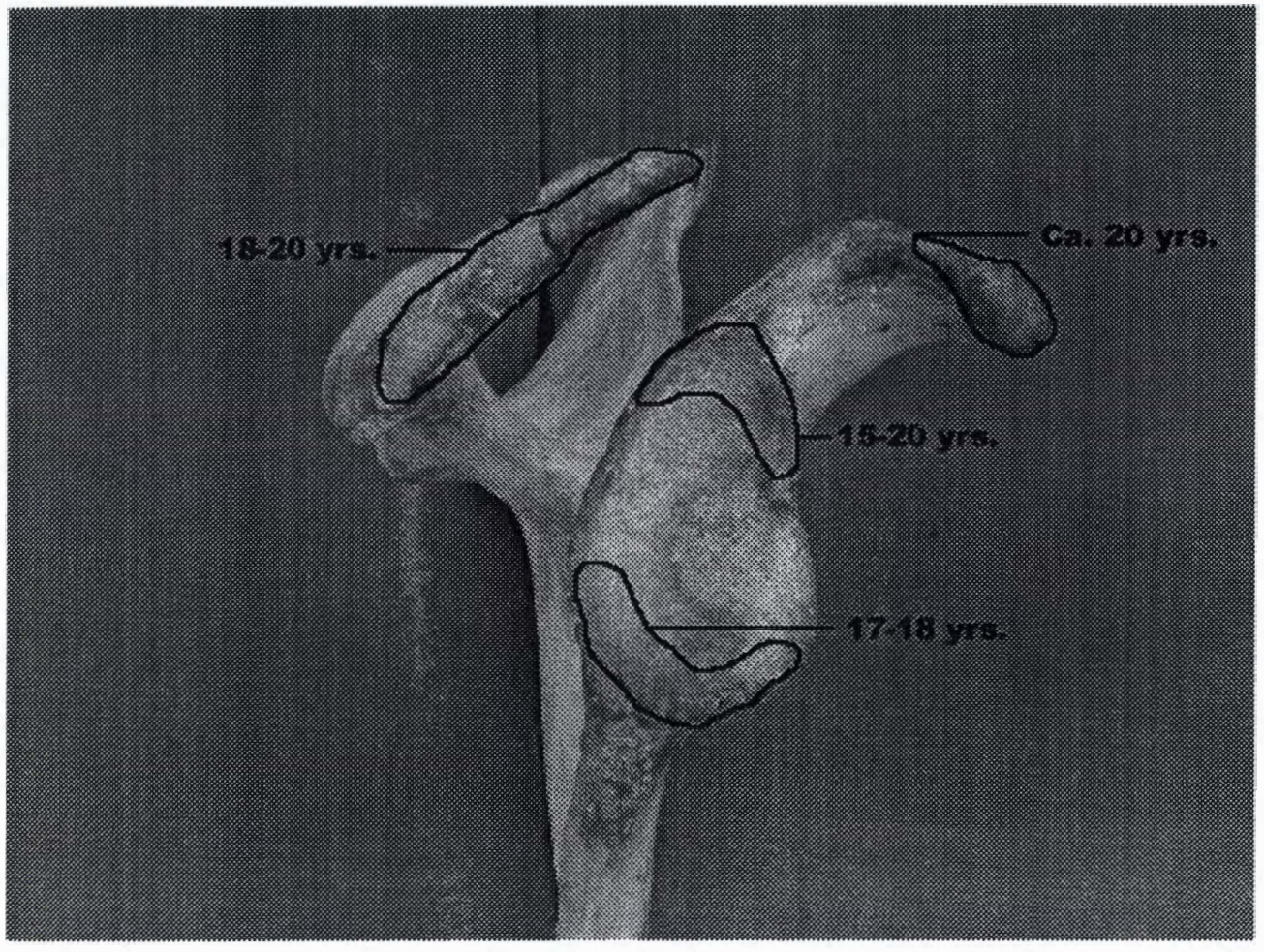



Figure 3.12. Age of epiphyseal fusion of the scapula (right scapula, lateral view).

uniting completely at approximately 17 to 18 years of age (Scheurer and Black, 2000).

The angle of the coracoid process may appear as a separate structure but more likely originates from the medial coracoid process. Appearing at approximately 14 to 15 years of age, fusion of the epiphysis is complete by approximately 20 years of age (Hodges, 1933; Garn et al., 1967; Birkner, 1978). Once fused, the epiphysis then unites with the epiphysis of the apex at approximately 13 to 16 years of age and is completely fused by approximately age 20 (Hodges, 1933; Birkner, 1978).

The secondary centers of ossification of the acromion appear between ages 14 and 16, and fusion is complete by age 20 (McKern and Stewart, 1957; Garn et al., 1967; Last, 1973; Ogden and Phillips, 1983; Williams et al., 1995). The base of the acromion forms at the lateral-most extension of the scapular spine and extends medially to the acromioclavicular joint (Figure 3.6). The epiphysis is located along the lateral border of the acromion and extends anteriorly to the tip of the acromion. Another center of ossification located between the acromioclavicular joint and the tip of the acromion spreads in both directions and fills the gap between the two centers (Williams et al., 1995).

Typically, the acromial epiphysis is comma-shaped in appearance with a thicker lateral border and a blunt tip, curving to form part of the acromioclavicular joint on its anterior border. Its characteristic shape is identifiable by early puberty (Scheurer and Black, 2000).

Non-union of a lateral portion of the acromion with the medial part is known as *os acromiale* (Edelson et al., 1993; Uri et al., 1997) and is a condition often associated with occupational injury, such as migrant farm labor (Wienker and Wood, 1988), rotator cuff injury (Mudge et al., 1984; Dennis et al.,1986; Warner et al., 1998), or congenital deformity. Frequently bilateral, non-union often occurs along the junction of the meso-acromion and meta-acromion portions (Liberson, 1937). This results in a quadrangular section of bone that is separated from the remainder of the acromion along a line connecting the acromioclavicular joint with the acromial angle (Miles, 1994). Miles (1994) population from Ensay, Scotland exhibited 11 examples of separation of the acromion in 220 scapulae. Stirland (1992), attributed non-union of 13.6 percent of the individuals of the Tudor warship Mary Rose to practicing archery at an early age, which prevented fusion of the epiphysis.

The epiphyses located at the inferior angle and the medial border (Figure 3.10) are the last scapular epiphyses to unite, typically beginning around age 15 to 17 with complete fusion around age 23 (Stevenson, 1924; Girdnay and Golden, 1952; McKern and Stewart, 1957; Basmajian and Slonecker, 1989). These epiphyses likely are composed of isolated centers of ossification rather than single centers, and closure results from coalescence between centers, beginning at the inferior angle. In the adult, the presence of fissures along the medial border represents incomplete fusion.

As with the medial border, the epiphysis of the inferior angle (Figure 3.13) commences closure around ages 15 to 17 and fusion is complete by age 23 (Stevenson; 1924; Hodges, 1933; McKern and Stewart, 1957; Basmajian and Slonecker, 1989). The inferior angle epiphysis fuses first at the inferior angle before spreading to the medial border.

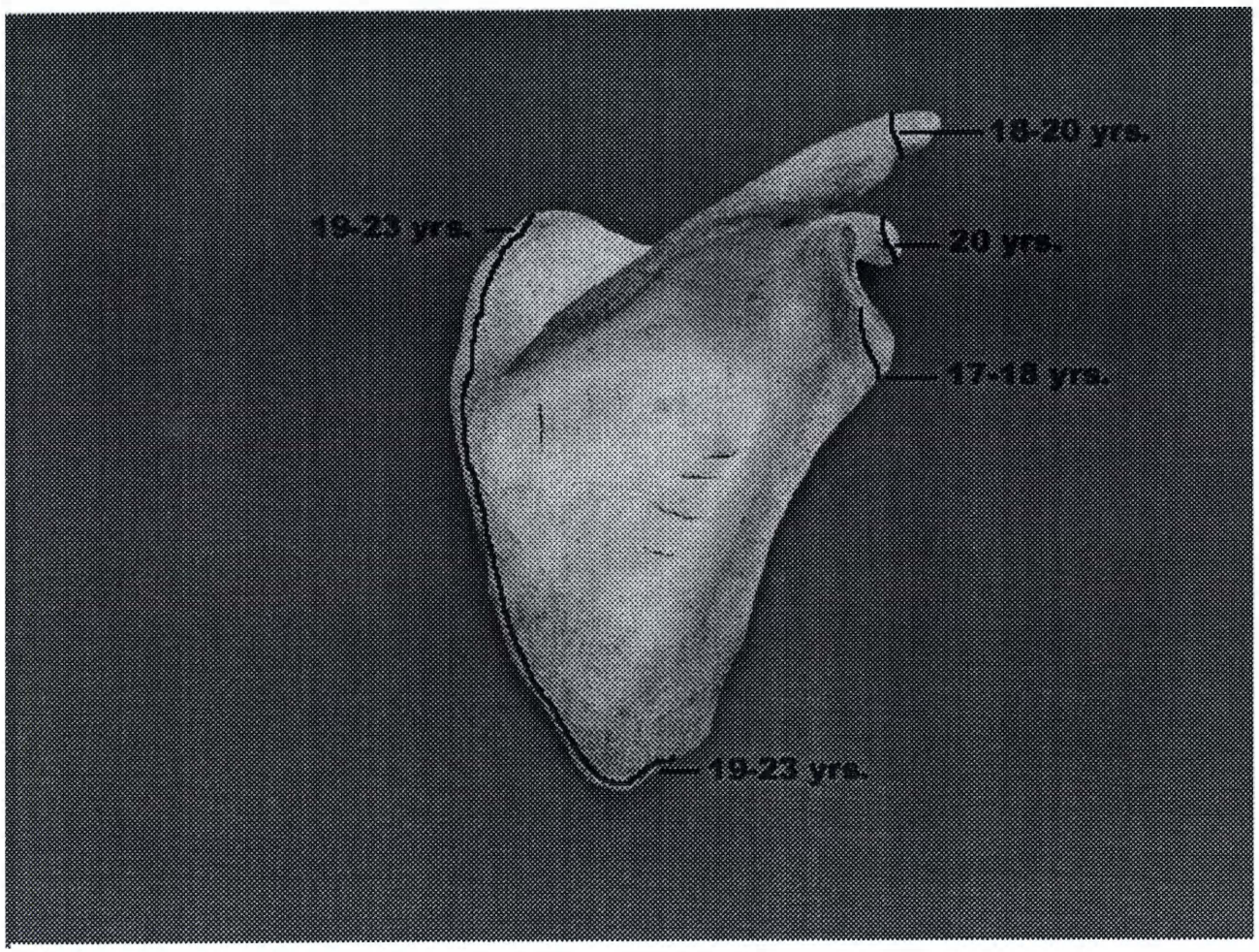



Figure 3.13. Age of epiphyseal fusion of the scapula (right scapula, dorsal view).

# CHAPTER 4

# Materials and Methods

## Scapulae

The skeletal material used was derived from the William M. Bass, III Donated and Forensic Collections, which are curated in the Department of Anthropology at The University of Tennessee, Knoxville. Both left and right scapulae were used whenever possible, although in some cases one scapula was absent or damaged to the extent that it could not be measured. Occasionally, only one scapula was available for analysis. The skeletal material used is comprised primarily of adult American white males (N=150), adult American white females (N=48), adult American black males (N=33), and adult American black females (N=10). Age ranges from 15 to 94 years with a median of 55 years and a mean of 54.4 years, indicating a wide and fairly symmetric age distribution. Only adult scapulae were used and skeletal material of unknown race and/or sex or exhibiting obvious anomalies or unfused epiphyses was excluded from analysis

## Landmarks

Ten landmarks that captured essential size and shape information and incorporated the primary morphological components of the scapula were used. Four landmarks, including the most superior point on the superior angle, the midpoint between the ridges of the scapular spine on the

vertebral border, the most inferior point on the inferior angle, and the midpoint on the dorsal border of the glenoid fossa are commonly used for measuring the height and breadth of the scapula (Hrdlička, 1952; Martin, 1957; Montagu, 1960; Bass, 1995). In addition, the most distal point on the acromion is commonly used to measure the length of the scapular spine (Bass, 1995), and the distance between the most superior and inferior points on the glenoid fossa is frequently used to determine sex (Dwight, 1894). The remaining landmarks, including the midpoint on the ventral border of the glenoid fossa, the most distal point on the coracoid process, and the most inferior point on the superior border were chosen because they capture the true morphology of the scapula. Several of the landmarks are non-traditional, necessitated by the need to adequately cover the morphology of the scapula. Table 4.1 provides a description of these landmarks and Figures 4.1, 4.2, and 4.3 provide a graphical representation of their locations.

Landmarks serve as the basis for which the explanation of biological change is grounded and by which it is measured (Bookstein, 1996). It is only through careful choice of landmarks that salient questions regarding functional and evolutionary change within and among homologous structures can be answered.

**Table 4.1. Scapular Landmarks and Descriptions**

| Landmark | Description |
|---|---|
| Superior angle | The most superior point on the superior angle. |
| Vertebral border | The point on the vertebral border that is midway between the two ridges of the scapular spine. |
| Inferior angle | The most inferior point on the inferior angle. |
| Inferior glenoid | The most inferior point on the glenoid fossa. |
| Superior glenoid | The most superior point on the glenoid fossa. |
| Dorsal glenoid | The midpoint on the dorsal border of the glenoid fossa. |
| Ventral glenoid | The midpoint on the ventral border of the glenoid fossa. |
| Lateral coracoid | The most lateral point on the coracoid process. |
| Lateral acromion | The most lateral point on the acromion process. |
| Scapular notch | The most inferior point on the scapular notch. |

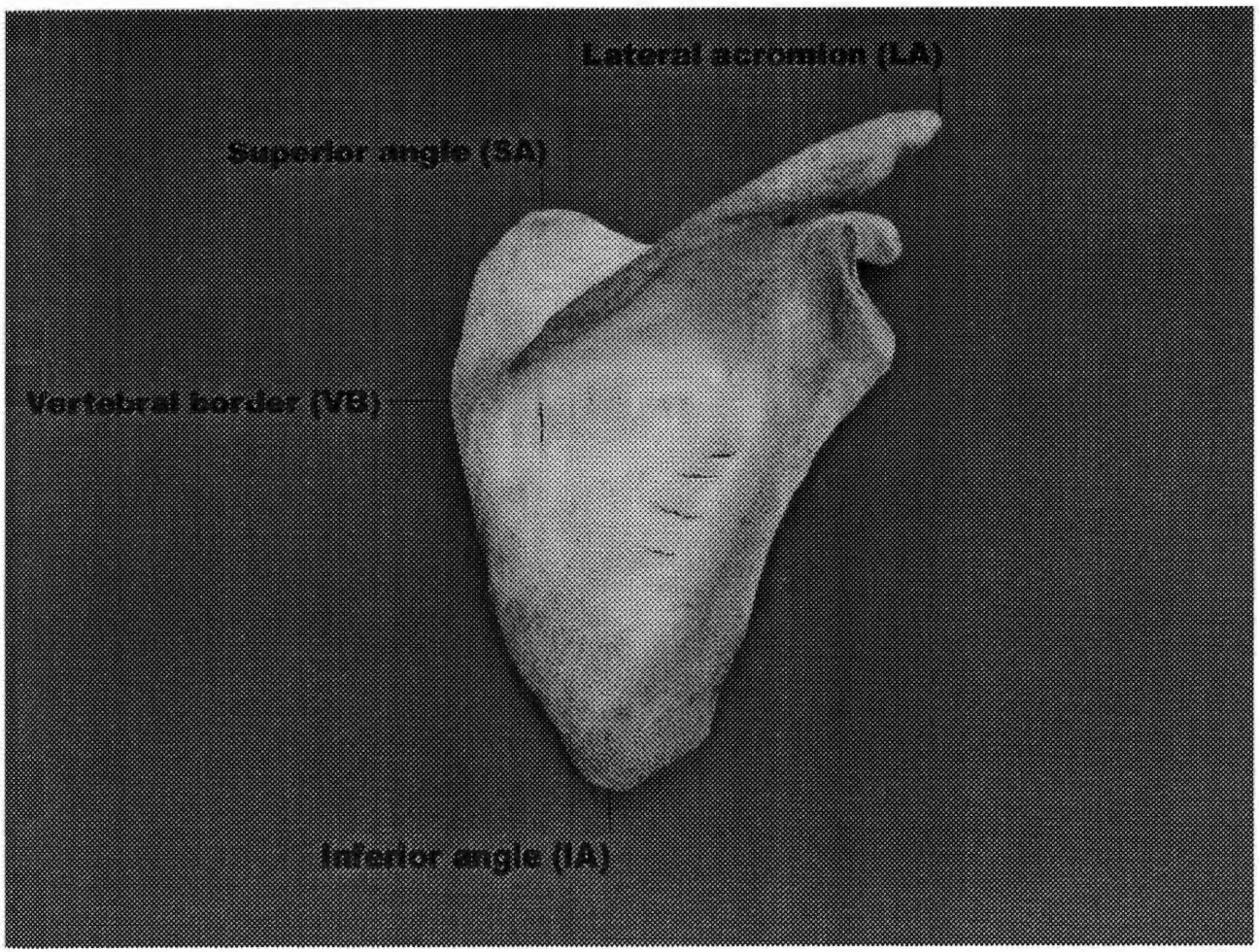



Figure 4.1. Scapular landmarks (dorsal view).

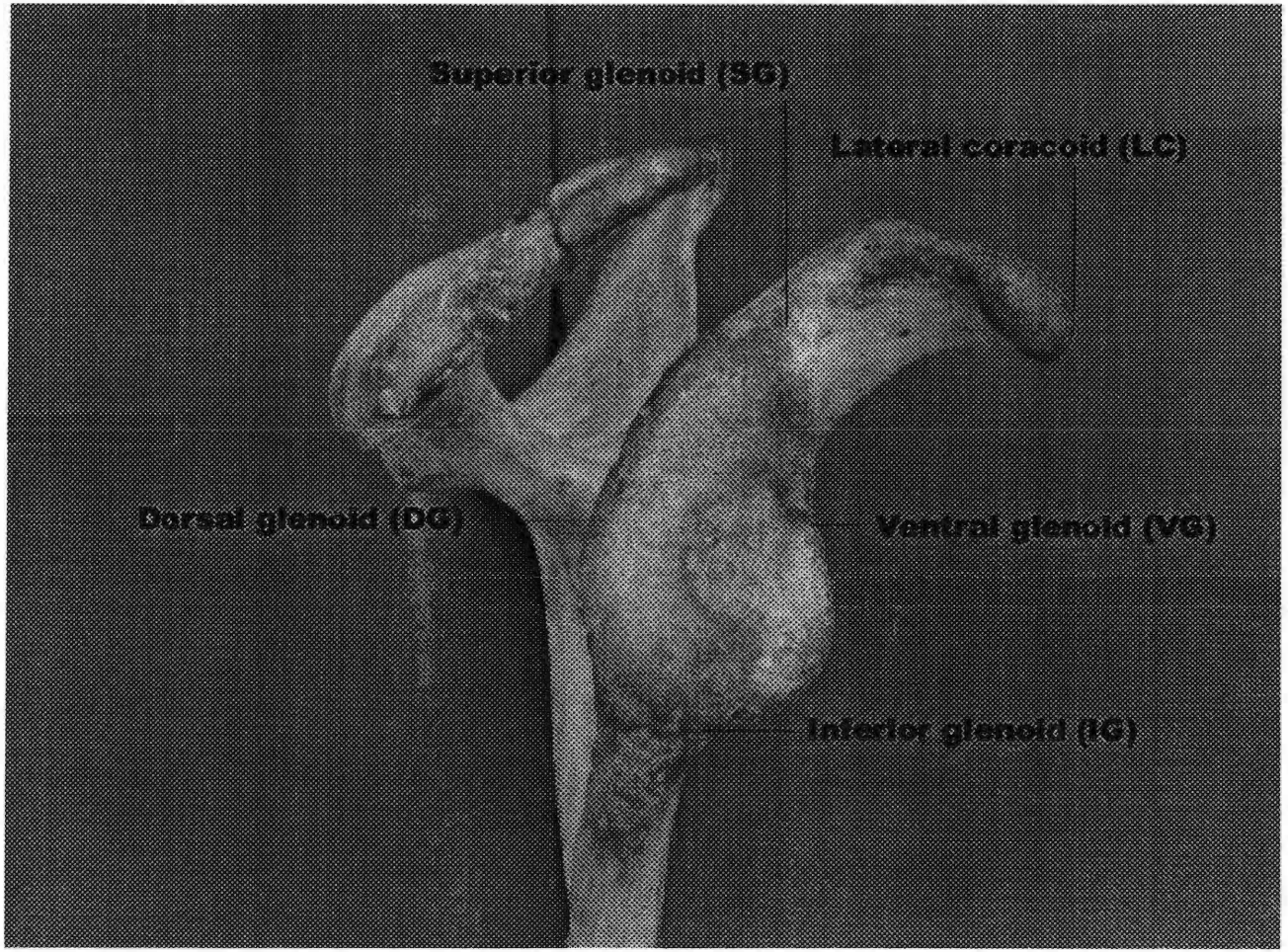



Figure 4.2. Scapular landmarks (lateral view).

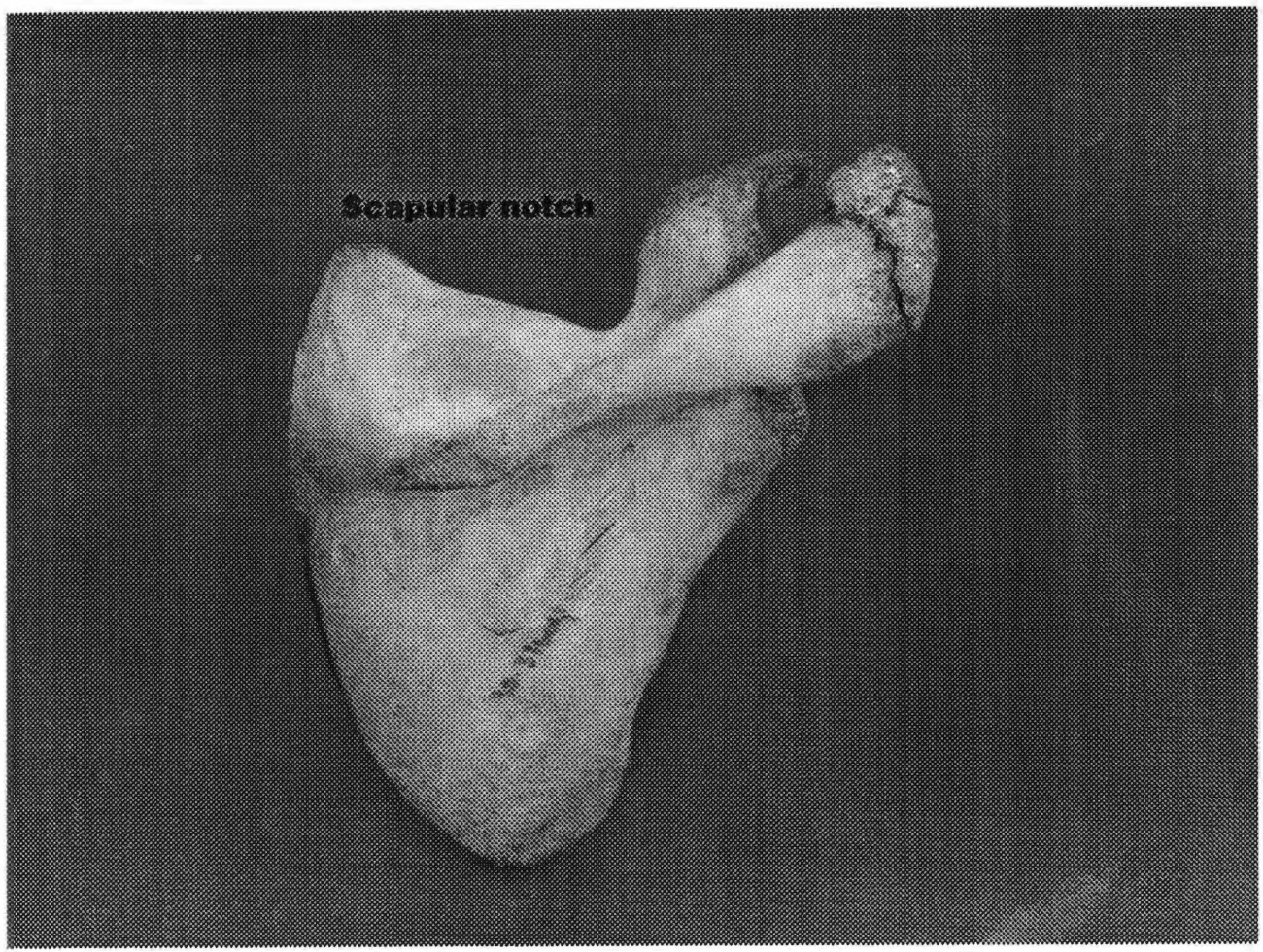



Figure 4.3. Scapular landmarks (scapular notch).

Rohlf (1996) offers three criteria for choosing landmarks:

1. The landmark should be repeatable. That is, they should be able to be located unambiguously on other specimens by other workers. The ability to do so requires a precise definition of the landmark and knowledge of the full range of variation likely to be encountered.
2. In order to adequately represent the object, the landmarks should be well distributed over it rather than localized in areas of particular interest. In addition, the use of three-dimensional geometric morphometry is preferable to two-dimensional representations in order to capture the maximum amount of information.
3. The locations of landmarks should be meaningful. They should be chosen in order to answer *a priori* questions of interest, and analytical methods should be used that best allow for comparison between structures.

For landmarks to be useful they must be homologous, meaning there is a correspondence between parts. In the context of geometric morphometry, homology must be considered a mapping function, such that there is a correspondence of points to points rather than parts to parts.

Landmarks can be categorized into three principal types:

Type 1. Type 1 landmarks represent "discrete juxtapositions of tissues" and typically are found at points in space where three structures

meet, such as cranial sutures or branching points of neural or arterial systems (Bookstein, 1991). Of the three types of landmarks, these are the most easily located due to their position at easily recognizable structure intersections, and likely provide the most plausible functional explanations, such as optimization of biomechanical strength or stiffness under changes in load. Craniometric examples of Type 1 landmarks include nasion, bregma, dacryon, and lambda.

Type 2. These landmarks are located at maxima of curvature or local morphogenetic processes, including tips of processes and invaginations (Bookstein, 1991). Type 2 landmarks represent application points of biomechanical forces, such at the tips of teeth and claws, as well as bone processes where muscle attachments are located. These landmarks may occur in response to a bulge located some distance from the area of study. Examples of Type 2 landmarks include basion and opisthion, which are the points at which the mid-sagittal plane intersects the anterior and posterior margins of the foramen magnum, respectively, and alare, which is the most lateral point on the anterior margin of the nasal aperature.

Type 3. Type 3 landmarks represent extremal points along an axis. Included are centroids, endpoints of diameters, intersections of interlandmark segments, and points located farthest away from other landmarks. Of the three types of landmarks, these are the least informative, given that they measure size more than shape. Examples of Type 3 landmarks include glabella (the most anterior point in the mid-sagittal plane

at the lower margin of the frontal bone between the supraorbital crests and superior to the nasal root), gnathion (the most inferior point on the inferior margin of the mandibular body in the mid-sagittal plane), and condylion (the most lateral points on the mandibular condyle).

Unlike the cranium, scapulae offer no intersections of structures for use as Type 1 landmarks. All ten landmarks used in this study are classified as Type 2 or Type 3.

**Missing Landmarks**

Many scapulae were missing one or more landmarks due to a variety of reasons. Scapulae from the William M. Bass, III Forensic Collection often suffered from carnivore scavenging, trauma, warping, or extreme weathering, rendering landmarks absent or unrecognizable. Similarly, scapular landmarks from the William M. Bass, III Donated Collection, which is comprised largely of skeletal material of older and often osteoporotic individuals, were often absent due to fracturing or unrecognizable because of bone extoses. Such landmarks as could be recognized were digitized. Rarely, when a reasonable approximation could be obtained, a landmark's position was estimated. Although 241 pairs of scapulae were digitized, scapulae with missing landmarks were excluded from further statistical analysis reducing the sample size to 194 left scapulae (5 Black females, 23 Black males, 35 White females, 131 White males) and 195 right scapulae (5 Black females, 24 Black males, 38 White females, 128 White males).

**Data Collection Protocol**

Prior to digitizing, all landmarks on left and right scapulae were first located using a Mitutoyo digital pointed jaw caliper (accurate to 0.01 mm) or a Hillson-Fitzgerald dental caliper (also accurate to 0.01 mm). Whenever possible the Hillson-Fitzgerald dental caliper was used, as needle points in the jaws of the caliper allowed very precise and consistent placement of landmarks. At each landmark location a small mark was placed with a graphite pencil.

All Cartesian coordinates were collected using a MicroScribe-3DX three-dimensional digitizer connected to a laptop computer. After each scapula was firmly anchored to an elevated wooden platform using modeling clay, landmarks were digitized and saved in an Excel spreadsheet.

# CHAPTER 5

## Analytical Methods

Although geometric morphometrics has been shown to be useful in determining ancestry and sexual dimorphism in crania, its utility in postcranial elements is largely untested. This dissertation tests the hypothesis that shape variation of the scapula can be quantified using geometric morphometry. If so, these methods can be used in conjunction with traditional morphometric and morphologic techniques to more accurately determine sex and ancestry.

Currently, almost all studies using geometric morphometry use Procrustes distance, Kendall's shape space, or tangent space approximations to analyze shape. These methods are known to have the best statistical power, impose the least constraints on patterns of variation that can be detected, and have the lowest mean-squared error (Kent, 1994). In addition, these methods conform to statistical theory regarding the definition of shape (Kendall, 1977) and how shape variation is analyzed (Kendall, 1984; Small, 1996).

Accordingly, traditional and non-traditional scapular landmarks were subjected to Procrustes analysis to produce residuals that were, in turn, used in univariate and multivariate analyses. Thin-plate spline analysis was then used to produce a graphical representation of the mean configurations.

The initial step, Procrustes fitting of 241 pairs of scapulae with ten landmarks each, was followed by principal component analysis of the residuals produced. Graphical representation of the principal components permits visualization of morphological variability among the scapulae. Finally, mean configurations produced by Procrustes analysis were subjected to thin-plate spline analysis to generate two-dimensional representations showing pairwise variability in sex and ancestry.

**Procrustes Analysis**

Generalized Procrustes analysis (GPA; often called generalized least squares in the earlier literature) is a method by which homologous landmarks of one organism are superimposed on those of another in order to optimize goodness of fit and is accomplished by taking into account translation, rotation, scale, and possibly uniform shape change. Initially, the centroid of each landmark configuration is translated (sliding in any direction along a plane) to its origin. Once centered, all configurations are scaled to a common unit size by dividing by centroid size. Centroid size, which is the square root of the sum of the variances of the landmarks about that centroid in *x*, *y*, and *z* directions, is used in geometric morphometrics because it is uncorrelated with all shape variables when the landmarks are distributed around the mean positions by noise in the same variance at all landmarks and in all directions. Landmark configurations are scaled to centroid size in order to plot them as a point in Kendall's shape space.

Finally, all landmark configurations are optimally rotated (movement around an axis) to minimize the squared differences between corresponding landmarks, such that homologous landmarks are in a common orientation. This consensus configuration optimizes some measure of fit to the entire sample and removes size differences while simultaneously computing mean shape, which cannot be estimated prior to superimposition. The model and notation used for the three-dimensional superimposition of GPA is:

$$\mathbf{X}' = \rho \mathbf{X}'\mathbf{H} + \mathbf{1}\tau$$

where **X'** is the result of translating, rotating, and scaling **X** by $\rho$, **H**, and $\tau$, respectively. In this model, **X** and **X'** are $p$ and $k$ matrices of the $k$ coordinates of the $p$ points in a configuration before and after fitting. In addition, ρ is a scalar, **H** is a transformation matrix, **1** is a $p$ x 1 matrix of ones, and $\boldsymbol{\tau}$ is a 1 x $k$ matrix of translation parameters. These parameters are estimated by comparing them to reference specimen **Y**, which is another $p$ x $k$ matrix representing another specimen or mean configuration (Slice, 1996).

Minimizing the sum of the distances between the homologous landmarks of a pair of objects by centering them on their origin, scaling them to unit centroid size, and optimally rotating them permits them to conform to a point in Kendall's (1984) shape space, which is the fundamental geometric construction underlying geometric morphometrics. This space is of $pk$-$k$-$k(k$-1$)$/2-1 dimensions. Procrustes distance is a measure of distance between points in this space and thus is non-Euclidean. In addition,

Procrustes distance between two shapes is the minimum distance between any two pre-shapes to which the two shapes belong (Rohlf, 1996).

Kendall's shape space uses geometric analysis of Procrustes distances among landmarks, with each point representing a shape of a configuration of points in Euclidean space, regardless of position, size, or orientation. Scatters of landmark configurations are represented by scatters of points, not just scatters of single landmarks. Using the illustration of a "spherical blackboard", for which chords correspond to Procrustes distances or geodesic distances along great circles on the surface of the sphere, Kendall (1984) describes shape space for three points in the plane. By varying one landmark in a circle about its centroid, while requiring all other landmarks to remain fixed, the corresponding shapes are all exactly the same distance from the central shape. Given the mathematical complexity of computing shape space, an alternative approach using tangent space in Euclidean geometry is often used. This method uses the projections of the objects in shape space onto a linear vector space that is tangent to shape space. Distances between pairs of points approximate Procrustes distances between corresponding pairs of landmarks.

General Procrustes analysis was carried out using the generalized least squares procedure in Morpheus (Slice, 1998), which fits multiple configurations to a consensus. Generally, the first reference object serves as the model for subsequent iterations, which are translated, scaled, and rotated to minimize the sums of the squared differences. Upon achieving

the reference consensus, a new consensus is derived from averaging these fitted configurations. Subsequent iterations are fitted to the new consensus form and the difference in fit between these iterations is calculated. These iterations continue until the sum of squares is minimized to some standard (Slice, 1998). Generalized Procrustes analysis was then used to superimpose all configurations of race and sex.

Procrustes residuals serve as coordinates in shape space and may thus be used for many different multivariate analyses. Analysis using generalized least squares (GLS) is often the first phase, the reduction of landmark locations in a digitizing plane to a point in shape space.

**Principal Component Analysis**

Principal component analysis (PCA) attempts to extract a set of components that explain as much of the total variance as possible. One of the primary reasons for using PCA is that information explaining variability rapidly decreases as the number of principal components increase. In most cases, the majority of the variance is explained by a relatively small number of uncorrelated components. Thus, groups that can be discriminated reasonably well from each other should be distinguished by discrete clouds of points (Reyment et al., 1984).

Although principal components are used primarily to observe variability both within and among groups, they can also be used with more traditional multivariate analyses to investigate variability. In addition,

because the variance is often explained by a small number of components, principal component analysis is well suited to the large data sets often generated by three-dimensional data. Also, analysis of Procrustes residuals by principal component analysis provides valuable information about shape variation and also provides a means for visual representation of this variability.

In principal component analysis, the original variable set's axis system is rotated to a new set of orthogonal axes, called principal axes, which coincide with the maximum variation of the original data set. Principal components are then computed as the linear combination of the original variables for each specimen. The original values are subtracted from the sample means equal to zero. After transformation the total variance accounted for remains the same, and principal components can then be arranged in decreasing order based on the variance. Given that these principal components are independent of each other, each principal component score for each specimen can then be graphed, the first principal component along the x-axis and the second along the y-axis.

Procrustes analysis of ten landmarks from each scapula produced residuals that were then subjected to principal component analysis using SAS (1996). Individuals with missing landmarks were excluded from analysis. Each scapula generated principal component scores that were used for further analysis.

## Canonical Discriminant Function Analysis

A canonical discriminant function analysis, which is a parametric method based on a multivariate normal distribution, was used to calculate canonical discriminant functions (SAS, 1996). Within-group covariance matrices were used to calculate distances; prior probabilities were set equal.

## Thin-plate Spline Analysis

A technique borrowed from the mathematical field of approximations theory, thin-plate spline is not a superposition technique. Rather, thin-plate spline analysis allows the visualization of any pair of forms in shape space of a Cartesian deformation of one form to another. Deformation of the mean form into another form along some directional Procrustes distance provides a graphical representation of the direction of shape space. Bookstein (1986) suggests that in order to fully understand this deformation it should be broken down into several orthogonal parts. One part, affine transformation, is uniform or global change required to keep parallel lines parallel within a transformation and does not require bending. In doing so, these transformations convert squares into parallelograms and circles into ellipses of the same shape. In three-dimensional space, affine transformations convert cubes into parallelopipeds and spheres into ellipsoids all of the same shape. Affine transformations can then be diagrammed as the pure strains required to bend a square into a rectangle on the same axis. When describing shape and ignoring scale, the sum of squares of the axes is

unchanging. Also, when describing shape, affine transformations can be diagrammed as pure shear, bending a square into a parallelogram that is unchanged in the base segment and height. Non-affine transformation (non-uniform) is the energy required for bending.

Using the generalized Procrustes procedure in Morpheus (Slice, 1998), consensus configurations for both sexes and both races were computed. Once computed, thin-plate spline analysis in Morpheus (Slice, 1998) was employed to graphically observe variation among all combinations of sex and ancestry.

# CHAPTER 6

# Results

## Procrustes Analysis

Three iterations of the general least squares procedure in Morpheus (Slice, 1998) were required to successfully fit all left and right scapulae shape configurations. All subsequent analyses, including principal component analysis, canonical discriminant function analysis, and thin-plate spline analysis used Procrustes residuals derived from the third iteration.

## Centroid Size

Centroid sizes were derived from generalized Procrustes analysis in Morpheus (Slice, 1998). In Morpheus, missing data points are scaled to those available, thus all 241 pairs of scapulae yielded centroid sizes. Centroid sizes were then compared among groups and analyzed using the univariate analysis of variance (ANOVA) in SAS (1996). In SAS, observations with missing values are not included in the analyses, reducing the sample size to 194 left scapulae and 195 right scapulae. Descriptive statistics are presented in Table 6.1 and Table 6.2. and are graphically depicted in Figure 6.1 and Figure 6.2. Mean centroid size for left scapulae of Black males was 210.45 mm, 207.39 mm for White males, 183.21 mm for White females, and 175.55 for Black females. For right scapulae, mean

**Table 6.1. Descriptive Statistics of Centroid Sizes of Left Scapulae of Black Females (BF), Black Males (BM), White Females (WF), and White Males (WM)**

| | N | Minimum | Maximum | Mean | Std. Deviation |
|---|---|---|---|---|---|
| **BF** | 10 | 160.45 | 188.81 | 175.55 | 8.49 |
| **BM** | 33 | 196.52 | 228.38 | 210.45 | 8.89 |
| **WF** | 48 | 166.60 | 205.40 | 183.21 | 9.00 |
| **WM** | 150 | 175.43 | 237.41 | 207.39 | 10.34 |

**Table 6.2. Descriptive Statistics of Centroid Sizes of Right Scapulae of Black Females (BF), Black Males (BM), White Females (WF), and White Males (WM)**

| | N | Minimum | Maximum | Mean | Std. Deviation |
|---|---|---|---|---|---|
| **BF** | 10 | 162.97 | 187.85 | 175.58 | 7.37 |
| **BM** | 33 | 196.42 | 233.53 | 211.87 | 10.72 |
| **WF** | 48 | 165.78 | 203.29 | 185.01 | 9.90 |
| **WM** | 150 | 179.88 | 242.89 | 208.73 | 11.02 |

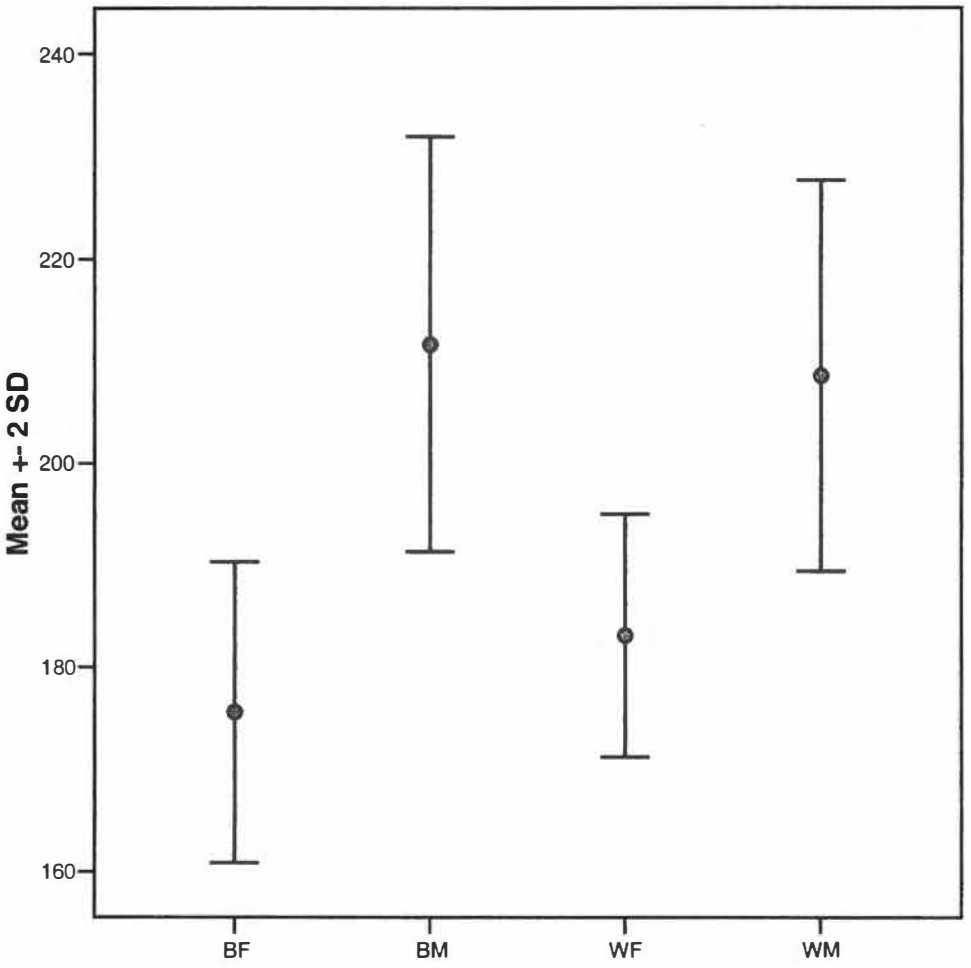



Figure 6.1. Means and standard deviations of centroid sizes of left scapulae.

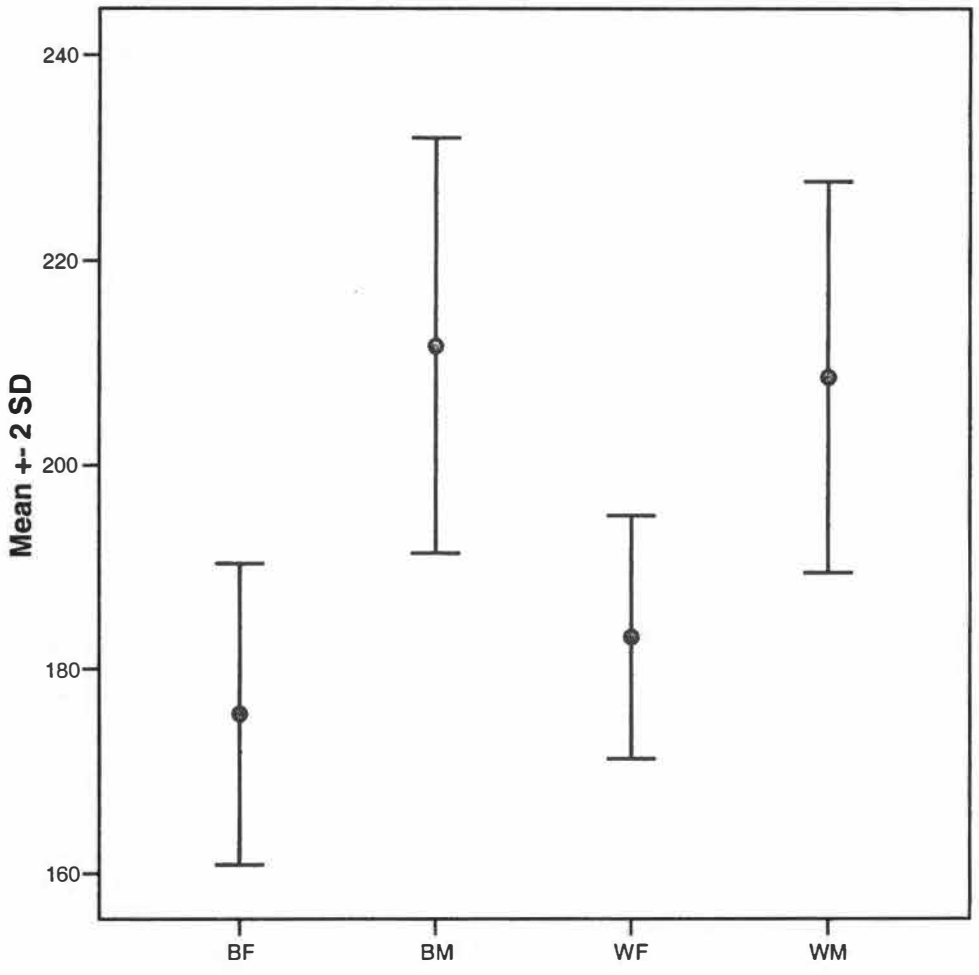



Figure 6.2. Means and standard deviations of centroid sizes of right scapulae.

centroid size of Black males was 211.87 mm, 208.73 mm for White males, 185.01 for White females, and 175.58 for Black females.

The ANOVA (Table 6.3, 6.4) suggests that mean centroid size did not differ between Blacks and Whites but did differ between the sexes. In addition, a significant ($p=0.006$ for left scapulae, $p=0.003$ for right scapulae) interaction of ancestry and sex indicates that sexual dimorphism is reversed in the ancestries. Differences of mean centroid size are larger for females than for males.

**Principal Component Analysis**

Analysis of the covariance matrix of the Procrustes residuals produced thirty non-zero principal components. A summary of the principal components and their associated eigenvalues, percent of variance, and cumulative percent of variance is presented in Table 6.5 for left scapulae and Table 6.6 for right scapulae. For left scapulae, the first 15 principal components accounted for 95 percent of the variance; for right scapulae, however, the first 15 principal components accounted for 96 percent of the variance. High principal component scores in the first principal components are largely due to eigenvectors associated with the *x* and *y* and to a lesser extent *z* coordinates, which represent superior-inferior, medial-lateral, and dorsal-ventral variation, respectively.

**Table 6.3. Analysis of Variance of Centroid Sizes of Left Scapulae**

| Source | Type III SS | df | Mean Square | F | Sig. |
|---|---|---|---|---|---|
| Corrected Model | 30621.900[a] | 3 | 10207.300 | 105.606 | .000 |
| Intercept | 3821795.685 | 1 | 3821795.685 | 39540.629 | .000 |
| Ancestry | 134.298 | 1 | 134.298 | 1.389 | .240 |
| Sex | 22114.459 | 1 | 22114.459 | 228.798 | .000 |
| Ancestry * Sex | 728.760 | 1 | 728.760 | 7.540 | .006 |
| Error | 22907.212 | 237 | 96.655 | | |
| Total | 9855062.992 | 241 | | | |
| Corrected Total | 53529.112 | 240 | | | |

[a]. R Squared= .572 (Adjusted R Squared= .567)

**Table 6.4. Analysis of Variance of Centroid Sizes of Right Scapulae**

| Source | Type III SS | df | Mean Square | F | Sig. |
|---|---|---|---|---|---|
| Corrected Model | 30557.331[a] | 3 | 10185.777 | 89.848 | .000 |
| Intercept | 3867241.266 | 1 | 3867241.266 | 34112.719 | .000 |
| Ancestry | 250.854 | 1 | 250.854 | 2.213 | .138 |
| Sex | 22810.464 | 1 | 22810.464 | 201.210 | .000 |
| Ancestry * Sex | 1001.484 | 1 | 1001.484 | 8.834 | .003 |
| Error | 26867.872 | 237 | 113.367 | | |
| Total | 9994592.729 | 241 | | | |
| Corrected Total | 57425.203 | 240 | | | |

[a]. R Squared= .532 (Adjusted R Squared= .526)

**Table 6.5. Eigenvalues of the Covariance Matrix of Left Scapulae**

| PC | Eigenvalue | Difference | Proportion | Cumulative |
|---|---|---|---|---|
| 1 | 0.00147225 | 0.00036689 | 0.2246 | 0.2246 |
| 2 | 0.00110536 | 0.00036464 | 0.1687 | 0.3933 |
| 3 | 0.00074071 | 0.00016887 | 0.1130 | 0.5063 |
| 4 | 0.00057185 | 0.00012174 | 0.0873 | 0.5936 |
| 5 | 0.00045010 | 0.00012927 | 0.0687 | 0.6623 |
| 6 | 0.00032083 | 0.00003204 | 0.0490 | 0.7112 |
| 7 | 0.00028879 | 0.00002231 | 0.0441 | 0.7553 |
| 8 | 0.00026648 | 0.00002374 | 0.0407 | 0.7959 |
| 9 | 0.00024274 | 0.00005348 | 0.0370 | 0.8330 |
| 10 | 0.00018926 | 0.00002121 | 0.0289 | 0.8618 |
| 11 | 0.00016805 | 0.00003459 | 0.0256 | 0.8875 |
| 12 | 0.00013346 | 0.00003014 | 0.0204 | 0.9079 |
| 13 | 0.00010333 | 0.00000903 | 0.0158 | 0.9236 |
| 14 | 0.00009430 | 0.00001897 | 0.0144 | 0.9380 |
| 15 | 0.00007533 | 0.00001957 | 0.0115 | 0.9495 |
| 16 | 0.00005575 | 0.00000757 | 0.0085 | 0.9580 |
| 17 | 0.00004819 | 0.00000873 | 0.0074 | 0.9654 |
| 18 | 0.00003946 | 0.00000360 | 0.0060 | 0.9714 |
| 19 | 0.00003586 | 0.00000348 | 0.0055 | 0.9769 |
| 20 | 0.00003238 | 0.00000654 | 0.0049 | 0.9818 |
| 21 | 0.00002585 | 0.00000135 | 0.0039 | 0.9857 |
| 22 | 0.00002449 | 0.00000593 | 0.0037 | 0.9895 |
| 23 | 0.00001856 | 0.00000884 | 0.0028 | 0.9923 |
| 24 | 0.00000972 | 0.00000090 | 0.0015 | 0.9938 |
| 25 | 0.00000882 | 0.00000081 | 0.0013 | 0.9951 |
| 26 | 0.00000801 | 0.00000097 | 0.0012 | 0.9964 |
| 27 | 0.00000704 | 0.00000066 | 0.0011 | 0.9974 |
| 28 | 0.00000638 | 0.00000092 | 0.0010 | 0.9984 |
| 29 | 0.00000546 | 0.00000045 | 0.0008 | 0.9992 |
| 30 | 0.00000501 | | 0.0008 | 1.0000 |

**Table 6.6. Eigenvalues of the Covariance Matrix of Right Scapulae**

| PC | Eigenvalue | Difference | Proportion | Cumulative |
|---|---|---|---|---|
| 1 | 0.00135158 | 0.00035582 | 0.2072 | 0.2072 |
| 2 | 0.00099576 | 0.00019122 | 0.1526 | 0.3598 |
| 3 | 0.00080454 | 0.00013286 | 0.1233 | 0.4831 |
| 4 | 0.00067169 | 0.00016548 | 0.1030 | 0.5861 |
| 5 | 0.00050620 | 0.00013685 | 0.0776 | 0.6636 |
| 6 | 0.00036936 | 0.00004653 | 0.0566 | 0.7203 |
| 7 | 0.00032282 | 0.00005280 | 0.0495 | 0.7697 |
| 8 | 0.00027002 | 0.00004101 | 0.0414 | 0.8111 |
| 9 | 0.00022901 | 0.00004990 | 0.0351 | 0.8462 |
| 10 | 0.00017911 | 0.00001849 | 0.0275 | 0.8737 |
| 11 | 0.00016062 | 0.00000899 | 0.0246 | 0.8983 |
| 12 | 0.00015163 | 0.00003978 | 0.0232 | 0.9215 |
| 13 | 0.00011185 | 0.00000922 | 0.0171 | 0.9387 |
| 14 | 0.00010263 | 0.00003574 | 0.0157 | 0.9544 |
| 15 | 0.00006689 | 0.00001587 | 0.0103 | 0.9647 |
| 16 | 0.00005102 | 0.00000921 | 0.0078 | 0.9725 |
| 17 | 0.00004181 | 0.00000912 | 0.0064 | 0.9789 |
| 18 | 0.00003269 | 0.00000572 | 0.0050 | 0.9839 |
| 19 | 0.00002697 | 0.00000109 | 0.0041 | 0.9880 |
| 20 | 0.00002588 | 0.00000534 | 0.0040 | 0.9920 |
| 21 | 0.00002053 | 0.00000473 | 0.0031 | 0.9952 |
| 22 | 0.00001581 | 0.00000552 | 0.0024 | 0.9976 |
| 23 | 0.00001029 | 0.00000526 | 0.0016 | 0.9992 |
| 24 | 0.00000502 | 0.00000492 | 0.0008 | 0.9999 |
| 25 | 0.00000010 | 0.00000001 | 0.0000 | 0.9999 |
| 26 | 0.00000009 | 0.00000001 | 0.0000 | 1.0000 |
| 27 | 0.00000008 | 0.00000002 | 0.0000 | 1.0000 |
| 28 | 0.00000007 | 0.00000000 | 0.0000 | 1.0000 |
| 29 | 0.00000006 | 0.00000000 | 0.0000 | 1.0000 |
| 30 | 0.00000006 | | 0.0000 | 1.0000 |

**Left scapulae**

A multivariate analysis of variance (MANOVA) was run using the 15 principal component scores for left scapulae as dependent variables and a single fixed factor representing sex by race groupings. The multivariate F-test (Wilks' Lambda) from the MANOVA indicated that at least one of the 15 components differed, on average, between at least two paired groups ($F=3.57$, $p<0.001$).

Subsequent univariate (ANOVA) tests conducted on left scapulae indicated that four principal components, 1, 3, 4, and 14, differed significantly by group membership once adjusted using the Bonferroni correction ($\alpha = 0.05/15 = 0.003$). Principal components 8 and 9 did not differ significantly but loaded in the second canonical discriminant function and were thus included. Of these, principal components 3, 4, and 14 load on the first canonical discriminant function, while principal components 1, 8, and 9 load on the second canonical discriminant function.

The first principal component (PC1) accounts for over 22% of the variance and is associated with variation at the inferior angle and with dorsolateral positioning of the dorsal glenoid fossa. Negative scores on the first principal component are associated with positioning of the inferior angle superiorly. Positive scores correspond to dorsolateral positioning of the dorsal glenoid. The third principal component (PC3) is associated with the position of the inferior angle as well as variability in the superior and ventral glenoid fossa. Positive scores are associated with a more inferior position of

the inferior angle as well as a more superior and ventral positioning of the superior and ventral glenoid fossa, respectively. Principal component 4 (PC4) is related to positioning of the superior angle, vertebral border, and inferior and ventral glenoid fossa. Specifically, positive scores indicate a more ventral position of the superior angle as well as more lateral positioning of the inferior glenoid fossa and vertebral border. Principal component 8 (PC8) is associated with the position of the superior angle, scapular notch, and vertebral border. Positive scores reflect a more inferior position of the superior angle and scapular notch, and negative scores represent ventral positioning of the vertebral border. Principal component 9 (PC9) reflects positioning of the superior and inferior glenoid fossa and lateral positioning of the vertebral border. Positive scores are associated with dorsal positioning of the superior glenoid fossa and lateral positioning of the vertebral border, and negative scores reflect a medial position of the inferior glenoid fossa. Principal component 14 (PC14) involves positioning of the vertebral border, acromion, superior angle, and inferior glenoid fossa. Positive scores reflect lateral positioning of the superior angle and inferior positioning of the inferior glenoid fossa, while negative scores are associated with medial positioning of the vertebral border and ventral positioning of the acromion.

**Right scapulae**

A MANOVA was conducted on the right scapulae using the 15 principal component scores as dependent variables and a single fixed factor

representing sex by ancestry groupings. The multivariate F-test (Wilks' Lambda) indicated that at least one of the 15 components differed, on average, between at least two of the paired groups. Univariate (ANOVA) tests indicated that a significant difference existed between the four groups in at least one of the 15 principal components once adjusted with the Bonferroni correction ($\alpha = 0.05/15 = 0.003$). Principal components 3 and 4 load on the first canonical discriminant function and principal component 1 loads on the second canonical discriminant function.

Principal component 1 (PC1) involves positioning of the superior and inferior angles. Positive scores reflect lateral positioning of the inferior angle and negative scores reflect medial positioning of the superior angle. Principal component 3 (PC3) is associated with positioning of the lateral coracoid and superior angle. Positive scores reflect a more dorsal position on the lateral coracoid, while negative scores indicate a more medial position on the superior angle. Principal component 4 (PC4) is associated with positioning of the lateral coracoid, lateral acromion, and superior angle. Positive scores reflect a lateral position on the lateral coracoid and a more dorsal position on the superior angle. Negative scores are associated with a medial position on the acromion.

**Canonical Discriminant Function Analysis**

Canonical discriminant function analysis indicates that sex and ancestry differences exist in scapular shape among individuals in this

sample. Eigenvalues of the covariance matrix for left and right scapulae have been previously presented in Tables 6.5 and 6.6, respectively. Class means on canonical variables of left scapulae are presented in Figure 6.3 and class means on canonical variables of right scapulae are presented in Figure 6.4. In both figures, racial separation is clearly shown by the clustering of White males and White females to the left side of the figure, while Black males and Black females tend toward the right side of the figure. Similarly, sex differentiation is evident in the clustering of White males and Black males toward the top of the figure, while White females and Black females tend toward the bottom of the figure.

**Left scapulae**

Canonical discriminant function 1 is comprised of principal components 3, 4, and 14 and effectively discriminated among individuals by ancestry. Among Blacks, the superior angle tends to be more dorsally positioned than in Whites, while the superior angle is more laterally positioned in Whites than Blacks. The inferior angle is more inferiorly located in Blacks than Whites. The superior glenoid fossa is more ventrally positioned in Blacks than Whites, while the ventral and inferior glenoid are more laterally positioned in Blacks than Whites. In addition, the vertebral border at its intersection with the scapular spine is more medially positioned in Blacks than in Whites.

Canonical discriminant function 2 is made up of principal components 1, 8, and 9 and is effective in discriminating between individuals on the basis

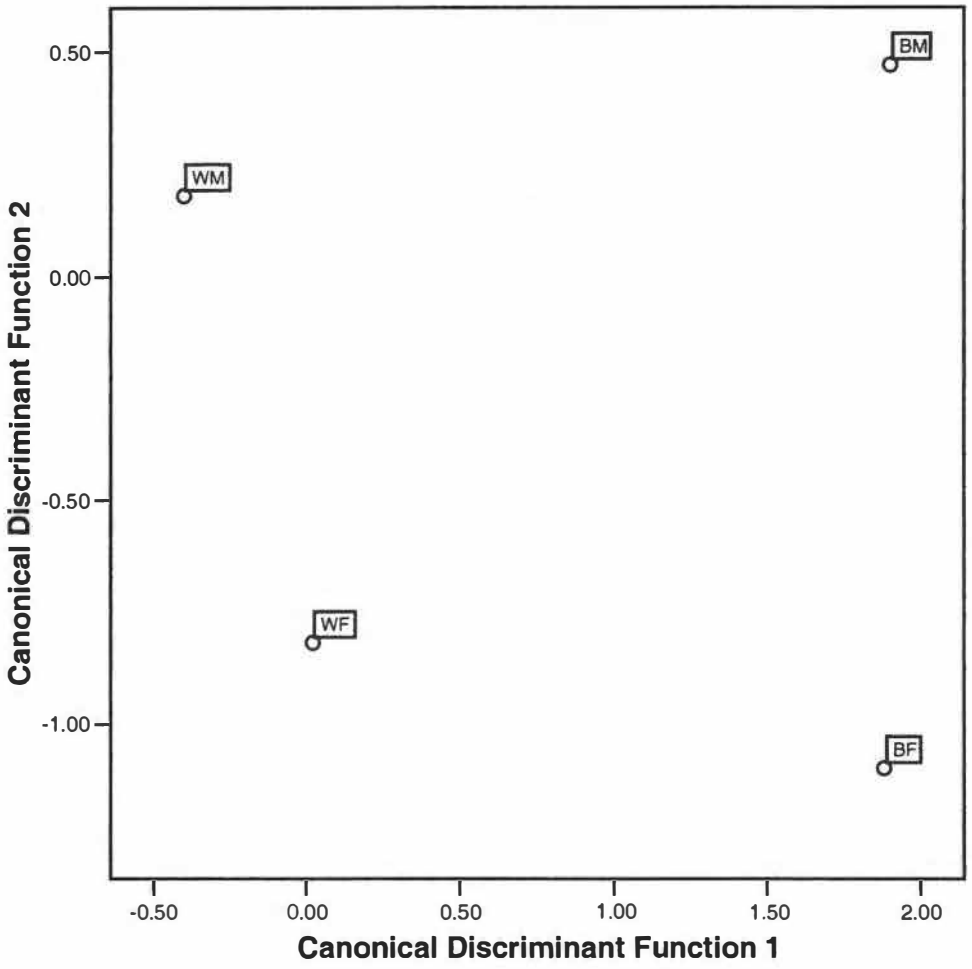



Figure 6.3. Class means on canonical variables of left scapulae.

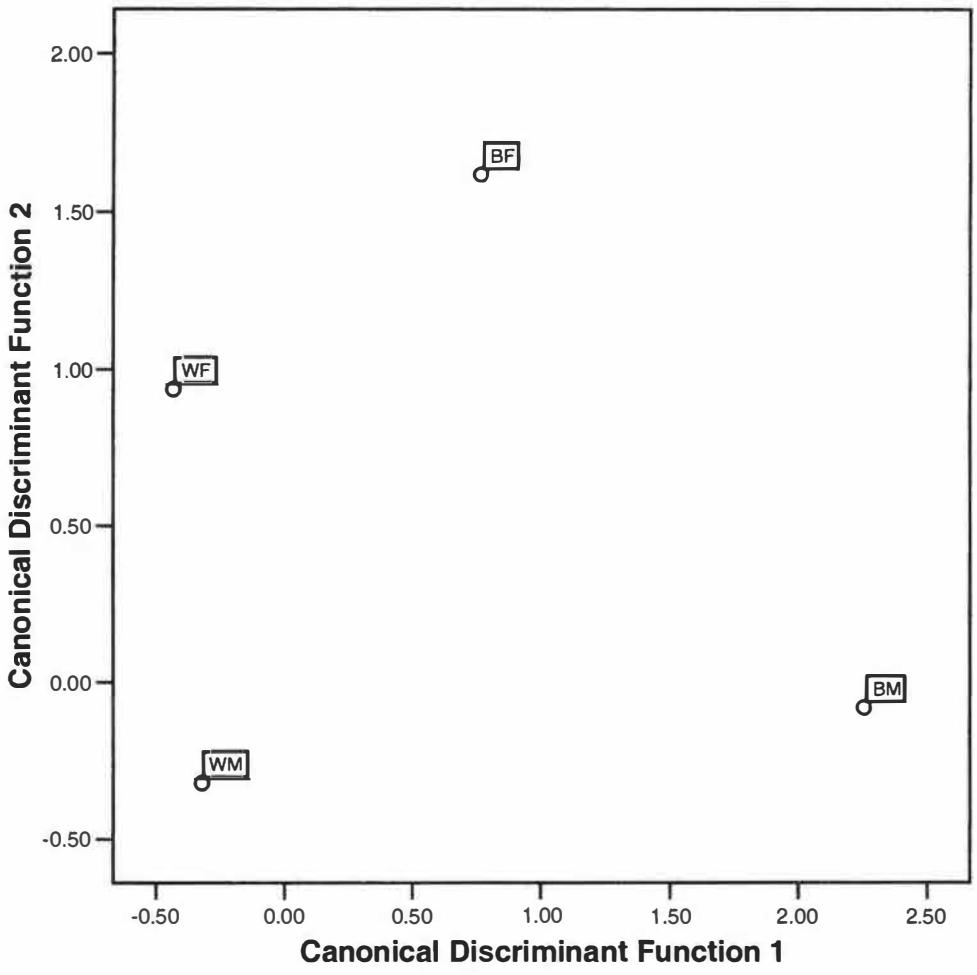



Figure 6.4. Class means on canonical variables of right scapulae.

of sex. For females, the inferior angle is more ventrally positioned than for males as is the vertebral border at its intersection with the scapular spine. In addition, the inferior glenoid is more medially positioned for females than for males. This triangle formed between the inferior glenoid, the inferior angle, and the vertebral border at its intersection with the scapular spine appears to be the primary area of the left scapula that distinguished males from females.

Mahalanobis distances and F-statistics are presented in Table 6.7 and Table 6.8, respectively. In addition, p-values of generalized squared distances (Mahalanobis distances) of left scapulae are significant across all combinations of ancestry and sex (Table 6.9).

**Right scapulae**

Principal components 3 and 4 comprise canonical discriminant function 1 and effectively partition ancestry differences among individuals. Among Blacks, the lateral coracoid is more dorsolaterally positioned than among Whites, while the superior angle is located more medially in Whites. The lateral acromion is positioned more medially in Whites than Blacks.

Canonical discriminant function 2 is comprised of principal component 1 and is useful is detecting sex differences. Specifically, in males the inferior angle is more medially positioned than in females. Also, the superior angle is more medially located on females than on males. Mahalanobis distances are presented in Table 6.10 and F-statistics are presented in Table 6.11. All p-values (Table 6.12) of generalized squared

**Table 6.7. Generalized Squared Distance of Left Scapulae of Black Females (BF), Black Males (BM), White Females (WF), and White Males (WM)**

| | BF | BM | WF | WM |
|---|---|---|---|---|
| **BF** | 0 | 6.94179 | 8.53440 | 9.89949 |
| **BM** | 6.94179 | 0 | 5.06197 | 5.37760 |
| **WF** | 8.53440 | 5.06197 | 0 | 1.39497 |
| **WM** | 9.89949 | 5.37760 | 1.39497 | 0 |

**Table 6.8. F Statistics for Generalized Squared Distance of Left Scapulae of Black Females (BF), Black Males (BM), White Females (WF), and White Males (WM)**

| | BF | BM | WF | WM |
|---|---|---|---|---|
| **BF** | 0 | 1.76067 | 2.30579 | 2.94431 |
| **BM** | 1.76067 | 0 | 4.33866 | 6.49732 |
| **WF** | 2.30579 | 4.33866 | 0 | 2.37939 |
| **WM** | 2.94431 | 6.49732 | 2.37939 | 0 |

**Table 6.9. P-Values for F Statistics of Generalized Squared Distance of Left Scapulae of Black Females (BF), Black Males (BM), White Females (WF), and White Males (WM)**

| | BF | BM | WF | WM |
|---|---|---|---|---|
| **BF** | 1.0000 | 0.0436 | 0.0051 | 0.0003 |
| **BM** | 0.0436 | 1.0000 | <.0001 | <.0001 |
| **WF** | 0.0051 | <.0001 | 1.0000 | 0.0038 |
| **WM** | 0.0003 | <.0001 | 0.0038 | 1.0000 |

**Table 6.10. Generalized Squared Distance of Right Scapulae of Black Females (BF), Black Males (BM), White Females (WF), and White Males (WM)**

| | BF | BM | WF | WM |
|---|---|---|---|---|
| **BF** | 0 | 6.36336 | 3.38125 | 5.95354 |
| **BM** | 6.36336 | 0 | 8.31685 | 6.78785 |
| **WF** | 3.38125 | 8.31685 | 0 | 1.65449 |
| **WM** | 5.95354 | 6.78785 | 1.65449 | 0 |

**Table 6.11. F Statistics for Generalized Squared Distance of Right Scapulae of Black Females (BF), Black Males (BM), White Females (WF), and White Males (WM)**

| | BF | BM | WF | WM |
|---|---|---|---|---|
| **BF** | 0 | 1.62674 | 0.92302 | 1.76991 |
| **BM** | 1.62674 | 0 | 7.55807 | 8.47536 |
| **WF** | 0.92302 | 7.55807 | 0 | 2.99501 |
| **WM** | 1.76991 | 8.47536 | 2.99501 | 0 |

**Table 6.12. P-Values for F Statistics of Generalized Squared Distance of Right Scapulae of Black Females (BF), Black Males (BM), White Females (WF), and White Males (WM)**

| | BF | BM | WF | WM |
|---|---|---|---|---|
| **BF** | 1.0000 | 0.0707 | 0.5397 | 0.0421 |
| **BM** | 0.0707 | 1.0000 | <.0001 | <.0001 |
| **WF** | 0.5397 | <.0001 | 1.0000 | 0.0003 |
| **WM** | 0.0421 | <.0001 | 0.0003 | 1.0000 |

distances generated by the DISCRIM procedure of SAS (1996) indicated that all combinations of ancestry and sex differ significantly except for Black females, which tend to differ from Black males (p=0.0707) but do not differ from White females (p=0.5397).

**Thin-plate Spline Analysis**

Thin-plate spline analysis in Morpheus (Slice, 1998) was employed to visually depict shape variation identified by canonical analysis. Figure 6.5 shows shape variation between left scapulae of White males and Black males. Using Black males as a reference and White males as the target, mean configurations indicate that grid deformation is most pronounced at the superior and inferior angles, coracoid process, and acromion. This area was identified as significantly different in shape in the first canonical discriminant function, which incorporates principal components 3, 4, and 14.

Figure 6.6 shows shape variation between left scapulae of White males and White females. The target, White females, was mapped onto the reference, White males. Grid deformation between the consensus configurations is evident at the superior angle and less so at the inferior angle. These two areas were identified in the second canonical discriminant function as being significantly different between the sexes.

Variation in the shape of right scapulae between White males and Black males is depicted in Figure 6.7. Grid deformation is most pronounced at the glenoid fossa and the superior angle, both of which were identified as

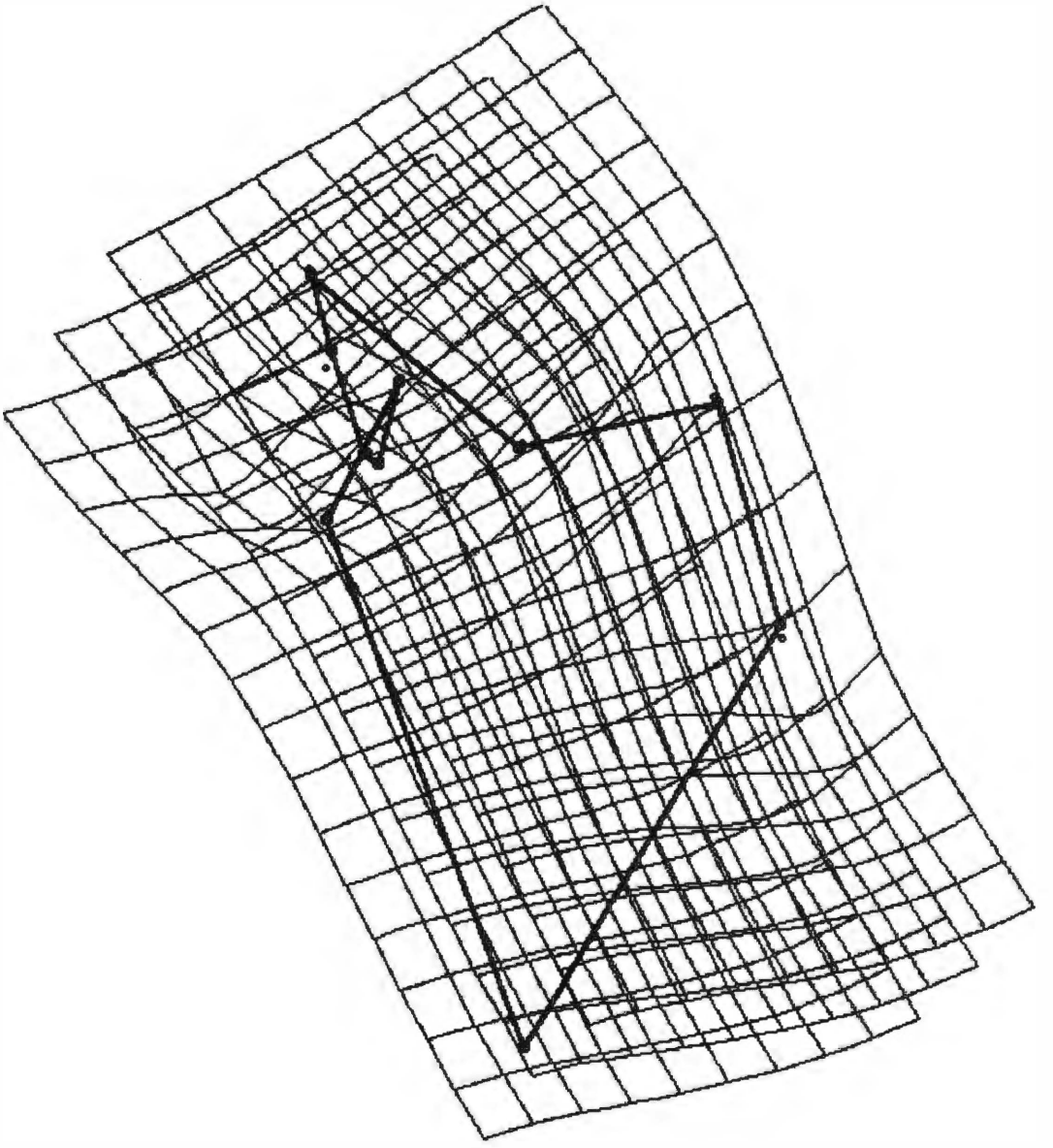


Figure 6.5. Thin-plate spline plot of mean White male and Black male configurations of left scapulae. Lateral is to the left and superior is to the top of the page.

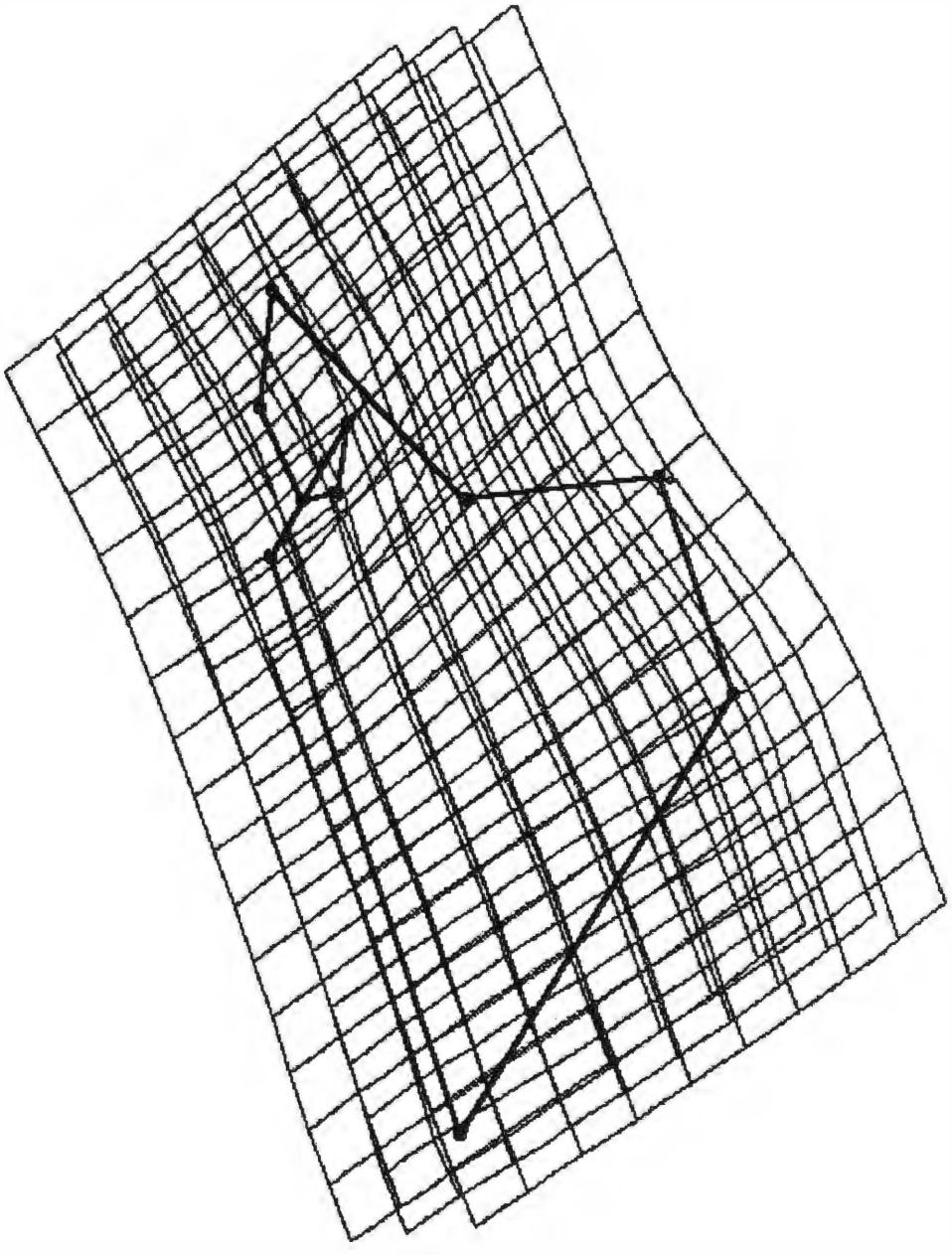


Figure 6.6. Thin-plate spline plot of mean White male and White female configurations of left scapulae. Lateral is to the left and superior is to the top of the page.

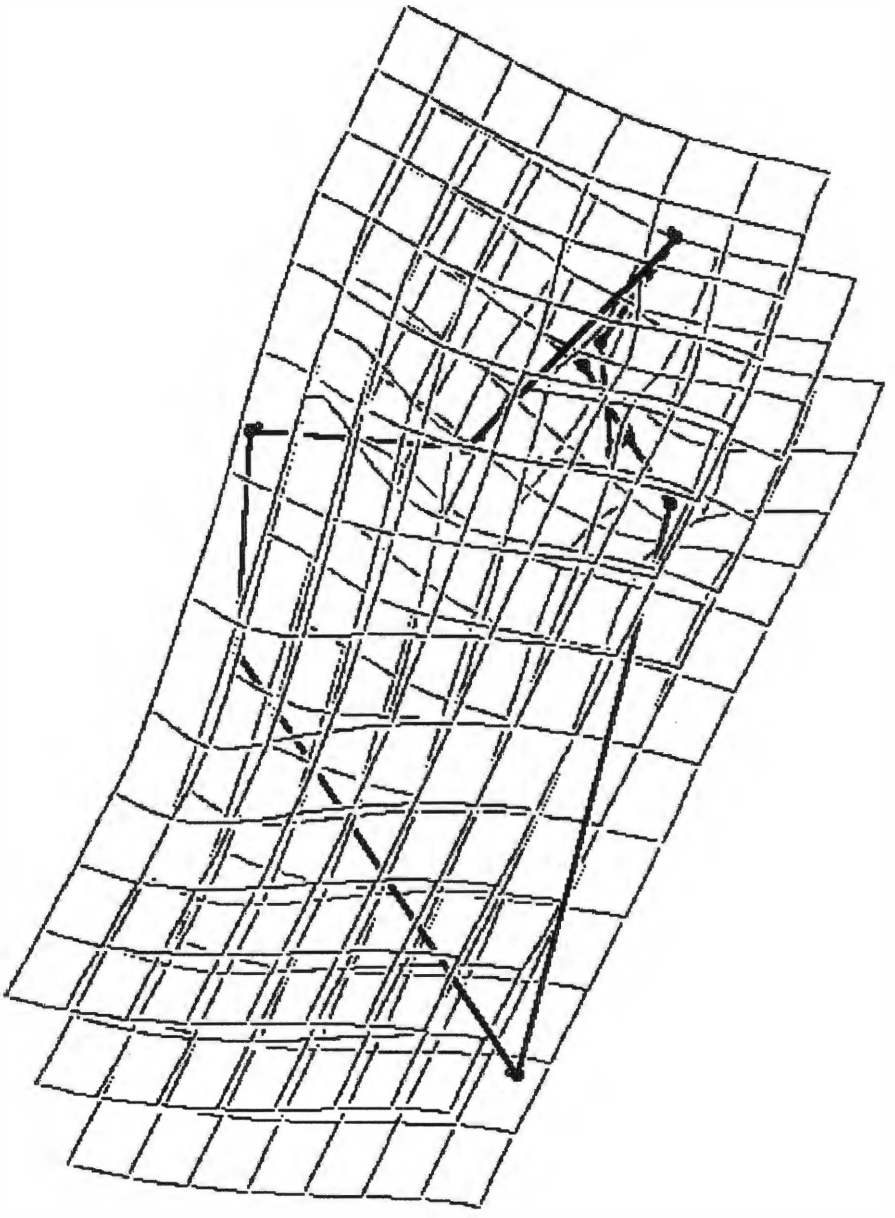


Figure 6.7. Thin-plate spline plot of mean White male and Black male configurations of right scapulae. Lateral is to the right and superior is to the top of the page.

areas of involvement in the canonical discriminant analysis. The first canonical discriminant function indicated that these areas of non-concurrence were responsible for the significant shape differences between the two ancestries.

The thin-plate spline depicted in Figure 6.8 shows obvious grid deformation at the glenoid fossa, vertebral border, and to a lesser extent at the inferior angle between right scapulae of White males and White females. These points of difference were identified in the second canonical discriminant function, which identifies sexually dimorphic shape differences when the consensus configurations are mapped onto one another.

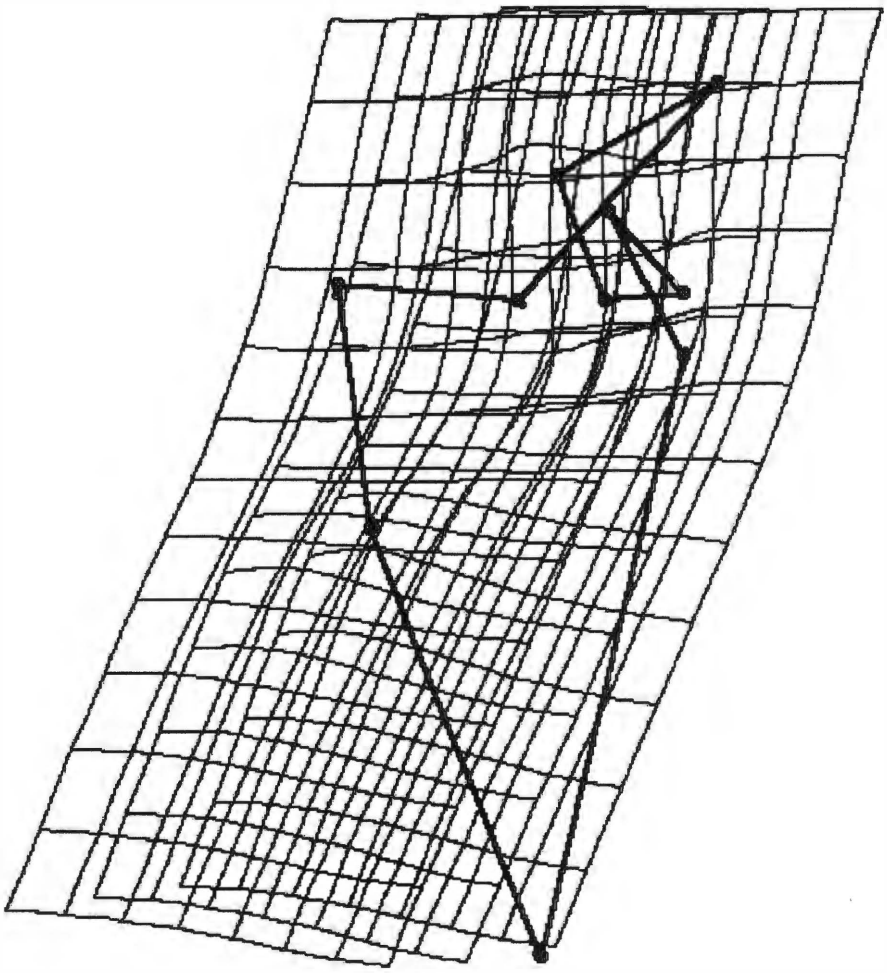


Figure 6.8. Thin-plate spline plot of mean White male and White female configurations of right scapulae. Lateral is to the right and superior is to the top of the page.

# CHAPTER 7

## Discussion and Conclusions

A paucity of successful studies regarding the determination of sex and ancestry from the scapula was, in part, responsible for the conception of this dissertation. As mentioned elsewhere in this text, numerous attempts have been made to determine sex and ancestry from the scapula, albeit with mixed results.

Early works by Broca (1878), Livon (1879), Flower (1879), Dwight (1887), Graves (1921, 1922, 1939), and others used variation in scapular measurements and scapular indices to assign individuals to various groups. Similarly, Vallois' (1924, 1926a, 1926b, 1927, 1928) extensive study of the scapula used a combination of metric and morphological traits to assign individuals to various races. Hrdlička, while realizing that trait frequency differed among groups, also recognized the importance of biomechanical stresses on the modification of scapular shape and acknowledged that classifications of the shape of the vertebral border, inferior angle, and scapular notch existed as a continuum rather than as discrete traits characteristic of a particular sex or race. Trait frequencies, such as the shape of the vertebral border, shape of the superior border, and the shape of the scapular notch, were shown by Hrdlička (1942a) to vary between the sexes but not enough to confidently assign gender.

The majority of these studies used traditional landmarks and measurements to formulate indices describing variability in size or morphometric traits describing variability in shape. Despite repeated efforts, however, few studies have shown that scapular morphological traits are sufficiently distinct to confidently assign ancestry or sex.

Discriminant function analysis, however, has been successfully used to determine sex from the scapula. Ren (1987) achieved correct sexing of 97% of Chinese adults using discriminant function analysis of the length of the glenoid cavity and length of the scapular spine. Discriminant function sexing using the length of the glenoid cavity, maximum distance from the acromion to the coracoid process, and maximum length of the coracoid process correctly sexed 95% of a sample of southern Italians (Di Vella et al., 1994), and Murphy (1995) correctly sexed 94% of individuals in a sample of prehistoric New Zealand Polynesian scapulae. Using the length of the scapula, Stewart (1979) correctly sexed 79% of a sample of American Blacks and Whites.

This dissertation tested the hypothesis that sex and ancestry differences in shape are present in the scapula and that this variation could be quantified using traditional and non-traditional landmarks coupled with geometric morphometry. In addition, this study incorporated several elements not commonly found in most analyses of ancestry and sex. First, geometric morphometry was used in conjunction with the more traditional discriminant function analysis. Because geometric morphometry removes

absolute size, shape variability of the scapulae was investigated in all dimensions. In addition, the use of non-traditional landmarks, such as the most inferior point on the scapular notch and the most lateral point on the coracoid process, allowed a more detailed analysis of the geometry of the scapulae. The use of non-traditional landmarks has been shown to be useful in the analysis of other skeletal elements, including the skull (McKeown, 2000), and os coxa (Synstelien, 2001).

To this end, the coordinate data derived from digitizing ten points on each of 241 pairs of left and and right scapulae were analyzed for differences in mean centroid size between Blacks and Whites and between the sexes. The data were then subjected to Procrustes analysis, which effectively removes size differences while computing mean shape. Principal component analysis and canonical discriminant function analysis were used to examine differences in scapular shape between Blacks and Whites and between males and females. Thin-plate splines graphically depicted shape differences between sexes and between ancestries.

Results of the analysis of variance of centroid sizes of left and right scapulae suggested that centroid size effectively discriminated between males and females but did not discriminate between Blacks and Whites. As expected, centroid sizes of males were larger than those of females. The significant interaction between ancestry and sex, however, cannot be explained. Mean centroid size differences were larger for females than for males, suggesting that sexual dimorphism in centroid size is reversed in the

ancestries. A larger sample size, particularly of Black females, is needed to explore this relationship further.

Similarly, geometric morphometry methods employed in this dissertation showed that shape variability exists between scapulae of Blacks and Whites and between the sexes. Plots of canonical discriminant function scores of left and right scapulae showed a clear differentiation between Blacks and Whites and between males and females. In addition, all p-values of generalized squared distances (Mahalanobis distances) of left scapulae were significant across all combinations of sex and ancestry. For right scapulae, all p-values were significant except for Black females, which did not differ from White females and tended to differ from Black males. Thus, it is clear that differences exist in scapular shape between the sexes and between ancestries. Although geometric morphometry has been successfully used to differentiate among other groups using other skeletal elements, such as the skull (Cheverud et al., 1992; O'Higgins and Dryden, 1993; Lynch et al., 1996), and humerus (Bacon, 2000), this is the first time it has been employed to identify sex and ancestry differences in scapular shape.

Less easily explained is the differential loading of the principal components in the canonical discriminant functions. For right scapulae, the principal components in the first canonical discriminant function, which discriminates on the basis of ancestry, involve positioning of the superior angles, acromion, and coracoid. For left scapulae, however, the first

canonical discriminant function, which also discriminates on the basis of ancestry, involves the position of glenoid fossa landmarks in addition to the superior and inferior angles. Similarly, principal components of the second canonical discriminant function, which discriminates on the basis of sex, largely involve positioning of the superior and inferior angles in right scapulae, whereas for left scapulae the second canonical discriminant function, in addition to the inferior angle, also involves positioning of glenoid landmarks and the vertebral border.

A number of factors may have contributed to the significant shape differences found in this study. First, in addition to a genetic component, bone shape also incorporates an environmental component. Initially, genetics drives the overall shape of the bone, which is later modified by extrinsic factors, such as environmental stress and biomechanical loading. Thus, the genetic component is likely to achieve maximum expression on bones where biomechanical expression is least. Given that musculature of the skull is limited largely to the muscles of mastication and the supporting musculature associated with the occipital, genetic expression of the skull is likely to be pronounced and more easily detected. Most postcranial elements, however, are intimately associated with locomotion, structural support, or manipulative activities. Unlike the skull, these postcranial elements require extensive musculature, which, although likely modifying scapular architecture somewhat, does not completely mask the effects of genetics.

The effects of muscle development on skeletal architecture have long been known. Biomechanical stresses are believed to be a major contributor to skeletal development (Ruff and Jones, 1981; Roy et al., 1994) as well as age- and sex-related ontogenetic factors (Helmkamp and Falk, 1990). Biomechanical loading of bone and its relationship to bone development has been the focus of radiographic (Garn et al., 1976; Jones et al., 1977) and photon absorptiometric (Nilsson and Westlin, 1971; Watson, 1973) studies. These studies of the living, particularly athletes, have attempted to explain bone mineral content in terms of physical activity.

Bilateral asymmetry studies, in particular, demonstrate the effects of exercise and muscle development on bone modification. Nilsson and Westlin (1971) found that although non-athletes showed no significant asymmetry in the bone mineral content of the distal femur of the dominant limb, athletes showed higher bone mineral content in the femur of the dominant limb. Similarly, Jones et al. (1977) observed cortical thickness of the humerus of the playing arms of professional tennis players exceeded cortical thickness in the non-dominant arm by 30% or more. Watson (1973) observed that although the humeri of young baseball players had higher bone mineral content in the dominant arm, the patterns of symmetry in the corresponding ulna and radius were inconsistent. These baseball players exhibited increasing bilateral asymmetry with age as well as increased bilateral asymmetry in the humerus compared to a small control sample. Watson cautioned that although unproven, higher bone mineral content in

the humerus appeared to be a function of exercise stress acting on the humerus.

Bone modification is also believed to result from other causes, not just from environmentally induced ones such as exercise stress. Asymmetry in femur and foot lengths in 4-month old human fetuses has been observed, before activity-related stress factors are operative (Schultz, 1926). In addition, one study showed that cortical thickness of the right second metacarpal was greater in both right- and left-hand dominant individuals, but the differences were significant only among right-handed individuals (Garn et al., 1976). Similarly, Plato et al. (1980) reported that measurements of the second metacarpal were greater in the right hand regardless of hand dominance. Measurements of total width, length, total area, and cortical area were significant only among the right-hand dominant. They suggested that the right second metacarpal inherently has more bone than the left, irrespective of hand dominance. Further, they stated that stress-related activity due to hand dominance could increase the bilateral difference in the right-handed and reduce it in the left-handed. A significant correlation existed between relative strength, as measured by combined grip and arm strength adjusted for age and body size, and some cortical bone dimensions.

Thus, the relationship between activity level and bilateral asymmetry is not unequivocal. Ruff and Jones (1981) stated that one of the main impediments in understanding bilateral asymmetry and its relationship to

activity level is that previous studies have focused almost entirely on highly select groups such as professional athletes, where asymmetry is likely to be pronounced. Few studies have been conducted on normal unselected populations, and of these, most have focused on less informative data such as long bone lengths or weights or structurally marginal areas such as the second metacarpal. Most studies have shown levels of asymmetry of a few percent, with higher levels attributable to higher levels of activity of the dominant side (Trinkaus et al., 1994).

Although most studies on skeletal asymmetry have focused on long bones, it is likely that most paired bones exhibit asymmetry in varying degrees. The scapula, which comprises a major part of the pectoral girdle and supports some of the same muscles that contribute to torsional and cortical bone asymmetry of the humerus, has received little attention regarding the effects of musculature bone modification. Nevertheless, Hrdlička (1942a) recognized that the scapula "...phylogenetically is almost entirely a muscular product, aside of its articular parts is completely dependent on the development and activity of its muscles, and in response to these, at all times of its existence, is adaptable in shape, size, strength, and most other conditions."

As with most bilaterally symmetric elements, the same gene system acts on both left and right scapulae and thus should produce mirror images of each other (Cartmill et al., 1987). As noted above, however, environmental conditions may differentially mediate genetic expression,

resulting in differential development, particularly in those areas most subject to muscular stress. It is clear that the effects of musculature are capable of affecting not only scapular size, but also scapular shape, as noted by Hrdlička (1942a). The muscles associated with the scapula are some of the strongest in the entire body. The wide platform provided by the scapula increases mobility of the shoulder as well as providing power to the joint. It is conceivable that bone modification in response to muscular development, particularly at the origins and insertions, differentially modified bilateral development of the scapula and accounted for the shape variability observed.

Thus, it is clear that a suite of complex and poorly understood variables act on scapular architecture to produce shape differences that are statistically significant between the sexes and between Blacks and Whites.

**Future Research**

That this study found significant differences in scapular shape between the sexes and between Blacks and Whites represents an important step forward in anthropology. With a complete set of skeletal remains the human skeleton can usually be accurately assessed for sex and often for ancestry. Individually, many bones in the human body can be sexed with reasonable certainty although very few are diagnostic for ancestry. Finding significant differences in the shape of the scapulae suggests that additional

postcranial elements may also be amenable to geometric morphology analysis.

Currently, the most common methods of ancestry determination are morphological methods and discriminant function analysis. Until recently, most discriminant function analyses have employed traditional landmarks. Increasingly, however, non-traditional landmarks are being used to differentiate between ancestries. Synstelien's (2001) study of the os coxa, for example, produced an overall classification of 82.9%, an accuracy rate exceeded only by measurements of the cranium, femur, or a combination of postcranial elements.

This study has shown that the nascent but growing field of geometric morphometry can advance the science of anthropology by using both traditional and non-traditional landmarks to examine differences in the shape of skeletal elements. Geometric morphometry is a relatively new technique, and the full range of its usefulness in answering anthropological questions remains unexplored. It is hoped that this study will spur researchers to examine other skeletal elements using other populations in order that population-specific standards of shape can be generated.

# List of References

# List of References


Ada, J.R. and Miller, M.E. (1991). Scapular fractures. Analysis of 113 cases. Journal of Clinical Orthopaedics and Related Research. 269:174-180.

Aiello, L. and Dean, C. (1990). An Introduction to Human Evolutionary Anatomy. London: Academic Press.

Anderson, W. (1891). Comment in the Proceedings of the Anatomical Society of Great Britain and Ireland. Feb. Journal of Anatomy and Physiology 25.

Anetzberger, H. and Putz, R. (1996). The scapula: principles of construction and stress. Acta Anatomica 156:70-80.

Bacon, A. (2000). Principal components analysis of distal humeral shape in Pliocene to recent African hominids: the contribution of geometric morphometrics. American Journal of Physical Anthropology 111:479-487.

Bainbridge, D. and Tarazaga, S. (1956). A study of the sex differences of the scapula. Journal of the Royal Anthropological Institute 86:109-134.

Barnett, N.D., Mander, M., Peacock, J.C., Bushby, K., Gardner-Medwin, D. and Johnson, G.R. (1995). Winging of the scapula: the underlying biomechanics and an orthotic solution. Proceedings of the Institute of Mechanical Engineers 209:215-223.

Basmajian, J.V. and Slonecker, C.E. (1989). Grant's Method of Anatomy. A Clinical Problem-solving Approach. Baltimore: Williams and Wilkins.

Bass, W.M. (1995). Human Osteology: A Laboratory and Field Manual of the Human Skeleton, 4th edition. Missouri Archaeological Society, Columbia, Missouri.

Benfer, R.A. (1975). Morphometric analysis of Cartesian coordinates of the human skull. American Journal of Physical Anthropology 42:371-382.

Birkner, R. (1978). Normal Radiographic Patterns and Variances of the Human Skeleton—An X-ray Atlas of Adults and Children. Baltimore: Urban and Schwarzenberg.

Blackith, R. and Reyment, G. (1971). Multivariate Morphometrics. London: Academic.

Boas, F. (1905). The horizontal plane of the skull and the general problem of the comparison of variable forms. Science 21:862-863.

Bookstein, F.L. (1982). Foundations of morphometrics. Annual Reviews of Ecology and Systematics 13:451-470.

Bookstein, F.L. (1986). Size and shape spaces for landmark data in two dimensions. Statistical Science 1:181-242.

Bookstein, F.L. (1990). Introduction to methods for landmark data. In Rohlf, F.J., and Bookstein, F., editors: Proceedings of the Michigan morphometric workshop. Ann Arbor: University of Michigan Museums, pp. 215-225.

Bookstein, F.L. (1991). Morphometric tools for landmark data. New York: Cambridge University Press.

Bookstein, F.L. (1992). A brief history of the morphometric synthesis. In Marcus, L., Bello, E., and Garcia-Valdecasas, A., editors: Contributions to morphometrics. Madrid: Museo Nacional de Ciencias Naturales, pp. 15-40.

Bookstein, F.L. (1996). Combining the tools of geometric morphometrics. In Marcus, L.F., Corti, M., Loy, A., Naylor, G.J.P., and Slice, D.E., editors: Advances in Morphometrics. New York: Plenum Press, pp. 131-152.

Boyer, D.W. (1975). Trapshooter's shoulder: stress fractures of the coracoid process. Journal of Bone and Joint Surgery 57A:862.

Brailsford, J.F. (1953). The Radiology of Bones and Joints, 5th edition. Baltimore: Williams and Williams.

Bright, A.S., Torpey, B., Magid, D., Codd, T. and McFarland, E.G. (1997). Reliability of radiographic evaluation for acromial morphology. Skeletal Radiology 26:718-721.

Broca, P. (1878). Sur les indices de largeur de l'omoplate chez l'homme, les singes et dans la série des mammifères. Bulletin de Societie d'Anthropologie de Paris I, 66.

Brookes, M. and Revell, W.J. (1998). Blood Supply of Bone--Scientific Aspects, 2nd edition. London: Springer.

Campobasso, C.P., Di Vella, G. and Introna, F. Jr. (1998). Using scapular measurements in regression formulae for the estimation of stature. Bollettino della Societaa Italiana di Biologia Sperimentale 74:75-82.

Carola, R., Harley, J.P. and Noback, C.R. (1992). Human Anatomy. London: McGraw-Hill.

Cartmill, M., Hylander, W.L. and Shafland, J. (1987). Human Structure. Cambridge: Harvard University Press.

Chambler, A.F. and Emery, R.J. (1997). Acromial morphology; the enigma of terminology. Knee Surgery, Sports Traumatology, Arthroscopy. 5:268-272.

Cheverud, J., Lewis, J.L., Bachrach, W. and Lew, W.D. (1983). The measurement of form and variation in form: an application of three-dimensional quantitative morphology by finite-element methods. American Journal of Physical Anthropology 62:151-165.

Cheverud, J., Kohn, L., Konigsberg, L. and Leigh, S. (1992). Effects of fronto-occipital artificial cranial vault modification on the cranial base and face. American Journal of Physical Anthropology 88:323-345.

Churchill, S.E. and Trinkaus, E. (1990). Neanderthal scapular glenoid morphology. American Journal of Physical Anthropology 83:147-160.

Cohn, I. (1921). Observations on the normally developing shoulder. American Journal of Roentgenology 8:721-729.

Cole, T.M. (1996). Early anthropological contributions to "Geometric Morphometrics." American Journal of Physical Anthropology 101:291-296.

Cummins, C.A., Anderson, K., Bowen, M., Nuber, G. and Roth, S.I. (1998). Anatomy and histological characteristics of the spinoglenoid ligament. Journal of Bone and Joint Surgery 80A:1622-1625.

Dennis, D.A., Ferlic, D.C. and Clayton, M.L. (1986). Acromial stress fractures associated with cuff tear arthropathy. Journal of Bone and Joint Surgery 68A:937-940.

de Palma, A.F. (1957). Degenerative Changes in the Sternoclavicular and Acromioclavicular Joints in Various Decades. Springfield: CC Thomas.

Di Vella, G., Campobasso, C.P., Dragone, M., and Introna, F., Jr. (1994). Skeletal sex determination by scapular measurements. Bollettino della Societaa Italiana di Biologia Sperimentale 70:299-305.

Doyle, W.J. (1976). Functionally induced alteration of adult scapular morphology. Acta Anatomica 99:173-177.

Dwight, T. (1887). The range of variation of the human shoulderblade. American Naturalist 21:627-638.

Dwight, T. (1905). The size of the articular surfaces of the long bones as characteristics of sex as an anthropological study. American Journal of Physical Anthropology 4:19-31.

Edelson, J.G. (1995a). Bony bridges and other variations of the suprascapular notch. Journal of Bone and Joint Surgery 77:505-506.

Edelson, J.G. (1995b). The 'hooked' acromion revisited. Journal of Bone and Joint Surgery 77:284-287.

Edelson, J.G. (1996). Variations in the anatomy of the scapula with reference to the snapping scapula. Clinical Orthopedics Jan:111-115.

Edelson, J.G., Zuckerman, J. and Hershkovitz, I. (1993). Os acromiale: anatomy and surgical implications. Journal of Bone and Joint Surgery 75B:551-555.

Elmiger, P. (1966). The early development of the scapula in humans. Acta Anatomica 65:58-137.

Fazekas, I.G. and Kósa, F. (1978). Forensic Fetal Osteology. Budapest: Akadémiai Kiadó.

Field, E.J. and Harrison, R.J. (1957). Anatomical Terms: Their Origin and Derivation. Cambridge: Heffler.

Finnegan, M. (1978). Non-metric variation of the infracranial skeleton. Journal of Anatomy 125:23-37.

Flower, W.H. (1879). On the scapular index as a race character in man. Journal of Anatomy and Physiology 14:13-17.

Frazer, J.E. (1948). The Anatomy of the Human Skeleton, 4th edition. London: Churchill.

Frey, H. (1923). Untersuchungen über die scapula, Speziell über ihre äussere Form und deren Abhängigkeir von der Funktion. Zeitschrift fur Anatomie Entwicklungsgeschichte 28:277-324.

Ganzhorn, R.W., Hocker, J.T., Horowitz, M. and Switzer, H.E. (1981). Suprascapular nerve entrapment. Journal of Bone and Joint Surgery 63A:492-494.

Garcia, G. and McQueen, D. (1981). Bilateral suprascapular nerve entrapment syndrome. Journal of Bone and Joint Surgery 63A:491e 492.

Garn, S.M., Rohmann, C.G. and Silverman, F.N. (1967). Radiographic standards for postnatal ossification and tooth calcification. Medical Radiography and Photography 43:45-66.

Garn, S.M., Mayor, G.H. and Shaw, H.A. (1976). Paradoxical bilateral asymmetry in bone size and bone mass in the hand. American Journal of Physical Anthropology 45:209-210.

Getz, J.D., Recht, M.P., Piraino, D.W., Schils, J.P., Latimer, B.M., Jellema, L.M. and Obuchowski, N.A. (1996). Acromial morphology: relation to sex, age, symmetry, and subacromial enthesophytes. Radiology 1993:737-742.

Girdnay, B.R. and Golden, R. (1952). Centres of ossification of the skeleton. American Journal of Roentgenology 68:922-924.

Goodall, C. (1991). Procrustes methods in the statistical analysis of shape. Journal of the Royal Statistical Society B53:285-339.

Gower, J. (1975). Generalized Procrustes analysis. Psychometrika 40:323-343.

Gowland, W.P. (1915). Preliminary note on a diarthordial articulation between the clavicle and the coracoid. Journal of Anatomy and Physiology 49:187-189.

Gradoyevitch, B. (1939). Coracoclavicular joint. Journal of Bone and Joint Surgery 21:918-920.

Graves, W.W. (1921). The types of scapulae: a comparative study of some correlated characters in human scapulae. American Journal of Physical Anthropology 4:111-128.

Graves, W.W. (1922). Observations on age changes in the scapula. American Journal of Physical Anthropology 5:21-33.

Graves, W.W. (1939). A note on the biological and clinical significance of inherited variation. I. The types of scapulae. Southern Medical Journal 32:740-745.

Gray, D.J. (1942). Variations in human scapulae. American Journal of Physical Anthropology 29:57-72.

Guangjin, R. (1982). Sexual diagnosis of scapula by discriminant function analysis. Acta Anthropologica Sinica 21:144-146.

Gumina. S., Postacchini, F., Orsina, L. and Cinotti, G. (1999). The morphometry of the coracoid process—its aetiologic role in subcoracoid impingement syndrome. International Orthopaedics 23:198-201e

Gupta, R., Sher, J., Williams, G.R. and Iannotti, J.P. (1998). Non-union of the scapular body: a case report. Journal of Bone and Joint Surgery 80A:428-430.

Hanihara, K. (1959). Sex diagnosis of Japanese skulls and scapulae by means of discriminant functions. Journal of the Anthropological Society of Nippon 67:21-27.

Helmkamp, R.C., and Falk D. (1990). Age- and sex-associated variations in the directional asymmetry of rhesus macaque forelimb bones. American Journal of Physical Anthropology 83:211-218.

Heyse-Moore, G.H. and Stoker, D.J. (1982). Avulsion fractures of the scapula. Skeletal Radiology 9:27-32.

Hodges, P.C. (1933). An epiphyseal chart. American Journal of Roentgenology 30:809-810.

Hojo, T. (1970). Secular changes in the form of the Japanese scapulae, compared with other races. Kumamoto Igakkai Zasshi 44:937-952.

Hollinshead, W.H. (1982). Anatomy for Surgeons, 3rd edition. Philadelphia: Harper and Row.

Howell, J.A. (1917). An experimental study of the effect of stress and strain in bone development. Anatomical Record 3:233-252.

Hrdlička, A. (1942a). The adult scapula: additional observations and measurements. American Journal of Physical Anthropology 29:363-415.

Hrdlička, A. (1942b). The scapula: visual observations. American Journal of Physical Anthropology 29:73-94.

Hrdlička, A. (1942c). The juvenile scapula: further observations. American Journal of Physical Anthropology 29:287-310.

Hrdlička, A. (1952). Practical Anthropometry, 4th edition, edited by T.D. Stewart. The Wistar Institute of Anatomy and Biology, Philadelphia.

Imatani, R.J. (1975). Fractures of the scapula: a review of 53 fractures. Journal of Trauma 15:473-478.

Iordanidis, P. (1961). Détermination du sexe par les os du sequelette. Annales de Médecine Légale 41:280-291.

Jacobson, S.R., Speer, K.P., Moor, J.T., Janda, D.H., Saddemi, S.R., MacDonald, P.B. and Mallon, W.J. (1995). Reliability of radiographic assessment of acromial morphology. Journal of Shoulder and Elbow Surgery 4:449-453.

Jones, H.H., Priest, J.D., Hayes, W.C., Tichenor, C.C. and Nagel, D.A. (1977). Humeral hypertrophy in response to exercise. Journal of Bone and Joint Surgery 59:204-208.

Kanagasuntheram, R., Sivanandasingham, P. and Krishnamurti, A. (1987). Anatomy: Regional, Functional and Clinical. Singapore: PG Publishing.

Kapandji, L.A. (1974). The Physiology of the Joints, Volume 3. The Trunk and Vertebral Column. London: Churchill Livingstone.

Keats, T.E. (1992). Atlas of Normal Roentgen Variants that may Simulate Disease, 5th edition. St. Louis: Mosby Yearbook.

Kendall, D.G. (1977). The diffusion of shape. Advances in Applied Probability 9:428-430.

Kendall, D.G. (1984). Shape-manifolds, Procrustean metrics and complex projective spaces. Bulletin of the London Mathematical Society 16:81-121.

Kent, J.T. (1994). The complex Bingham distribution and shape analysis. Journal of the Royal Statistical Society, Series B 56:285-299.

Krogman, W.M. (1962). The Human Skeleton in Forensic Medicine. Springfield, Illinois: C.C. Thomas.

Kuhns, J.G. (1945). Variations in the vertebral border of the scapula: their relation to muscular function. Yearbook of Physical Anthropology 109-112.

Kumar, V.P., Satku, K., Liu, J. and Shen, Y. (1997). The anatomy of the anterior origin of the deltoid. Journal of Bone and Joint Surgery 79:680-683.

Last, R.J. (1973). Anatomy, Regional and Applied, 5th edition. Edinburgh: Churchill Livingstone.

Lele, S. (1993). Euclidean distance matrix analysis (EDMA): estimation of mean form and mean form distance. Mathematical Geology 25:573-602.

Lele, S. and Richtsmeier, J. (1991). Euclidean distance matrix analysis: a coordinate-free approach for comparing biological shapes using landmark data. American Journal of Physical Anthropology 86:415-428.

Liberson, F. (1937). Os acromiale - a contested anomaly. Journal of Bone and Joint Surgery 19:683-689.

Livingstone, S.K. (1937). Sprengel's deformity. Journal of Bone and Joint Surgery 19:539-540.

Livon, M. (1879). De l'omoplate et de ses indices de largeur dans les races humaines. Thése pour le Doctorate en Médecine Paris, 1-64.

Lynch, J., Wood, C. and Luboga, S. (1996). Geometric morphometrics in primatology: craniofacial variation in *Homo sapiens* and *Pan troglodytes*. Folia Primatology 67:15-39.

Macalister, A. (1893). Notes on the acromion. Journal of Anatomy and Physiology 27:245-251.

MacGillivray, J.D., Fealy, S., Potter, H.G. and O'Brien, S.J. (1998). Multiplanar analysis of acromion morphology. American Journal of Sports Medicine 26:836-840.

Marcus, L. and Corti, M. (1996). Overview of the new, or geometric morphometrics. In Marcus, L.F., Corti, M., Loy, A., Naylor, G.J.P. and Slice, D.E., editors: Advances in Morphometrics. New York: Plenum Press, pp. 1-13.

Martin R. (1957). Lehrbuch der Anthropologie. Revised Third Edition, Volume 3, edited by Karl Saller. Gustav Fischer Verlag, Stuttgart.

Martin, C.P. (1933). The cause of torsion of the humerus and of the notch on the anterior edge of the glenoid cavity of the scapula. Journal of Anatomy 67:573-582.

McClure, J.G. and Raney, R.B. (1974). Double acromion and coracoid processes: case report of an anomaly of the scapula. Journal of Bone and Joint Surgery 56A:830-832.

McClure, J.G. and Raney, R.B. (1975). Anomalies of the scapula. Clinical Orthopedics 110:22-31.

McGahan, J.P., Rab, G.T. and Dublin, A. (1980). Fractures of the scapula. Journal of Trauma 20:880-883.

McKern, T.W. and Stewart, T.D. (1957). Skeletal age changes in young American males. Headquarters, Quartermaster Research and Development Command, Technical Report EP-45. Quartermaster Research and Development Center Environmental Protection Research Division, Natick, Massachusetts.

McMinn, R.M.H. and Hutchings, R.T. (1977). Color Atlas of Human Anatomy. Chicago: Year Book Medical Publishers.

Mendes-Corrêa, A.A. (1919). Osteometria Portuguesa, II Cintura escapular. An Acad. Polytechn. (Porto) 13:1-45.

Miles, A.E.W. (1994). Non-union of the epiphysis of the acromion in the skeletal remains of a Scottish population of ca. 1700. International Journal of Osteoarchaeology 4:149-163.

Miles, A.E.W. (1996). Humeral impingement on the acromion in a Scottish island population of c. 1600 AD. International Journal of Osteoarchaeology 6:259-288.

Miles, A.E. W. (1997). The glenoid notch and the shape of the glenoid cavity of the scapula. Journal of Anatomy 191:475.

Miles, A.E.W. (1998). New light on the acromial attachment of the human coraco-acromial ligament. International Journal of Osteoarchaeology 8:274-279.

Miles, A.E.W. (1999). Observations on the undersurface of the skeletalized human acromion in two populations. International Journal of Osteoarchaeology 9:131-145.

Montagu, M.F.A. (1960). A Handbook of Anthropometry. Charles C. Thomas, Springfield, Illinois.

Moran, A.J. and Chamberlain, A.T. (1997). The incidence of dorsal sulci of the scapula in a modern human population from Ensay, Scotland. Journal of Human Evolution 33:521-524.

Mudge, M.K., Wood, V.E. and Frykman, G.K. (1984). Rotator cuff tears associated with os acromiale. Journal of Bone and Joint Surgery 66A:427-429.

Murphy, A.M.C. (1995). Sex determination of prehistoric New Zealand Polynesian scapulae. New Zealand Journal of Archaeology 17:29-34.

Nicholson, G.P., Goodman, D.A., Flatow, E.L. and Bigliana, L.U. (1996). The acromion: morphologic condition and age-related changes. A study of 420 scapulas. Journal of Shoulder and Elbow Surgery 5:1-11.

Nilsson, B.E. and Westlin, N.E. (1971). Bone density in athletes. Clinical Orthopedics 77:179-182.

Ogata, S. and Ulthoff, H.K. (1990). Acromial enthesopathy and rotator cuff tear. Clinical Orthopedics and Related Research 254:39-48.

Ogden, J.A. and Phillips, S.B. (1983). Radiology of postnatal skeletal development. VII. The scapula. Skeletal Radiology 9:157-169.

O'Higgins P. and Dryden, I. (1993). Sexual dimorphism in hominoids: further studies of craniofacial shape differences in *Pan*, *Gorilla*, and *Pongo*. Journal of Human Evolution 24:183-205.

O'Higgins, P. and Vidarsdottir, U. (1999). New approaches to the quantitative analysis of craniofacial growth and variation. In Hoppa, R. and Fitzgerald, C., editors: Human Growth in the Past. Cambridge: Cambridge University Press.

Olivier, G. and Pineau, H. (1957). Biométrie du scapulum; Asymétrie, corrélations et différences sexuelles. Archives d'Anatomie de Paris 33:67-88.

Ozaki, I., Fujimoto, S., Nakagawa, Y., Masuhara, K. and Tamai, S. (1988). Tears of the rotator cuff of the shoulder associated with pathologic changes in the acromion. Journal of Bone and Joint Surgery 70A:1224-1230.

Palmqvist, P. and Péres-Claros, J.A. (1996). Comparative morphometric study of a human phalanx from the Lower Pleistocene site at Cueva Victoria (Murcia, Spain), by means of Fourier analysis, shape coordinates of landmarks, principal and relative warps. Journal of Archaeological Science 23:95-107.

Pate, D., Kursunoglu, S., Resnick, D. and Resnick, C.S. (1985). Scapular foramina. Skeletal Radiology 14:270-275.

Patte, D. (1990). The subcoracoid inpingement. Clinical Orthopedics and Related Research 254:55-59.

Peat, M. (1986). Functional anatomy of the shoulder complex. Physical Therapy 66:1855-1865.

Peng, S. (1983). Estimation of stature from skull, clavicle, scapula, and os coxa of male adults of southern China. Acta Anthropologica Sinica 2:253-259.

Penning, R. and Müller, S. (1988). Sexual dimorphism of the scapula. Zeitschrift für Rechtsmedizin 101:183-196.

Phelps, E. (1932). A critique of the principle of the horizontal plane of the skull. American Journal of Physical Anthropology 17:71-98.

Plato, C.C., Wood, J.L. and Norris, A.H. (1980). Bilateral asymmetry in bone measurements of the hand and lateral hand dominance. American Journal of Physical Anthropology 52:27-31e

Prescher, A. and Klümpen, T. (1997). The glenoid notch and its relation to the shape of the glenoid cavity of the scapula. Journal of Anatomy 190:457-460.

Ren, G. (1987). Sexual diagnosis of scapula by discriminant function analysis. Acta Anthropologica Sinica 6:144-146.

Rengachary, S.S., Burr, D., Lucas, S., Hassanein, K.M., Mohn, M.P. and Matzke, H. (1979). Suprascapular entrapment neuropathy: a clinical, anatomical and comparative study. Part 2: Anatomical Study. Neurosurgery 5:447-451e

Reyment, R., Blackith, R., and Campbell, N. (1984). Multivariate Morphometrics, 2nd edition. London:Academic Press.

Riesenfield, A. (1966). The effects of experimental bipedalism and upright posture in the rat and their significance for the study of human evolution. Acta Anatomica 65:449-521.

Rohlf, F.J. (1996). Morphometric spaces, shape components and the effects of linear transformations. In Marcus, L.F., Corti, M., Loy, A., Naylor, G.J.P., and Slice, D.E., editors: Advances in Morphometrics. New York: Plenum Press, pp. 11e-129.

Rohlf, F. and Marcus, L. (1993). A revolution in morphometrics. Trends in Ecological Evolution 8:129-132.

Ross, A., McKeown, A. and Konigsberg, L. (1999). Allocation of crania to groups via the "New Morphometry." Journal of Forensic Sciences 44:584-587.

Rowe, C.R. (1968). An atlas of anatomy and treatment of mid-clavicular fractures. Clinical Orthopedics and Related Research 58:29-42.

Roy, T.A., Ruff, C.B. and Plato, C.C. (1994). Hand dominance and bilateral asymmetry in the structure of the second metacarpal. American Journal of Physical Anthropology 94:203-211.

Ruff, C.B. and Jones, H.H. (1981). Bilateral asymmetry in cortical bone of the humerus and tibia—sex and age factors. Human Biology 53:69-86.

SAS (1996). SAS System for Windows, Release 6.12. SAS Institute, Inc., Cary, North Carolina.

Schultz, A.H. (1926). Fetal growth of man and other primates. Quarterly Review of Biology 1:465-521.

Schurer, L. and Black, S. (2000). Developmental Juvenile Osteology. London: Academic Press.

Shulin, P.and Fangwu, Z. (1983). Estimation of stature from skull, clavicle, scapula and os coxa of male adult of Southern China. Acta Anthropologica Sinica 2:253-259.

Siegel, A. and Benson, R. (1982). A robust comparison of biological shapes. Biometrics 38:341-350.

Slice, D.E. (1996). Three-dimensional, generalized resistant fitting and the comparison of least-squares and resistant-fit residuals. In Marcus, L.F., Corti, M., Loy, A., Naylor, G.J.P., and Slice, D.E., editors: Advances in Morphometrics. New York: Plenum Press, pp.177-199.

Slice, D.E. (1998). Morpheus et al.: Software for Morphometric Research. Revision 1/30/98. Department of Ecology and Evolution, State University of New York, Stony Brook, New York.

Small, C.G. (1996). The Statistical Theory of Shape. Springer-Verlag, New York.

Sneath, P. (1967). Trend-surface analysis of transformation grids. Journal of Zoology 151:65-122.

Steele, D.G. and Bramblett, C.A. (1988). The Anatomy and Biology of the Human Skeleton. College Station: Texas A&M University Press.

Stevenson, P.H. (1924). Age order of epiphyseal union in man. American Journal of Physical Anthropology 7:53-93.

Stewart, T.D. (1979). Essential of Forensic Anthropology. Springfield, IL: C.C. Thomas.

Stirland, A. (1992). Comparisons of the scapula in young adult medieval males: an application of Hrdlička. Anthropologie 30:5-7.

Stone, R.J. and Stone, J.A. (1997). Atlas of Skeletal Muscles. Dubuque, IA: William C. Brown.

Sun, C. (1986). Observation on the Chinese scapulae. Acta Anthropologica Sinica 5:372-376.

Synstelien, J. (2001). Differences in Os Coxae Between Blacks and Whites: a Musculoskeletal Approach to Human Variation. The University of Tennessee, Knoxville, Master's Thesis.

Tachdjian, M.O. (1972). Pediatric Orthopedics. Philadelphia: W.B. Sanders.

Thompson, D. (1917). On Growth and Form. London: Cambridge University Press.

Thompson, D.A., Flynn, T.C., Miller, P.W. and Fischer, R.P. (1985). The significance of scapular fractures. Journal of Trauma 25:974-977.

Trinkaus, E., Churchill, S.E. and Ruff, C.B. (1994). Postcranial robusticity in Homo. II:Humeral bilateral asymmetry and bone plasticity. American Journal of Physical Anthropology 93:1-34.

Turner, W. (1886). The scapula. Report on the human crania and other bones of the skeleton. Challenger Reports 16:81-88.

Uhthoff, H.K., Hammond, D.I., Sarkar, K., Hooper, G.J. and Papoff, W.J. (1988). The role of the coraco-acromial ligament in the impingement syndrome. International Orthopedics 12:97-104.

Uri, D.S., Kneeland, J.B. and Herzog, R. (1997). Os acromiale: evaluation of markers for identification on sagittal and coronal oblique MR images. Skeletal Radiology 26:31-34.

Vallois, H.V. (1924). La formation de l'omoplate humaine. Annales d'Anatomie Pathologique de d'Anatomie Normale 3:111-113.

Vallois, H.V. (1926a). Les anomalies de l'omoplate chez l'homme. Bulletin de la Sociétié d'Anthropologie de Paris 7:19-36.

Vallois, H.V. (1926b). Variations de l'échancrure coracoidienne de l'omoplate. Annales d'Anatomie Pathologique de d'Anatomie Normale. 3:129-168.

Vallois, H.V. (1927). L'omoplate des Négrilles et celle des Négritos. Bulletin de la Sociétié d'Anthropologie de Paris 7:1-3.

Vallois, H.V. (1928). L'omoplate humaine, étude anatomique et anthropologique. Bulletin de la Sociétié d'Anthropologie de Paris 7:129-168.

Vanarthos, W.J. and Monu, J.U. (1995). Type 4 acromion: a new classification. Contemporary Orthopedics 30:227-229.

Van Dongen, R. (1963). The shoulder girdle and humerus of the Australian Aborigine. American Journal of Physical Anthropology 21:469-489.

Vangsness, C.T., Jorgensen, S.S., Watson, T. and Johnson, D.L. (1994). The origin of the long head of the biceps from the scapula and glenoid labrum. Journal of Bone and Joint Surgery 76B:315-327.

Wang, J.C. and Shapiro, M.S. (1997). Changes in acromial morphology with age. Journal of Shoulder and Elbow Surgery 6:55-59.

Warner, J.J.P., Beim, G.M. and Higgins, L. (1998). The treatment of symptomatic os acromiale. Journal of Bone and Joint Surgery 80A: 116-120.

Watson, R.C. (1973). Bone growth and physical activity in young males. International Conference on Bone Mineral Measurement. R.B. Mazess, editor. U.S. Department of Health, Education, and Welfare Publication No. (NIH) 75-683. U.S. Government Printing Office, Washington, D.C., pp. 380-386.

Weiner, D.S. and MacNab, I. (1970). Superior migration of the humeral head. Journal of Bone and Joint Surgery 52B: 524-527.

Wienker, C.W. and Wood, J.E. (1988). Osteological individuality indicative of migrant citrus laboring. Journal of Forensic Sciences 33:562-567.

Wilber, M.C. and Evans, E.B. (1977). Fractures of the scapula. Journal of Bone and Joint Surgery 59A: 358-362.

Williams, P.L., Bannister, L.H., Berry, M.M., Collins, P., Dyson, M., Dussek, J.E. and Ferguson, M.W.J. (1995). Gray's Anatomy, 38th edition. Edinburgh: Churchill Livingstone.

Wilson, C.L. and Duff, G.L. (1943). Pathologic study of degeneration and rupture of the supraspinatus tendon. Archives of Surgery 47:121-135.

Wolffson, D.M. (1950). Scapula shape and muscle function, with special reference to the vertebral border. American Journal of Physical Anthropology 8:331-342.

Wood Jones, F. (1953). Buchanan's Manual of Anatomy, 8th edition. London: Baillière Tindall and Cox.

Wood, C. and Lynch, J. (1996). Sexual dimorphism in the craniofacial skeleton of modern humans. In Marcus, L.F., Corti, M., Loy, A., Naylor, J.P.G. and Slice, D.E., editors: Advances in Morphometrics. New York: Plenum Press, pp. 407-414.

Yazici M., Kopuz, C., and Gulman, B. (1995). Morphologic variants of acromion in neonatal cadavers. Journal of Pediatric Orthopedics 15: 744-647.

Zuckerman, J.D., Kummer, F.J., Cuomo, F. and Greller, M. (1997). Interobserver reliability of acromial morphology classification: an anatomic study. Journal of Shoulder and Elbow Surgery 6:286-287.

# Vita

Frederick J. Snow was born in Louisville, Kentucky and attended elementary school and high school in Knoxville, Tennessee. He received a Bachelor of Arts in English from Georgia State University in 1970. After working as a police officer and a hazardous materials specialist, he entered The University of Tennessee and received a Master of Arts in Anthropology in 1989. While working on his doctorate, he was employed as a forensic anthropologist in both Bosnia and Kosovo. After returning from the Balkans, he was hired by the Georgia Bureau of Investigation as a forensic anthropologist. He continued his doctoral education at The University of Tennessee and was awarded his Ph.D. in Anthropology in 2004.

5996 2951 1
06/23/04 MRB